EPR of Uranium Ions

I. Ursu and V. Lupei

Central Institute of Physics
P.O. Box 5206
Bucharest, Romania

I. INTRODUCTION

Actinides, the last known group of the Periodic Table are the subject of a special interest, both practical and scientific. Though their use is mainly based on their unique nuclear properties, the electronic structure is of no little interest because it is of paramount importance in determining the physical and chemical properties of the actinides and their compounds. Despite the common tendency to consider the actinides group as a new rare-earth group, similar to the lanthanides, numerous data show that this group has a definite identity, evidenced mainly in the first half of the group. At the beginning of the actinides group, a contraction of the 5f electronic shell takes place (actinide contraction), but this is not so sharply manifested as the contraction of the lanthanides 4f shell. In the actinide group the energy separation of the 5f, 6d, and 7s electronic levels is small, whereas for the lanthanides the 4f electrons are strongly localized. This leads to a strong competition between the 5f, 6d, and 7s electrons in determining the electronic properties of the actinides and their compounds. Another consequence of the weaker 5f contraction is that the ionic radius of the actinide ions is greater than that of the corresponding lanthanide ions. A determinant factor for actinides is the increased importance of the relativistic effects, mainly shown in the increase of the spin-orbit coupling (which is usually twice that of the lanthanides), which combined with a decrease in the Coulomb interelectronic repulsion, leads to a severe

breakdown of the Russell-Saunders coupling. These main factors together with other effects due to the complexity of the atomic systems under discussion lead to clear characteristics of the actinides, as follows:

(a) A great variety of valence states. Whereas with lanthanides the usual valence state in compounds +3 and sometimes also +2 and/or +4, with actinides the whole series of ions, from +2 to +6 (or even +7) is often found;

(b) The most stable valence state of the actinides is usually larger than for lanthanides, especially at the beginning of the group;

(c) The crystal field effects are about twice as strong as with the lanthanides;

(d) The extreme breakdown of the Russell-Saunders coupling makes it necessary to consider fully intermediate coupling in crystal field calculations.

These effects, shown especially with the lighter actinides, lead to the interesting situation that some of their properties are similar to those of the 3d elements rather than to the lanthanides. However, it would be incorrect to overemphasize this similarity, and the best way is to consider the actinides not only as f elements, but also to consider the whole electronic structure and the effective radii of the electronic shells. The stronger contraction of the 5f shell in the second half of the actinide group allows closer similarity with the lanthanides, but even here it is not perfect.

The great variety of valence states of the actinides makes it possible that the ions of a given element span a wide range of $5f^n$ configurations. For example, uranium ions span all the electronic configurations (from +6 to +2) at the beginning of the series, where the identity of the actinide group is chiefly manifested.

The very complex behavior of the actinides combined with, in many cases, a lack of spectroscopic data of free ions, makes it necessary to study their compounds by a multitude of physical methods. It is not the aim of this review to discuss fully the electronic properties of the actinides, but to show what results can be obtained by the use of electron paramagnetic resonance (EPR). This task is difficult since excellent reviews on the subject have been given by Abragam and Bleaney (1) and by Boatner and Abraham (2). However, some new results obtained since these reviews have been published, many of them by the present authors, makes it useful to present this review. A review of magnetic resonance studies on uranium compounds, related mainly to their use in nuclear energetics has recently been published (3).

EPR has been very effective in the study of uranium ions in crystals; the main results being as follows:

(a) Determination of the nuclear spin, the nuclear magnetic moment and electric quadrupole moment for the isotopes 233 and 235;

(b) Identification of the valence state of uranium ions in crystals;

(c) Identification of the symmetry and structure of different uranium centers in crystals;

(d) Identification of the ground state of uranium ions in crystals and of the influence of other electronic states on this. These results show the importance of the intermediate coupling in the case of actinides;

(e) Crystal field studies, emphasizing the role of covalency.

We hope that this review clearly shows these results and also indicates that the EPR studies of uranium ions in crystals have further potential.

II. URANIUM IONS IN CRYSTALS

A. Electronic Structure of Uranium and its Ions

1. General Properties

Uranium was discovered in 1789 by M. H. Klaproth in pitchblende. In 1841 E. Peligot showed that the semimetallic substance separated by Klapworth was in fact the uranium dioxide. At the formulation of the periodic system of elements by D. Mendeleeff, uranium was the heaviest known element. In 1896 H. Becquerel discovered the radioactivity of uranium. This discovery gave a strong impetus to studies on uranium, and in 1939, when nuclear fission was discovered (Hahn and Strassman) uranium became one element of the greatest scientific and practical interest. This is because ^{235}U is the only natural nuclide which undergoes nuclear fission in a reaction with slow neutrons.

Uranium has fourteen isotopes, with mass numbers from 227 to 240. Only three of these, namely 234, 235, and 238 isotopes occur in nature with abundances of 0.006%, 0.71%, and 99.28% and with lifetimes for α-decay of 2.45×10^5 y, 7.1×10^8 y, and 4.51×10^9 y, respectively (4). For nuclear power, of great importance are the natural isotopes 235 and the synthetic isotope 233 (α-active, lifetime of 1.6×10^5

y) as fissile materials and the isotope 238 as a fertile material. The nuclei of the even isotopes have zero nuclear spin and magnetic moments, while the odd isotopes have half-integral values of the nuclear spin quantum number and non-zero nuclear magnetic moment.

The electronic structure of atomic uranium and its ions or compounds is still not completely clear. The optical spectra of neutral [U(I)], singly ionized [U^+ or U(II)], four-fold ionized [U^{4+} or U(V)], and five-fold ionized [U^{5+} or U(VI)] uranium are known, and there is no reported analysis on the free-ion spectra of the other ions. On the other hand, in the condensed state only the ions U^{6+} to U^{2+} have been stabilized.

The ionic radii of the different uranium ions are not very large (1.03 Å for U^{3+}, 0.93 Å for U^{4+}, 0.88 Å for U^{5+}, and 0.82 Å to 0.73 Å for U^{6+} (5), and they can easily substitute in crystals the alkali or alkaline-earth ions as well as other diamagnetic cations such as La^{3+}, Y^{3+}, or Th^{4+}. Uranium ions can substitute for cations of a much lower valence in crystals; the electric charge difference being compensated by different means such as substitutional anions of higher valence, interstitial anions, cationic vacancies, substitutional cations of lower valency and so on. Thus a great variety of uranium centers in diamagnetic crystals can be obtained and detailed information on the electronic structure of the uranium ions can by inferred from these studies. However, much care must be exercised because the covalency in crystals may severely alter the properties of the ions in crystals as compared with the free ions.

The electronic structure of uranium has been the subject of a long debate. Though as early as 1923, Bohr (6) suggested that the filling of the 5f shell must begin around the element 91, early arguments in favor of uranium as a 6d element have been raised (7). This controversy lasted almost two decades until firm data on chemical properties of the uranium compounds, emission spectroscopy, optical absorption spectra in solutions and crystals, crystallographic, and magnetic studies have clearly established some of the main electronic properties of uranium and its compounds. The findings have subsequently been confirmed or completed by refined physical methods such as neutron diffraction, photoelectronic emission spectroscopy, and EPR.

2. Brief Theoretical Account

A theoretical study of the atomic structure of uranium is a very difficult task due to the inherent complications which arise in the study of large quantum systems (8-10). Many calculations have been performed in order to ascertain the electronic structure, spectroscopic parameters, and other parameters of interest such as the radial integrals for crystal field studies. Due to the complex interactions in such systems, the wave equation can be solved only approximately. We consider here a free atom without nuclear spin.

In a non-relativistic theory, the main terms in the Hamiltonian are the kinetic term $\sum_i p_i/2m$, the electron-nuclear electrostatic interaction $\sum_i -Ze^2/r_i$, the interelectronic repulsion $\sum_{ij} e^2/r_{ij}$, and the spin-orbit coupling $\sum_i \zeta_i l_i \bullet s_i$. The main part of this Hamiltonian is composed of the first three which are of an order of magnitude of 10^6 cm^{-1}. Because of the lack of spherical symmetry of the interelectronic repulsion, the wave equation for these three terms cannot be solved exactly. For this reason the interelectronic repulsion is divided into two parts: the spherical symmetric part (the most important) is introduced together with the first two terms in the zeroth-order Hamiltonian H_1 while the asymmetric part H_2 (of order 10^4-10^5 cm^{-1}) acts as a perturbation on the states of H_1. The wave equation with the Hamiltonian H_1 is solved by Hartree or Hartree-Fock methods (12), which lead to the transformation of the multielectronic equation in a sum of unielectronic equations with central potential.

In the Hartree method the total wavefunction of the system is a product of unielectronic wavefunctions, with the only restriction given by the Pauli principle. The central potential represents in this case the spherical potential created at the site of a given electron by the nucleus and the other electrons. This potential does not include the exchange effects, and there is no correlation between the states of the different electrons. In the Hartree-Fock method, the multielectronic wavefunction is a totally antisymmetric determinantal product of unielectronic wavefunctions which leads to an additional exchange term in the central potential. Because the exact calculation of the exchange potential by the Hartree-Fock method is very difficult, different approximations such as the Slater potential (13), the Kohn-Sham potential (14), the parametrized Slater potential (15), the X α-potential (16) have been used. The unielectronic energies depend only on the quantum numbers n and l, while the unielectronic wavefunctions depend on n, l, m_l, and m_s. The energy state characterized by the quantum numbers (n_i, l_i) specifies a $2(2l_i + 1)$ degenerate electronic shell. The solution of the

multielectronic equation is a series of energy states specified by a sequence of quantum numbers

$$(n_1 l_1)^{i_1} (n_2 l_2)^{i_2} \ldots (n_N l_N)^{i_N}$$

and called electronic configurations.

The nonspherical Hamiltonian potential H_2 acts usually as a perturbation on the central field wavefunctions within a given configuration. This approximation which neglects the configuration interaction may not be always correct, especially in case of the heavy atoms. When the interaction H_2 is much stronger than the spin-orbit coupling, it splits the electronic configurations in spectral terms characterized by the total orbital momentum L and total spin S quantum numbers (the so-called Russell-Saunders coupling). In the calculation of the effect of H_2 in a given electronic configuration (of equivalent or non-equivalent electrons) or in the calculation of the configuration mixing, two kinds of integrals (the electrostatic $F^{(k)}$ and exchange $G^{(k)}$) must be computed. For a configuration of equivalent electrons the effect of H_2 can be completely described by the electrostatic parameters $F^{(k)}$, with k = 0,2,4, and 6.

The spin-orbit coupling of uranium is about 2×10^3 cm^{-1}. This interaction couples the spin and the orbital angular momentum, and in the Russell-Saunders treatment L and S are coupled to give a total angular momentum J. This causes splitting of each spectral term into a number of energy levels characterized by the quantum number J which has values between |L-S| and L+S. This splitting can be expressed with the spin-orbit radial integral ζ_{nl}. A level is (2J+1) degenerate, each state being characterized by the quantum numbers (n l L S J M_J). When the spin-orbit interaction is very strong, it can couple different spectral terms. This leads to a breakdown of the Russell-Saunders coupling, and the only "good" quantum number is the total angular momentum J. The wavefunction for each level contains admixtures from different L and S states but of the same J. This situation is called intermediate coupling and each level is labeled, besides the "good" quantum number J, by the L and S of the main component of the wavefunctions. The extreme situation when the spin-orbit coupling is stronger than the interaction H_2, leads to a coupling of the individual spin and orbital momentum to give the total angular momentum j of each electron, then these are coupled to give the total momentum J of the atom. This coupling (j-j coupling) is a good approximation only for some particular levels in heavy atoms and does not describe well a general situation even for the heaviest element known.

For heavy atoms, where the product $Z\alpha$ approaches unity (α being the fine structure constant), the relativistic effects become very important. These can be taken into account with different degrees of approximation. The simplest is to consider the intermediate coupling, due to strong spin-orbit interaction and a reduced H_2 interaction, both of these being relativistic effects. Another approximation is to use a non-relativistic theory and apply correction factors obtained by comparing the relativistic and non-relativistic calculations on simple systems.

However, many cases exist when a rigorous relativistic theory is necessary. In this case the unielectronic interactions are replaced by the Dirac Hamiltonian and the interelectronic term is corrected with the Breit interaction (17) which is treated as a first-order perturbation. The wave equation is solved in the same manner as in the non-relativistic case. Many variants exist, depending on how the exchange potential is taken into account. Thus almost all the variants found in the non-relativistic treatment have been adapted for relativistic calculations, and we have the relativistic Hartree (RH) method (18), the relativistic Hartree-Fock, or the Dirac-Fock method (DF) (19,20), the relativistic Hartree-Fock-Slater or Dirac-Slater method (D-S) (21) and so on (22). Since the Dirac Hamiltonian contains the spin-orbit coupling, the unielectronic wavefunctions are the eigenfunctions of the total angular momentum j = l + s. The unielectronic states are labeled by the quantum numbers nlj, the number l being retained in order to show the parity of states and the value of l to which a state of given j is reduced in the non-relativistic limit.

The atomic wavefunction is an antisymmetric product of unielectronic wavefunctions and is an eigenfunction of the total atomic angular momentum j. This leads to a j-j coupling. However, because this coupling is never achieved and usually it is necessary to use the intermediate coupling, the mixing of different configurations must be taken into account [mixed configuration Dirac-Fock-MDF-method (23)].

A comparison of the few existing methods, shows that the relativistic parameters rather than the non-relativistic ones approach more closely the experimental ones. The need for intermediate coupling is emphasized by the relativistic calculations (especially by the theories which include the exchange), which show a decrease in the electrostatic Slater parameters $F^{(k)}$, especially for the heavy ions. Atomic

Table 1. The Electronic Radial Parameters ζ_{5f}, $\langle r^2 \rangle$, $\langle r^4 \rangle$, and $\langle r^6 \rangle$ for the Free Uranium Atom and Ions

Ion	Configuration	ζ, cm^{-1}		$\langle r^2 \rangle$, a.u.				$\langle r^4 \rangle$, a.u.				$\langle r^6 \rangle$, a.u.			
		DS[b]	DF[c]	HFS[a]	DS	DF	MDF[d]	HFS	DS	DF	MDF	HFS	DS	DF	MDF
U	$5f^3 6d\ 7s^2$	1503	1503		3.091				28.43				773.8		
U^+	$5f^3 7s^2$	1905			2.769				18.05				253.6		
U^{2+}	$5f^4$	1725	1391		3.278				27.19				472.6		
U^{3+}	$5f^3$	1977	1632	1.86	2.541	2.359	2.346	6.47	13.50	11.48	10.906	39.1	133.3	92.47	90.544
U^{4+}	$5f^2$	2212	1846	1.68	2.156	2.044	2.042	5.00	8.79	7.66	7.632	24.4	61.64	48.056	47.774
U^{5+}	$5f^1$	2442	2051		1.905	1.833	1.833		6.45	5.84	5.838		35.64	29.81	29.793

a) Parametrized Hartree-Fock-Slater values (24). b) Dirac-Slater values (25). c) Dirac-Fock values (25). d) Mixed configuration Dirac-Fock values (26).

parameters of neutral uranium and its ions, computed by non-relativistic parameterized Hartree-Fock-Slater (24), Dirac-Slater and Dirac-Fock (25), and mixed configuration Dirac-Fock (26) methods are given in Table 1.

The radial parameters $<r^i>$ in the relativistic calculations are defined as

$$<r^i> = \int_0^\infty [P^2(r) + Q^2(r)]r^i dr,$$

where P(r) and Q(r) are respectively, the large and small components of the one-electron radial wavefunctions (22). The relativistic values in Table 1 represent the weighted average of the values calculated for the relativistic $5f_{7/2}$ and $5f_{5/2}$ configurations: $<r^i> = (6/14)<r^i>_{5/2} + (8/14)<r^i>_{7/2}$.

Free-ion spectroscopic data are available only on the neutral uranium, U^{4+} and U^{5+}. For all the other uranium ions, the free-ion data have been deduced from studies on ions in crystals. However, the free-ion data deduced from the spectroscopic studies on uranium ions in crystals depend on the system under study. Two major effects are responsible for this. First, some atomic parameters are modified due to the fact that the ion is in a crystal. Thus the electron delocalization produces an orbital reduction which in turn modifies the spin-orbit coupling to a degree which differs for each particular system. Secondly, the interaction with the neighboring charges in a crystal produces considerable splitting and mixing of states and may even alter the relative energies of the levels. Due to these effects, systematic data obtained by a multitude of methods on a given ion in different crystals are necessary in order to deduce reliable "free-ion" values.

3. Spectroscopic Studies

3a. Neutral Uranium

The uranium atom has an extremely rich emission spectrum with about 100,000 identified lines (27,28). More than 1,000 energy levels have already been identified. New techniques such as multistep laser photoionization spectroscopy (29-31) and dye laser fluorescence spectroscopy (32, 33) allowed the identification of new high energy levels, including Rydberg states. In 1946 the ground state of uranium was identified as $(Rn)5f^3 6d^1 7s^2$ with the lowest level $^5L_6$ (34, 35). The uranium spectrum has been identified as an analogue of the element neodymium from the lanthanide group. We must note, however, that the ground configuration of neutral neodymium is $(Xe)4f^4 6s^2$ with the lowest level $^5I_4$ (10, 36). This difference shows the effect of the competition between the 5f and 6d orbitals in determining the electronic properties of the actinides. Subsequent studies (37-39) have confirmed this identification for uranium. The theoretical treatment shows that the energy levels of a given configuration of uranium encompass a very broad energy spectrum and some levels of the ground configuration go beyond the ionization limit (6.1941 eV) (31). The labeling of the energy levels is very difficult because often none of the couplings (Russell-Saunders or j-j) allow for an intermediate coupling wavefunction with a dominant component, weighted at more than 30% (27). The lowest levels of the excited configurations are very close to the lowest level of the ground state, and a strong configuration mixing takes place. The theoretical parameters differ according to the method used, e.g. the spin-orbit parameter ζ_{5f} is 2480 cm^{-1} (H-F-S) (40), 1856 cm^{-1} (D-S) (25, 40), 1503 cm^{-1} (D-F) (25), or 1717 cm^{-1} (D-S with an exchange scaling factor $\alpha = 0.7$ (40)) as compared with the experimental values of 1773 cm^{-1} (41) or 1754 cm^{-1} (39). The theoretical value for ζ_{6d} is 1848 cm^{-1} (H-F-S), 1475 cm^{-1} (D-S), or 1363 cm^{-1} (α-D-S) (40).

3b. Single-ionized Uranium

The emission spectrum is again very complex (27,28). More than 3,000 lines have been identified so far. A very strong competition between the 5f, 6d, and 7s orbitals in determining the electronic properties of this ion is observed. The ground configuration is $5f^3 7s^2$ with the nearest excited configurations $5f^3 6d7s$, $5f^3 6d^2$, and $5f^4 7s$. The theoretical (D-S) value for the ζ_{5f} constant is 1905 cm^{-1} for the ground configuration and 1682 cm^{-1} for the configuration $5f^4 7s$ (25).

3c. Divalent Uranium

No analysis of the free-ion spectra of this ion have been reported. Estimations of the theoretical structure are contradictory. The ground configuration for U^{2+} is given as $5f^3 6d$ with the ground state $^5L_6$ (27) while elsewhere (42) the $5f^3 7s$ configuration is the ground state, with $5f^3 6d$ and $5f^4$ at about 700 cm^{-1}. Considering the approximations used in these estimations (e.g. the estimated (42) ground state for U^+ is $5f^3 6d7s$ with an error of 500 cm^{-1}, while the experimental data clearly show that it is $5f^3 7s^2$), it is not possible to reach a correct

conclusion without clear experimental evidence. In a systematic study of the optical spectra of uranium ions in fluorite, Hargreaves (43, 44) claims to have found a spectrum with an EPR signal from a non-Kramers ion, with $g_{\parallel} = 3.28$ and $g_{\perp} < 0.1$. Though initiallly the ground configuration was identified as $5f^3\,6d$ with the lowest level $^5L_6$ (43), a subsequent analysis (44) replaced this with $5f^3\,7s$ with the ground level $^5I_4$. On the other hand the actinide Np^{3+} (45-47) and Pu^{3+} (48) in condensed media, and the lanthanide ion Nd^{2+} (49) and Pm^{3+} (50) have the ground configuration $5f^4$ and $4f^4$, respectively, with the lowest level $^5I_4$. It is likely that for U^{2+} the ground configuration is $5f^4$. Situations in which the 5f shell becomes lower than 6d when passing from neutral atom to ions are known (for instance the ground configuration is $6d^2\,7s^2$ for neutral thorium, 5f6d for Th^{2+} and 5f for Th^{3+} (51-54).

The calculated spin-orbit parameter for the $5f^4$ configuration of U^{2+} is 1725 cm^{-1} (D-S) or 1391 cm^{-1} (D-F) (25).

3d. Trivalent Uranium

The only data on this ion come from optical spectra in crystals and solutions. The absorption study of U^{3+} in $LaCl_3$ has demonstrated that the ground state of this ion is $5f^3$ with a ground level $^4I_{9/2}$ (45) in agreement with an estimate (42). The optical spectra (45) allowed an estimation of the spectral parameters and of the spin-orbit coupling $\zeta_{5f} = 1666$ cm^{-1}. However, this value is affected by the orbital reduction and is not a good estimate of the "free-ion" spin-orbit parameter. The calculations gave for this parameter the values of 1977 cm^{-1} (D-S) or 1632 cm^{-1} (D-F) (25). By comparing the values of the calculated spin-orbit parameters with the experimental values it was concluded (25) that the D-S values are closer to the experimental data and the agreement is quite good. With a numerical correction, the estimated value of the spin-orbit parameter for U^{3+} is 1787 cm^{-1}. The states of U^{3+} reflect the intermediate coupling. The ground level $^4I_{9/2}$ contains 83% ^4I and 15% ^2H. The first excited level at 4278.4 cm^{-1} has 95 % $^4I_{11/2}$, then at 7377.7 cm^{-1} a $^4F_{3/2}$ level has 46% ^4F and 25% ^2D. The next levels are at 7948.8 cm^{-1} with 92% $^4I_{13/2}$, at 9490.9 cm^{-1} a level with J =9/2 and 38% ^2H, 33% ^2G, 12% ^4I, 11% ^4F and so on. The first excited configuration $5f^2\,6d$ is not far from the ground configuration (27.1×10^3 cm^{-1} (42)) and shows itself as a group of broad absorption bands in the visible part of the absorption spectra of U^{3+} in crystals. The system $CaF_2:U^{3+}$ was the second crystal to lase (55-57, 44), although the structure of the active centers and the details of the spectra are still not completely elucidated.

3e. Tetravalent Uranium

The optical spectra of U^{4+} in crystals (43, 44, 58-60) established that the ground configuration is $5f^2$. The ground level is $^3H_4$ with 89% ^3H and 10% ^1G, the level at 3500 cm^{-1} has J = 2 with 92% ^3F and 7% ^1D, the level $^3H_5$ at 5981 cm^{-1} and $^3F_3$ at 7033 cm^{-1} have pure LS composition, while the next level, at 7748.8 cm^{-1} with J = 4 has 47% ^3F and 44% ^1G. The spectral parameters depend on the particular system under study. For instance ζ_{5f} is 1870 cm^{-1} for $CaF_2:U^{4+}$, 1780 cm^{-1} for $ZrSiO_4:U^{4+}$, and 1800 cm^{-1} for U^{4+} in Cs_2UCl_6. The theoretical values for ζ_{5f} are 2212 cm^{-1} (D-S) and 1846 cm^{-1} (D-F) (25), from which the free-ion value of 1982 cm^{-1} is estimated.

The recently reported optical spectra of the free ion (61,62) are in good agreement with these results: the ground level has J = 4 with 89.3% ^3H and 9.8% ^1G and the first excited level is at 4160.6 cm^{-1} and has J = 2 with 86.3% ^3F and 12.95% ^1D; the levels $^5H_5$ at 6136.9 cm^{-1} and $^3F_3$ at 8983.5 cm^{-1} have indeed pure Russell-Saunders composition. The measured spin-orbit coupling parameter for the free ion is 1968 ± 2 cm^{-1}, sensibly larger than that measured from optical spectra of U^{4+} in crystals.

3f. Pentavalent Uranium

The optical spectra of the free ion U^{5+} (63) confirmed the ground configuration to be $5f^1$, determined previously from optical spectra in crystals. The two levels of this configuration, $^2F_{5/2}$ (ground level) and $^2F_{7/2}$ are separated by 7608.6 cm^{-1}, which gives the spin-orbit parameter $\zeta_{5f} = 2173.9$ cm^{-1}. The calculated values for ζ_{5f} are 2442 cm^{-1} (D-S) or 2051 cm^{-1} (D-F) from which a value of 2172 cm^{-1} was estimated (25), in excellent agreement with the experimental data. The excited configurations lie very high (over 100,000 cm^{-1}) and have no noticeable influence on the ground configuration.

3g. Hexavalent Uranium

This ion has the closed electronic configuration of the inert gas radon. The ion U^{6+} is very stable in compounds and can form strong

covalent bonds with its neighbors in a crystal. Strong optical transitions have been found between the molecular orbitals of these bonds. Particularly strong are the bonds with oxygen with which uranium can form stable groups like the linear uranyl group UO_2^{2+} or the uranate (octahedral or tetrahedral) group, in which the uranium ion is equally or almost equally bonded to six or four oxygens.

The ground state of an octahedral U^{6+} complex is a singlet A_{1g} which characterize a molecular electronic configuration composed of four γ_8 relativistic unielectronic orbitals with a majority 2p ligand character (64-69). The excited unielectronic molecular orbitals are non-bonding and have mainly uranium character: the first five states are γ_7', γ_8', γ_7'', γ_8'', and γ_6' (with over 95% uranium character), then states which originate mainly from 6d levels of uranium (over 87%), and after that levels with 7s uranium character (over 75%). The first excited molecular electronic configuration of the complex is $(\gamma_8)^3\gamma_7'$, which has three energy levels, E, T_1, and T_2. Thus, a charge transition of an electron from the ground $(\gamma_8)^4$ configuration to the first excited configuration $(\gamma_8)^3\gamma_7'$ under the action of an electromagnetic field (such as light) is accompanied by three optical absorption lines, from the ground level A_{1g} to these three levels. Usually these transitions are in the visible range of the spectrum and their intensity is governed by suitable selection rules.

An axial distortion of the octahedral complex splits the molecular states. Two major cases can be encountered:

(i) weak distortion (weaker than the interelectronic Coulombic interaction) which splits the excited levels (T_1 A_2 + E, T_2 B_2 + E, E A_1 + B_1) but not the ground state;

(ii) strong distortion (stronger than the interelectronic interaction) which splits the unielectronic γ_8 levels in doublets $\gamma_6 = \gamma_7$. The ground configuration is now $(\gamma_7)^2$ and has a single electronic level A_{1g}, and the first electronic configuration is $\gamma_7\gamma_7'$ and has three levels, A_1, A_2, and E.

As can be seen, the picture of the electronic levels and of the corresponding optical transitions differ for the two cases. A careful analysis of the optical spectra, taking into account the additional information which can be obtained from such measurements as Zeeman effect or magnetic circular dichroism, could lead to an unambiguous assignment of the levels, and thus of the strength of distortion.

The U^{6+} complexes have a very large electron affinity (6 to 8 eV). The electron is trapped on the lowest excited electronic level which originates from the γ_7' unielectronic state. Since this state is almost a pure uranium 5f state, the trapping of the electron practically transforms the U^{6+} ion into U^{5+} which is paramagnetic and can be studied by EPR. The electron charge is almost the same in both cases (67), and this situation is expected for uranates too. Thus the trapping of the electron in the antibonding γ_7'(5f) orbital does not modify the symmetry of the complex and does not alter significantly the unielectronic orbitals.

A similar situation holds for the uranyl complexes.

B. Uranium Ions in Crystals

1. General Account

If the ions are introduced in crystals (substitutionally or interstitially), an additional interaction with their neighbors takes place. The source of this interaction is the so-called crystal field which has a definite symmetry, closely connected to the symmetry of the crystalline environment around the ion in question, the electric charges of the neighbors, and their nature and the presence of some point defects. The magnitude of the crystal field interaction depends on the electric charges of the ion and of its neighbors, the nature of the ion and the symmetry of the crystal field, the dipole and quadrupole polarization of the ion, the modifications of the effect of the ligand charge due to its finite charge distribution (charge penetration and exchange penetration), overlap and exchange, covalence (charge transfer) effects, the ligand-ligand exchange charge, and triangular path contributions (70).

The crystal field interaction affects the electronic structure of the open-shell ions. The main effects of the crystal field are modification of the free-ion spectroscopic parameters (the Slater $F^{(k)}$ parameters (71), the spin-orbit parameter) and a splitting ($\sim 10^3$ cm^{-1} in case of the actinides) of the energy states of the free ion. An exact treatment of the crystal field interaction is very difficult. Usually, approximate methods are used that take into account the relative intensities of the crystal field interaction H_c, the nonspherical interelectronic interaction H_2 and the spin-orbit coupling. Three main cases are observed:

(a) Weak crystal field, when the H_c is weaker than $H_{s\text{-}o}$. This implies calculation of matrix elements of H_c between functions of type $|n\ l\ s\ L\ J\ M_j>$ (pure or as parts of the intermediate-coupling wavefunctions).

The crystal field interaction leads to a partial or even to a total removal of the degeneracies of the energy levels. For the ions with odd numbers of electrons a residual degeneracy of minimum two is always left (the Kramers theorem). The J quantum number is often used to label the levels, though the mixing of the J levels through the crystal field combined with the intermediate-coupling effects can lead to crystal field states containing considerable admixture from many energy levels. This situation is characteristic for U^{3+} and U^{4+} in crystals.

(b) Intermediate crystal field, when H_c is stronger than H_{s-o}, but weaker than H_2. The matrix elements of H_c are calculated with the states $|n\ l\ S\ L\ M_S\ M_L>$ inside a given LS term. The crystal field leads to a partial removal of the M_L degeneracy. This situation is characteristic for U^{5+} in crystal fields of octahedral symmetry.

(c) Strong crystal field effects when H_c is of the same order of magnitude or stronger than H_2.

2. Symmetry Considerations

The study of the crystal field effects can be substantially simplified by using group theory (72). In a free ion the $(2J+1)$ wavefunctions characterized by M_z form the basis for the irreducible representation D^J of the three-dimensional rotation group R_3. The symmetry of the crystal field corresponds to one of the 32 crystallographic point groups which are subgroups of R_3. As a consequence, under the action of a weak crystal field, the irreducible representation D^J of the rotation group is reduced according to the irreducible representations Γ_i of the crystal field point group. Physically, this corresponds to a splitting of the $(2J+1)$ degenerate J level into a number of components, each component being labeled by an irreducible representation of the point group and having a residual degeneracy equal to the dimension of the representation. In the intermediate field case, the same arguments are valid for the $(2L+1)$-dimensional representation D^L of the rotation group.

When the angular momentum quantum number is integer, the groups involved are the simple point groups. For instance, in a cubic field, the representation D^L is reduced according to the irreducible representations $\Gamma_1, \Gamma_2, \Gamma_3, \Gamma_4$, and Γ_5 (of dimensions 1, 1, 2, 3, and 3) of the group O_h.

If J is half-integer, the reduction of D^J is done according to the irreducible representations of the double point groups. The cubic double point group has eight representations, the first five being the same as for the simple group, and threee new representations, Γ_6, Γ_7, and Γ_8 of dimensions 2, 2, and 4, respectively.

Group theory shows only how a given spectral term or energy level is split in a crystal field of a known symmetry (the number of components and their degeneracy) but cannot give any information concerning the ordering of the levels and the splittings. This can be obtained only by an actual calculation of the crystal field effect on the free ion states.

3. The Fictitious Angular Momentum

In the reduction of D^J in a cubic field, for some values of J the representation D^J of the rotation group is reduced to only one representation Γ of the cubic group. This suggests the possibility of classifying the basis functions of these representations Γ as the eigenfunctions of a fictitious angular momentum J. Thus the reduction $D^1 \rightarrow \Gamma_4$ shows that the three basis functions of the representation Γ_4 (regardless of the value of J) can be identified as the eigenfunctions of a fictitious J with $J = 1$. The three functions $|\pm 1>$, $|0>$ of a fictitious J with $J = 1$, can be taken also as basis functions for the representation Γ_5. The reduction $D^{1/2} \rightarrow \Gamma_6$ shows that the basis functions of the Γ_6 doublet can be considered as the eigenfunctions of a fictitious angular momentum with $J = 1/2$. and this can also be demonstrated for Γ_7. Finally, the reduction $D^{3/2} \rightarrow \Gamma_8$ shows that the states of the quartet correspond to the projections of a fictitious angular momentum $J = 3/2$ (even for J larger than 3/2).

4. The Crystal Field Potential

To evaluate the crystal field splittings and the ordering of the levels, one must know the form of the Hamiltonian H_c. Since this interaction must reflect the symmetry of the crystal field, we can anticipate that the Hamiltonian H_c will be a combination of operators acting on the free-ion states and that the coefficients multiplying these operators and reflecting the strength of the interaction must be determined by experiment. However, it is important to have a theoretical model of the crystal field parameters. As shown above, many mechanisms can contribute to the crystal field interaction, and a theoretical consideration of all these interactions is a difficult task. Thus, simplified models are used which take into account only one or a few interactions

which are supposed to give an essential contribution to the crystal field potential.

In the electrostatic crystal field model, the crystal field interaction is determined only by the electrostatic interaction of the ion with its neighbors in a crystal (73). The electric charges of these neighbors are considered as point charges localized at the lattice sites. In the electrostatic approximation, the crystal field potential $V(r_i,\Theta_i,\Phi_i)$ acting on the electron (r_i,Θ_i,Φ_i) of the ion satisfies the Laplace equation $V(r_i,\Theta_i,\Phi_i) = 0$, i.e. there is no interpenetration of the electron charge and of its neighbors. As a first approximation, only the nearest neighbors of the ion in the crystal are taken into account. If we expand in spherical harmonics , the electrostatic potential of the crystal field interaction can be written as

$$H_c = \Sigma\, a_k^q r_i^k Y_k^q(\Theta_i,\Phi_i). \qquad (1)$$

In tesseral harmonics, an expression in Cartesian coordinates can be obtained

$$H_c = \Sigma\, A_k^q P_k^q(x_i,y_i,z_i). \qquad (2)$$

Some restrictions on the expressions of equations 1 and 2 must be imposed. Thus, the definition of the spherical harmonics $Y_k^q = (-1)^q Y_k^{-q}$ imposes that $a_k^{q*} = (-1)^q a_k^{-q}$. Also, the triangular rule $k \leq 2l$ for electrons in an (nl) shell must hold. When the crystal field has inversion, the odd k spherical harmonics have vanishing matrix elements inside a given (nl) state, so they can be omitted from H_c. Inside a given k, the number of components q is limited by the crystal field symmetry, provided a suitable choice of the reference frame is made. The term $k = 0$ is usually omitted since it gives an equal shift of all the lines in a given (nl) configuration.

The crystal field calculations for a multielectronic ion can be simplified by using the Wigner-Eckart theorem which allows the replacement of the unielectronic operators in equations 1 and 2 by operators acting directly on the eigenfunctions of the free ion. Thus, the Hamiltonian in equation 1 can be written as a combination of tensor operators U_k^q (53) having the same transformation properties as the spherical harmonics,

$$H_c = \Sigma\, B_k^q U_k^q. \qquad (3)$$

If the Hamiltonian has the form of equation 2, the functions P_k^q can be replaced by the so-called equivalent operators O_k^q (74), with the same transformation properties and with matrix elements inside a given J proportional to those of P_k^q:

$$\langle JM_J|\Sigma_i\, p_k^q(r_i)|JM_J\rangle =$$

$$\Theta_k\langle r^k\rangle\langle JM_J|O_k^q(j)|JM_J\rangle$$

where Θ_k are the proportionality factors labeled usually $\Theta_2 = \alpha_J, \Theta_4 = \beta_J, \Theta_6 = \gamma_J$, their value depending on the particular J level and $\langle r^k\rangle$ are the radial integrals $\int R_{nl}^* r^k R_{nl} dr$. The equivalent operators can be obtained by replacing the Cartesian coordinates in p_k^q by the corresponding components of the angular momentum, by taking into account the commutation rules.

While the method of the equivalent operators is valid only inside a given J (or L), the tensorial operator method is more general. Tables with matrix elements of the tensorial operators are available (75).

5. Crystal Field Models

The coefficients A_k^q and B_k^q are estimated from a model of the crystal field. The electrostatic field models give the Hamiltonians of equations 1 or 2. However, a comparison of the theory with experiment shows that even if the parametrization in the Hamiltonians of equations 1 or 2 is correct, there is very poor agreement between the theoretical and experimental crystal field parameters. The equations 1 or 2 are far more general than their derivation in the nearest neighbor electrostatic approximation. Improvements to the calculated crystal field parameters were made by performing lattice sums, by introducting the overlap, exchange and covalency (charge transfer), and other effects. The configuration interaction effect is also included by calculating the shielding of the crystal field interaction of the inner electronic configuration, by the outer closed electronic shells (e.g. the shielding of the crystal field interaction of the 5f electrons by the closed $6s^2 6p^6$ shells). This leads to a decrease of the crystal field parameters expressed in terms of a shielding factor σ_k such as

$$A_k^q\langle r^k\rangle_{sh} =$$

$$(1 - \sigma_k)A_k^q\langle r^k\rangle_{\text{point charge}}. \qquad (4)$$

The calculated values of σ_2, σ_4, and σ_6 are 0.83, 0.026, and -0.039 for U^{3+}, and 0.88, 0.012, and -0.046 for U^{4+}, respectively (76).

An improvement in the crystal field potential has been introduced by the superposition model (70, 77). This model assumes that the total

crystal field can by considered as a superposition of individual contributions from each of the ions in the crystal. These individual crystal fields have cylindrical symmetry and, with the z-axis along this individual symmetry axis, the interaction potential can be described, for f-electrons, by only three "intrinsic" parameters, $\bar{A}_2^0$, $\bar{A}_4^0$, and $\bar{A}_6^0$, which depend on the distance R_i between the central ion and the ion which produces the individual field. The total crystal field parameters are then

$$A_k^q \langle r^k \rangle = n_{kq}(i)\bar{A}_k(R_i) \qquad (5)$$

where $n_{kq}(i)$ are factors that depend on the angular position of the ions, which are the source of the crystal field. This method has considerable advantages over the traditional method in carrying out crystal field potential calculations.

6. An Example: The Cubic Field

As an example, we consider the case of an ion with an f electron in a crystal field of cubic symmetry. For a weak crystal field, when there is no J mixing, we can use equation 2 of the crystal field Hamiltonian, which in this particular symmetry becomes (if the reference frame is parallel to the cube edges)

$$H_C = A_4(P_4^0 + 5P_4^4) + A_6(P_6^0 - 21P_6^4)$$
$$= A_4 P_4 + A_6 P_6. \qquad (6)$$

If we introduce the equivalent operators defined above, this becomes

$$H_C = A_4 \langle r^4 \rangle \beta_J O_4(J) + A_6 \langle r^6 \rangle \gamma_J O_6(J)$$
$$= B_4 O_4(J) + B_6 O_6(J) \qquad (7)$$

where

$$O_4(J) = O_4^0(J) + 5O_4^4(J),$$

$$O_6(J) = O_6^0(J) - 21O_6^4(J).$$

In a nearest neighbor electrostatic crystal field approximation, the coefficents A_4 and A_6 are

(a) for eightfold cubic coordination

$$A_4 = -\frac{7}{18}\frac{Ze^2}{R^5} \quad A_6 = \frac{1}{9}\frac{Ze^2}{R^7}$$

(b) for octahedral coordination

$$A_4 = \frac{7}{16}\frac{Ze^2}{R^5}; \; A_6 = \frac{3}{64}\frac{Ze^2}{R^7},$$

where Z_e is the charge of the ligand and R the distance from the central ion to the ligands.

For the splitting of the energy levels in a weak cubic crystal field (78), the crystal field Hamiltonian, equation 7, has been transformed into

$$H_C = B_4 F(4) O_4 / F(4) + B_6 F(6) O_6 / F(6) \qquad (8)$$

where F(4) and F(6) are scaling factors given by

$$B_4 F(4) = Wx \text{ and}$$

$$B_6 F(6) = W(1 - |x|), \text{ with } -1 \le x \le 1 \qquad (9)$$

This Hamiltonian becomes

$$H_C = W[xO_4(J)/F(4) + (1-|x|)O_6(J)/F(6)] \; . \qquad (10)$$

The sign of W is determined by B_4, while that of x is given by B_6.

The diagnolization of the Hamiltonian of equation 10 for a given J multiplet for given values of x allows the determination of the energy eigenvalues of different crystal field levels as a function of the energy parameter W, which can be estimated from experiment. The eigenfunctions for each Γ_i state in terms of the magnetic quantum states $|M_J\rangle$ are also obtained. If a given representation enters in the reduction of D^J only, once its wavefunctions do not depend on the parameter x; then the plot of the energy level versus x is a straight line. For the representations that enter more than once in the reduction of D^J, the wavefunctions depend on x, i.e. on the ratio of the sixth- to the fourth-order components of the crystal field potential, and the plot of the energy level versus x is a curved line.

7. The Ground State of Uranium Ions in Weak Cubic Crystal Field

The ground states for the uranium ions are $5f^1\ ^2F_{5/2}$ for U^{5+}, $5f^2\ ^3H_4$ for U^{4+}, $5f^3\ ^4I_{9/2}$ for U^{3+}, and either $5f^3\ 6d^5L_6$, $5f^3\ 7s\ ^5I_4$ or $5f^4\ ^5I_4$ for U_2^{+}.

In the case of a weak cubic field, which does not produce J mixing, there are five cases as follows:

(a) The free ion $^2F_{5/2}$ level is split into $\Gamma_7 + \Gamma_8$. For octahedral symmetry, the ground state is the doublet Γ_7, while in eightfold cubic or tetrahedral symmetry Γ_8 is lowest. The excited level $^2F_{7/2}$ is split

into $\Gamma_6 + \Gamma_7 + \Gamma_8$.

(b) The level $^3H_4$ reduces to $\Gamma_1 + \Gamma_3 + \Gamma_4 + \Gamma_5$. In octahedral symmetry, the ground state is the singlet Γ_1, while in eightfold cubic or in tetrahedral symmetry, the ground state can be Γ_1 (for $x < 10/19$) or the triplet Γ_5 (for $x > 10/19$).

(c) The level $^4I_{9/2}$ is split by a cubic field into $\Gamma_6 + 2\Gamma_8$. In octahedral symmetry the ground state can by Γ_6 or one of the Γ_8 representations, while in eightfold cubic and in tetrahedral field, the ground state is Γ_8.

(d) The level $^5I_4$ (as well as $^3H_4$) reduces to $\Gamma_1 + \Gamma_3 + \Gamma_4 + \Gamma_5$. The ground state in the octahedral field can be Γ_1 or Γ_5 (depending on x), while in eightfold cubic or tetrahedral symmetry, the ground state is the singlet Γ_1.

(e) The level $^5L_6$ is split into $\Gamma_1 + \Gamma_2 + \Gamma_3 + \Gamma_4 + 2\Gamma_5$. In an octahedral field, the lowest state can be Γ_1 or Γ_2, while in eightfold cubic or in tetrahedral symmetry the ground state can be the singlet Γ_2 or the doublet Γ_3.

As can be seen, in the decomposition of some J levels in cubic crystal field, some representations show up more than once. The wavefunctions which form the basis for these representations depend in an intricate way on the composition parameter x of the crystal field potential. Usually this dependence is computed numerically and tables of wavefunctions calculated for a given increment of x are available (78). It is, however, a difficult and time consuming task to extract this parameter from experimental data which provide the matrix elements of some operators between such wavefunctions. In order to overcome these difficulties, an analytical method which gives explicit expressions for the wavefunctions appearing more than once in the cubic crystal field splitting of a given J level versus x has been recently reported (79, 80). This method is based on the complete use of the transformation properties of an electronic wavefunction in a cubic symmetry. For some values of J these analytical functions are particularly simple. For instance (79), in case of a J = 9/2 level, which in a cubic crystal field is split according to the rule $D^{(9/2)} \rightarrow 2\Gamma_8 + \Gamma_6$, the wavefunctions of one of the Γ_8 representations (which are isomorphous to a fictitious angular momentum J = 3/2) can be written as functions of the magnetic quantum components $|M_J>$ according to:

$$|\Gamma_8',\pm 3/2> = \pm(\sin\Theta|\pm 5/2> + \cos\Theta|\pm 3/2>,$$

$$|\Gamma_8',\pm 1/2> = \pm[-(\sqrt{21}\cos\Theta + 3\sin\Theta)|\pm 9/2> +$$

$$(\sqrt{6}\cos\Theta + \sqrt{14}\sin\Theta)|\pm 1/2> +$$

$$(\sqrt{21}\cos\Theta - 5\sin\Theta)|\mp 7/2> \qquad (11a)$$

where the fictitious angle Θ is connected to the composition parameter

$$x' = \frac{B_6}{B_4} = \frac{\gamma A_6 <r^6>}{\beta A_4 <r^4>}$$

$$= \frac{F(4)}{F(6)} \frac{(1-|x|)}{x} \qquad (11b)$$

with the relation

$$\tan 2\Theta = \sqrt{\frac{3}{28}} \frac{5 + 336\,x'}{1 - 12x'} \qquad (11c)$$

The wavefunctions of the other Γ_8" representation have a similar form as for Γ_8' but with the replacement

$$\Theta(\Gamma_8") = \Theta(\Gamma_8') + \pi/2.$$

Suitable expressions for other J values can be written in a similar manner. The matrix elements calculated between such wavefunctions are explicit functions on the composition parameters; thus the experimental measurement of such matrix elements leads to an easy and direct determination of this parameter.

8. Lower Symmetries

For lower symmetries additional terms must be introduced in the crystal field Hamiltonian. Symmetry arguments can be used to deduce the form of the crystal field Hamiltonian.

The crystal field splits the J manifold into a number of states according to the reduction of D^J into the irreducible representations of the point group in question. If the crystal field potential is $\sum_{kq} B_k^q O_k^q$, the wavefunctions of the states inside a given J are mixtures of states of different M_J's which differ by multiples of q and can be written as $\sum_M C_{JM}|J,M>$ with $\sum_M C_{JM}^2 = 1$. Sometimes the crystal field can produce admixtures from states of different J's, and the wavefunctions are $\sum_M C_{JM}|J,M> + \sum_M C_{J',M}|J',M>$.

9. Intermediate Coupling

The problem of the crystal field splitting in the intermediate coupling becomes very complex (10, 76, 81, 82). This case is frequently

encountered for the actinides where the non-spherical interelectronic interaction H_2 is of the order 5×10^4 to 10^5 cm^{-1}, and the spin-orbit coupling is of order 2×10^3 to 4×10^3 cm^{-1}. A crystal field interaction of 10^3 cm^{-1} produces a considerable mixing of states of different J values. In fact, the crystal field interaction often approaches the spin-orbit coupling, and the only meaningful quantum numbers which can label the states are the irreducible representations of the crystal field symmetry group. This complex situation implies crystal field ground states strongly influenced by the mixing with the excited states, at least with those situated at several eV above it. Calculations for the electronic configurations $5f^2$ - $5f^6$ [considering the mixing from all the levels up to about 2 eV from the ground state in octahedral fields (81) and for the $5f^2$ configuration in octahedral and eightfold symmetry (76)] have shown a strong influence of the excited states on the crystal field splitting of the ground level. Thus, the plots for the energies of different crystal field states Γ_i versus the fourth-order cubic crystal field parameter $A_4\langle r^4\rangle$ (drawn for different ratios of the sixth- to the fourth-order component) have shown that even the representations which enter once in the reduction of D^J become curved lines, and important modifications in the crossing points of the different crystal field levels occur. This can change substantially the order of the crystal field levels as compared to the case of no mixing. Thus, for large B_6/B_4 values and for reasonable $A_4\langle r^4\rangle$ parameters, the ground state of a $5f^2$ ion in eightfold cubic symmetry can be Γ_1 instead of Γ_5.

10. The Relativistic Crystal Field

The use of the relativistic Hartree-Fock wavefunctions leads to an additional complication since for each (n l j) electron in a crystal field there are two radial integrals F and G (83). The relativistic crystal field radial integrals for the uranium ions have been calculated by various relativistic atomic methods (25, 26), and some of them are given in Table 1 together with the non-relativistic values (24). A fully relativistic crystal field calculation is rarely used. However, hybrid methods, using the classical formalism, but replacing the radial integrals by effective relativistic integrals are already in common use, as are, for instance, the integrals $\langle r^n\rangle$ for f-shells, obtained by a degeneracy-weighted average of the integrals calculated for the relativistic $f_{5/2}$ and $f_{7/2}$ shells.

11. The Intermediate Crystal Field

As mentioned earlier, the actinide contraction at the beginning of the series is smaller than in the case of the lanthanides. As a consequence, the radial charge distribution for the 5f electrons extends over those of the 6s and 6p electrons (at distances of 2 to 4 a.u. from the nucleus), unlike the lanthanides where the 4f electrons are well localized inside the 5s and 5p closed shells (84).

The larger extent of the 5f function at the beginning of the series implies an intermediate crystal field (85). Spectroscopic studies have shown that this is indeed the case for $5f^1$ in crystal fields of octahedral symmetry (1, 9, 85-95). The simultaneous diagonalization of the octahedral crystal field and spin-orbit interactions in the space spanned by the 14 functions $|lm_l sm_s\rangle$ with $l = 3$ and $s = 1/2$ is difficult so that the symmetry properties are used to simplify the problem. To begin with, we suppose that the crystal field interaction is stronger than the spin-orbit coupling.

An octahedral crystal field splits the sevenfold orbit degeneracy of the 5f level, giving a singlet (Γ_2 or a_2) and two triplets Γ_4 or t_1 and Γ_5 or t_2) of energies

$$E_{\Gamma_2} = -12b_4 - 48b_6$$

$$E_{\Gamma_5} = -2b_4 + 36b_6$$

$$E_{\Gamma_4} = 6b_4 - 20b_6$$

where $b_4 = (3/33)A_4\langle r^4\rangle$ and $b_6 = -(80/42)A_6\langle r^6\rangle$.

The order of the levels depends on the ratio b_6/b_4. For b_6/b_4 smaller than or equal to 5/42, the ground level is Γ_2. Over this limit Γ_5 becomes lowest. Usually the first case holds, and the order of the levels is $E_{\Gamma_2} < E_{\Gamma_5} < E_{\Gamma_4}$. The energy differences are usually labeled as[4] $V = E_{\Gamma_5} - E_{\Gamma_2}$ and $V' = E_{\Gamma_4} - E_{\Gamma_2}$ (75) or as $\Theta = E_{\Gamma_4} - E_{\Gamma_5}$ and $\Delta = E_{\Gamma_5} - E_{\Gamma_2}$ (77). Since the two spin eigenfunctions are the basis of the irreducible representation Γ_6 of the octahedral group, the 14 spin-orbit wavefunctions can be classified according to the products of representations $\Gamma_2\times\Gamma_6 \rightarrow \Gamma_7$, $\Gamma_5\times\Gamma_6 \rightarrow \Gamma_7 + \Gamma_8$ and $\Gamma_4\times\Gamma_6 \rightarrow \Gamma_8 + \Gamma_6$. Since the spin-orbit coupling is invariant under the octahedral group operators and commutes with J_z, it can be diagonalized inside each of the three representations Γ_6, Γ_7, and Γ_8. The energy matrices are

$$\Gamma_8 \begin{vmatrix} V + k_{t_2 t_2}\zeta & 3\sqrt{5}k_{t_1 t_2}\zeta/4 \\ 3\sqrt{5}k_{t_2 t_2}\zeta/4 & V' - k_{t_1 t_2}\zeta \end{vmatrix}$$

$$\Gamma_7 \begin{vmatrix} 0 & \sqrt{3}k_{a_2 t_2}\zeta \\ \sqrt{3}k_{a_2 t_2}\zeta & V' - k_{t_2 t_2}\zeta/2 \end{vmatrix}$$

$$\Gamma_6 \; | V' + 3k_{t_1 t_2}\zeta/2 | \qquad (12)$$

where k_{ij} are the orbital reduction factors (95) defined as

$$k_{ij} = \frac{\langle f^n \Gamma_i | U | f^n \Gamma_j \rangle}{\langle f \Gamma_i | U | f \Gamma_j \rangle}$$

where the functions of the denominator are the purely ionic wavefunctions of the representation Γ_k, and the functions used in the numerator are the molecular orbitals for the same representations. The orbital reduction can be substantial, so while $k_{a_2 t_2}$ is of the order 0.9 to 1, $k_{t_2 t_2}$ can sometimes be as small as 0.5 (95).

The ordering of the five energy levels which are the basis of equations 12 depends on the relative magnitudes of the spin-orbit coupling and crystal field interaction. Figure 1 shows schematically the splitting of a $5f^1$ configuration in an octahedral crystal field. Diagrams showing the effect of the relative magnitude of the crystal field effect and of the spin-orbit coupling on the relative positions of the crystal field levels for particular ratios of b_6/b_4 can be constructed [e.g. Figure 2.3 of (9)]. In an octahedral crystal field, the ground state is always a doublet which contains admixtures from the Γ_7 level (originating from the orbital Γ_2 singlet) and from the Γ_7 level (from Γ_5).

The wavefunctions of this doublet are

$$|+\rangle = \cos\Theta|\Gamma_7 +\rangle - \sin\Theta|\Gamma_7' +\rangle$$

$$|-\rangle = \cos\Theta|\Gamma_7 -\rangle - \sin\Theta|\Gamma_7' -\rangle \qquad (13)$$

where

$$\tan 2\Theta = 2\sqrt{3}k_{a_2 t_2}\zeta/(V - \tfrac{1}{2}k_{t_2 t_2}\zeta).$$

The first excited state can be Γ_7' or Γ_8, the crossover occurring (90) when $\zeta(4\Delta/\Theta + 15\Theta/4\Delta + 17/2) = \Theta + \Delta$.

If Θ is about twice the value of Δ, the crossover takes place at $\Delta \simeq 6\zeta$, i.e. at quite strong crystal fields.

An axial distortion splits the Γ_8 quartets, giving rise to new levels. Thus a tetragonal distortion splits the Γ_8 quartet into two doublets, Γ_6^t and Γ_7^t, their order being determined by the sign of the distortion. At the same time, the axial distortion will produce a displacment of the original doublets. However, the splitting $\Gamma_7' - \Gamma_7$ is little affected by the distortion. If the tetragonal distortion is of moderate intensity, the ground state remains Γ_7^o but will contain admixure from all four Γ_7^t states. If the axial distortion is strong, it may happen that Γ_6^t crosses the original Γ_7^o and becomes the ground state for the system (91). For a trigonal distortion, the Γ_8 levels are split into a doublet Γ_6^T and a pair of singlets Γ_4^T and Γ_5^T, and the doublets Γ_7 are transformed into doublets Γ_6^T. Thus, five Γ_6^T doublets will be mixed in order to obtain the wavefunction of the ground doublet. If the distortion is very strong and its sign is suitable, the pair of singlets $\Gamma_4^T + \Gamma_5^T$ become lowest in energy. Instead of considering first the interaction with the crystal field, we could start by considering initially the effect of the spin-orbit coupling and then diagonalize the crystal field interaction.

A tetrahedral or an eightfold cubic crystal field has very little effect on the free-ion states of a $5f^1$ ion even in the case when the crystal field parameters are large (90). In this case, the

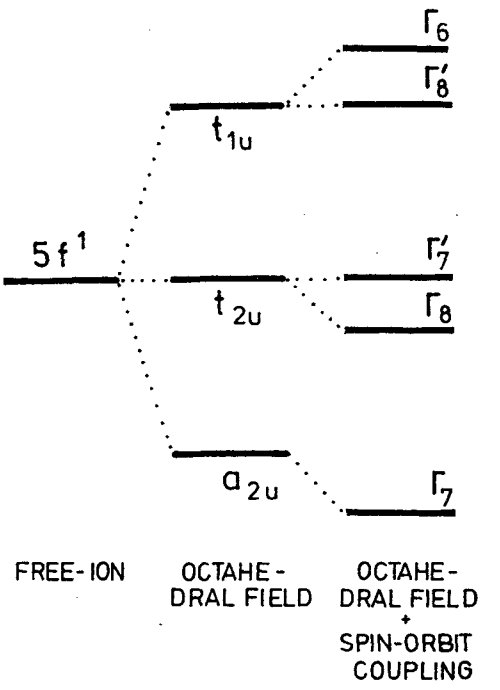

Figure 1. The splitting of the $5f^1$ configuration in a cubic octahedral crystal field (intermediate-field case).

treatment for the weak crystal field can be applied, regardless of the value of the crystal field parameters. The lowest electronic level $^2F_{5/2}$ of the free ion is split in a cubic field into a doublet Γ_6 and a quartet Γ_8. They are bunched together and the ratio between the crystal field strength and the spin-orbit parameters determines which of these two levels is lowest. In weak fields Γ_8 is lowest, but a crossing takes place in the intermediate field region when $\zeta(4\Delta/\Theta + 15\Theta/4\Delta - 17/2) = \Theta - \Delta$ where $\Delta = E_{a_1} - E_{t_1}$, $\Theta = E_{t_2} - E_{t_1}$, and the order of the levels in the strong field limit is $E_{a_1} > E_{t_2} > E_{t_1}$. For $\Delta \simeq 2\Theta$, the crossing point is at $\Theta = 11\zeta/8$. As in the case of the octahedral symmetry, a tetragonal distortion splits Γ_8 into the doublets $\Gamma_6{}^t$ and $\Gamma_7{}^t$, while a trigonal distortion splits Γ_8 into the doublet $\Gamma_6{}^T$ and a pair of singlets $\Gamma_4{}^T$ and $\Gamma_5{}^T$.

12. Determination of the "Free-ion" Parameters from Data in Crystals

The optical adsorption spectra of the paramagnetic ions in crystals for the weak crystal field consists of groups of lines centered around the positions of the free-ion lines. These groups correspond to transitions between the crystal-split levels. In principle, a correct consideration of the crystal field effects should allow the estimation of the free-ion spectroscopic parameters from crystal data. However, often the free-ion parameters are determined by using an average energy (or center of gravity) of the group of crystal-field components. Sometimes additional parameters, not discussed above, are introduced to take into account other interactions in the free ion, as for instance, the interactions between states from different configurations.

Thus, the effect on the energy levels of a f^n configuration from the interaction with levels of a $f^{n-2}l'l''$ configuration can be expressed with the Tress parameters α, β, and γ (96), while the effect of the levels from a $f^{n-1}l'$ configuration is described with the Judd parameters T^2, T^3, T^4, T^6, T^7, and T^8 (97). A complete analysis must also take into account weak interactions such as spin-spin or spin-other-orbit (98).

These "free-ion" values differ from the real free-ion parameters. One of the main reasons is that even these parameters are influenced by the crystalline environment (the orbit reduction and the reduction of the spectroscopic Slater parameters). For this reason, the calculated "free-ion" values differ from system to system, depending also on the method used and the levels chosen for the determination. However, it must be emphasized that the free-ion eigenstates determined with these parameters are the best starting wavefunctions in the calculation of the crystal field effects for the given system.

The accuracy of this method is strongly affected by the intermediate coupling, hence those levels must be chosen for the estimation of the "free-ion" values which show the closest approach to the Russell-Saunders coupling (44). An example of "free-ion" parameters estimated from the spectra of ions in crystals is the case of the trigonal U^{4+} center in calcium fluorite (44): where $F_0 = 13175$, $F_2 = 200$, $F_4 = 40$, $F_6 = 8.05$, $\zeta = 1660$, $\alpha = 26$ (in cm^{-1}), as compared with the data reported earlier (58) on the same system: $F_2 = 204.56$, $F_4 = 29.1$, $F_6 = 3.24$, $\zeta = 1870$ as compared with the values $F_2 = 230.84$, $F_4 = 35.22$, $F_6 = 3.77$, $\zeta = 1968$, $\alpha = 35.5$, $\beta = -664$, $\gamma = 744$, $p^2 = 573$, $p^4 = 524$, $p^6 = 1173$ obtained from free-ion spectra (62).

13. The Dynamic Crystal Field

The previous discussion has been based on the static approximation of the crystal field, characterized by fixed positions for the paramagnetic ion and its neighbors. In fact, they undergo vibrations with known frequencies. The electronic states of the ion can couple with the vibrational movement of its neighbors, and its electrons will be characterized by the vibronic states (99, 100). The vibronic states of a paramagnetic ion in a crystal have definite symmetry properties.

One of the main consequences of the vibronic coupling is the Jahn-Teller effect. Given initially for molecules (101), the Jahn-Teller theorem has been extended for ions in crystals (102-104). This theorem states (104) that "an orbitally degenerate state of a nonlinear molecule or crystalline defect is unstable and removes some of the degeneracy." The driving force of the Jahn-Teller instability is the vibronic coupling (103). In the case of very strong coupling, the complex may exhibit a static Jahn-Teller distortion, while in the case of a weak coupling a dynamic Jahn-Teller effect shows up, manifested in the modification of some orbital interactions. A discussion of the application of the Jahn-Teller effect to actinides is given elsewhere (105).

C. Hyperfine Interactions

In the preceding sections, we have considered only the electrostatic interaction between nuclei and electrons, assuming the nucleus as a point charge. In fact, the nuclei are complex systems with odd power (i.e. dipole, octapole, etc.)

magnetic moments and even power (quadrupole, hexadecapole, etc.) electric moments which can interact with the magnetic or electric fields. These magnetic or electric fields can be created by the electrons of the atom, molecule or crystalline environment or by the nuclei of the neighboring atoms in molecules or crystals. These interactions lead to an additional splitting of the energy levels, which are very small (less than 1 cm^{-1}) and are known as hyperfine interactions. The hyperfine interactions are dominated by the interaction of the nuclear magnetic moment with the spin and orbital moments of the electrons (the magnetic hyperfine interaction) and by the interaction of the nuclear quadrupole moment with the gradient of the electric field (produced by electrons and/or the external charges) at the nucleus (the quadrupole interaction).

For an even Z element, as uranium, the ground nuclear state for even A isotopes has zero nuclear spin, while the odd isotopes have half-integer spin quantum numbers: I = 5/2 for ^{233}U and I = 7/2 for ^{235}U.

For the magnetic fields used in magnetic resonance, the magnetic dipole moment is $\mu_I = \gamma\beta_n I$, i.e. is proportional to the angular momentum I of the nuclear ground state, γ being the nuclear spectroscopic factor and β_n the nuclear magneton. The nuclei with spins greater than 1/2 possess an electric quadrupole moment. An accurate knowledge of these moments is very helpful for the nuclear theories. Thus, while the spin and magnetic moments show the validity of the nuclear models, the nuclear electric quadrupole moment gives information concerning the departure from the spherical symmetry of the nuclear electric charge distribution. The study of the hyperfine interactions can supply information on the electronic structures of the system, the validity of the atomic structure calculations, the bonding in crystals, and the local structure of the crystals. Various nuclear (nuclear orientation, NMR, perturbed angular correlation, Mössbauer effect) or electric (optical spectroscopy of free ions and atoms, optical pumping, EPR of the ions in crystals, electron-nuclear double resonance, atom beam magnetic resonance, multistep laser photoionization spectroscopy, laser-radiofrequency double resonance) methods can be used in order to study these interactions. For uranium, the nuclear methods are not useful in the study of these interactions (106), and almost all data come from electronic measurements. For this reason we will treat the hyperfine interactions mainly with regard to their influence on the electronic structure of the uranium atoms and ions.

1. Magnetic Hyperfine Interaction in Free Atoms or Ions

Since the hyperfine interaction is very small compared to the other interactions in a free atom or ion, its effects can be treated as small perturbations on the fine-structure levels. Thus, the hyperfine structure calculations are a real test of the accuracy of the wavefunctions of electronic ground states.

The relativistic effects (107-110) are expected to be significant for uranium ions. However, for sake of simplicity, we will not consider here a full relativistic treatment but rather use some relativistic modifications of the classical hyperfine interactions. Inside a given (nl) configuration with l different from zero, the relativistic magnetic dipole hyperfine interaction can be written as:

$$H_{hf} = 2\gamma\beta_e\gamma_n \sum_i [l_i \langle R_l^{-3} \rangle - \sqrt{10}(sC^2)_i^1 \langle r_{sC}^{-3} \rangle + s\langle r_s^{-3} \rangle] I. \quad (14)$$

The first term in equation 14 is the interaction of the nuclear moment I with the orbital momentum of the electrons, the second represents the dipolar interaction between the nuclear and electronic spins where $\sqrt{10}(sC^2)_i^1$ is the electronic spin dipole operator (111) identical to $[s_i - 3r_0(r_0 s_i)]$, r_0 is a unit vector parallel to r, the electron position, and the last term has a similar form to the classical contact interaction (112) (which is zero except for the s electrons), but can be non-zero for any electron. The radial parameters in equation 14 are defined as combination of integrals $\langle r^{-3} \rangle_{jj'}$, computed between electronic states of the two relativistic subshells. For j = 7/2 and j = 5/2, subshells of a nf shell:

$$\langle r_l^{-3} \rangle = (1/49)[24\langle r^{-3} \rangle_{7/2,7/2} + 24\langle r^{-3} \rangle_{5/2,5/2} + \langle r^{-3} \rangle_{7/2,5/2}]$$

$$\langle r_{sc}^{-3} \rangle = (1/49)[-80\langle r^{-3} \rangle_{7/2,5/2}] + 144\langle r^{-3} \rangle_{5/2,5/2} - 15\langle r^{-3} \rangle_{7/2,5/2}]$$

$$\langle r_s^{-3} \rangle = (1/49)[64\langle r^{-3} \rangle_{7/2,7/2} - 48\langle r^{-3} \rangle_{5/2,5/2} - 16\langle r^{-3} \rangle_{7/2,5/2}]$$

with

$$\langle r^{-3} \rangle_{jj'} = \frac{-2}{\alpha a_0 (K+K'+2)} \int_0^\infty (PQ' + QP') R^{-2} dr \quad (16)$$

where α is the fine structure constant, a_0 is the Bohr radius, K = -4 for j = 7/2 and +3 for j = 5/2, P and Q are the large and small radial components of the relativistic one-electron wavefunctions; K refers to j and K' refers to j'. In the non-relativistic limit $\langle r_l^{-3} \rangle = \langle r_{sc}^{-3} \rangle$ and $\langle r_s^{-3} \rangle = 0$.

The matrix elements of the hyperfine interactions within a given J manifold can be evaluated in two coupling schemes. In the absence of any external fields, the electronic angular moment *J* and the nuclear spin moment *I* couple together to give the total angular momentum *F* = *I* + *J*. Each J level is split into levels characterized by the hyperfine quantum numbers F, which can take values |I - J| and I + J. Each F level is (2F + 1)-fold degenerate in the quantum number M_F. In this case, we must calculate matrix elements between states $|\sigma JIFM_F\rangle$, where σ denotes the other quantum numbers of the level J. Because the matrix elements between states of different J are very small, we will consider the diagonal matrix elements (which are also diagonal in M_F) and are equal to $(1/2)A[F(F+1) - J(J+1) - I(I+1)] \equiv (1/2)AK$. The parameter A is known as the magnetic hyperfine structure parameter. The non-relativistic calculation of this parameter (10) has been extended for the relativistic case in (25) where it is shown that for each Russell-Saunders component of an intermediate coupling wavefunction:

$$A = (2\gamma\beta_e\beta_n/I)\{[(2 - g)\langle r_l^{-3} \rangle + (g - 1)\langle r_s^{-3} \rangle + 2[\{14(2J + 1)/J(J + 1)\}^{\frac{1}{2}} \times \langle \sigma SL|V^{(12)}|\sigma'S'L'\rangle \times \begin{Bmatrix} S & S' & 1 \\ L & L' & 2 \\ J & J' & 1 \end{Bmatrix}] \langle r_{sC}^{-3} \rangle\} \quad (17)$$

where

$$(2\text{-}g) = \langle \sigma SLJ \| L \| \sigma SLJ \rangle / [J(J+1)(2J+1)]^{\frac{1}{2}}$$

and

$$(g\text{-}1) = \langle \sigma SLJ \| S \| \sigma SLJ \rangle / [J(J+1)(2J+1)]^{\frac{1}{2}}$$

are diagonal in the SLJ representation, while the tensor operator $V^{(12)}$ may have non-diagonal matrix elements and makes A very sensitive to the use of the intermediate coupling (113).

In the presence of an external magnetic field, large compared to the interaction between I and J, each of these moments are quantized in the external field, and a more suitable coupling scheme is $(2JM_J Im_I)$. In this scheme, the matrix elements, for which $M = M_J + m_I$ is conserved, have nonzero values. The diagonal matrix elements are equal to $AM_J m_I$ with A defined as above.

Various relativistic calculations have been performed in order to obtain the hyperfine radial parameters. Table 2 gives the D - S (25), D - F (25), and MDF (26) values together with the classical $\langle r^{-3} \rangle$ parameters (24) for the uranium atom and ions. In order to compare the relativistic and non-relativistic results, the weighted average relativistic values, as well as the "effective" values (106), are given.

The "effective" radial integrals have been estimated as follows. The hyperfine interaction can be considered as an interaction between the nuclear spin moment *I* and a hyperfine electronic magnetic field H_{hf}^{rel}, which is composed of three parts, H_l, H_{sC}, and H_s. In order to compare the relativistic and non-relativistic form as

$$H^{rel} = 2\beta\Sigma_i[l_i \cdot \sqrt{10}(sC^2)_i^1]\langle r^{-3} \rangle_{eff} \quad (18)$$

where the effective radial parameter is

$$\langle r^{-3} \rangle_{eff} = \frac{H_l + H_{sC} + H_s}{H_l/\langle r_l^{-3} \rangle + H_{sC}/\langle r_{sC}^{-3} \rangle}. \quad (19)$$

The $\langle r^{-3} \rangle_{eff}$ values for different uranium ions have been estimated by using the hyperfine fields calculated for the pure Hund's rule states of these ions (106).

The existence of different radial parameters for the various contributions to the hyperfine interaction has been clearly demonstrated by precise experimental measurements on different atoms or ions, which show differences up to about 10% between $\langle r_{sC}^{-3} \rangle$ and $\langle r_l^{-3} \rangle$. An examination of Table 2 shows also that the non-relativistic theories lead to serious overestimates (of about 30%) of $\langle r^{-3} \rangle$.

Another source of error in the calculation of the magnetic hyperfine parameter comes from the approximation used in the central-field theories. For this reason, effects such as the excited configuration mixing must be taken into account as well as the polarization of the closed-shell electrons by the electrons from incomplete shells, resulting in unpaired spin density at the nucleus. The last effect, known as "core polarization," can give large contributions to the hyperfine structure. An accurate calculation of the core polarization is extremely difficult for actinides. The very few data existing for core-polarization electronic hyperfine fields in actinides can be described by an empirical relation (106, 114).

Table 2. The Hyperfine Radial Parameter $\langle r^{-3} \rangle$ for Uranium Atom and Ions (in a.u.)

Ion	Configuration	HFS[a]	DS				MDF[c]			$\langle r^{-3} \rangle_{eff}^{e}$
			5/2,5/2	7/2,7/2	5/2,7/2	DWA	5/2,5/2	7/2,7/2	DWA	
U	$5f^3 6d\ 7s^2$		5.434	4.979	5.136	5.174				
U^+	$5f^3 7s^2$		5.556	5.130	5.271	5.312				
U^{2+}	$5f^4$		5.044	4.604	4.758	4.793				
U^{3+}	$5f^3$	7.23	5.718	5.310	5.441	5.485	5.914	5.417	5.630	5.633
U^{4+}	$5f^2$	7.82	6.366	5.966	6.805	6.137	6.528	6.024	6.240	6.312
U^{5+}	$5f^1$		6.999	6.600	6.711	6.771	7.130	6.612	6.834	6.999

a) Non-relativistic Hartree-Fock-Slater values (24). b) Dirac-Slater values (25). c) Mixed configuration Dirac-Fock values (26). d) Degeneracy-weighted average values $\langle r^{-3} \rangle = (6/14)\langle r^{-3} \rangle_{5/2} + (8/14)\langle r^{-3} \rangle_{7/2}$. e) "Effective" values (106).

$$H_{core} \simeq (600 + 100)(g_J - 1)\langle J_z \rangle \qquad (20)$$

where g_J is the Lande factor and H_{core} is expressed in kOe. This equation shows that the core-polarization effects are very strong in the case of actinides, about 6-7 times stronger than for the lanthanides. For the ground level of U^{3+}, H_{core} is estimated to be 740 kOe from a total hyperfine magnetic field of 4900 kOe, for U^{4+}, 480 kOe out of 4600 kOe, and for U^{5+}, 210 kOe out of 3200 kOe (106).

2. Electric Quadrupole Interactions in Free Atoms and Ions

A relativistic treatment of the nuclear electric quadrupole interaction is very complex because additional terms in the interaction can appear. However, it can be shown (109) that the expectation values of the relativistic and non-relativistic quadrupole interactions are quite similar in value and exception to this can only be expected when all the diagonal matrix elements vanish, and the off-diagonal elements become dominant. This situation arises in the case of the half-filled shells. None of the uranium ions are in such a position, so we will restrict our discussion to the non-relativistic quadrupole interaction.

The Hamiltonian which describes the quadrupole interaction between a distribution of nuclear charges and a distribution of electronic charges can be written as a product of second rank tensor operators that act only in the nuclear space (A_2^q) or in the electronic space (B_2^q) respectively. This can be transformed to give

$$H_Q = \sum_{i,j} V_{ij} Q_{ij} \qquad (21)$$

where

$$V_{ij} = \partial^2 V / \partial x_i \partial x_j |_{r=0}$$

and $V_{(x,y,z)}$ is the electrostatic potential created by electrons. The Q_{ij} in equation 21 are defined as

$$Q_{ij} = [eQ/6I(2I-1)][(3/2)(I_iI_j + I_jI_i) - \delta_{ij}I(I+1)]. \qquad (22)$$

The parameter Q is the nuclear quadrupole moment (115).

The two second-order tensors V_{ij} and Q_{ij} can be brought to the principal axes (x,y,z). In this case, the electric field gradient can be completely described by two parameters: V_{zz} and the asymmetry parameter $\eta = (V_{xx} - V_{YY})/V_{ZZ}$.

For a given electronic level J, the electronic operators can be replaced by equivalent operators, and the quadrupole interaction can be written as:

$$H_Q = [B/2I(2I-1)J(J-1)][3(JI)^2 + 3(I - J(J+1)I(I+1)] \qquad (23)$$

where

$$B = -J(2J-1)e^2 Q \langle r_q^{-3} \rangle \langle J \| \alpha \| J \rangle = e^2 q_J Q \qquad (24)$$

The matrix elements $<J\|\alpha\|J>$ are given in (74).

In the absence of an external field, the diagonal matrix elements of the quadrupole interaction for a given F state are equal to

$$[B/2I(2I-1)J(2J-1)][(3/4)K(K+1) - I(I+1)J(J+1)].$$

The radial integral $<r_q^{-3}>$ can be calculated by relativistic and non-relativistic methods. In non-relativistic theories, this parameter is equal to that used in the magnetic dipolar interaction. In a relativistic treatment, the quadrupole radial integral is defined as

$$<r_q^{-3}>_{jj'} = \int_0^\infty (FF' + GG')r^{-3}\,dr,$$

which is different from those used in the magnetic dipole interaction. A calculation has been made of the values $<r^{-3}{}_q>_{jj'}$ by D-S and D-F methods for uranium atom and ions (25).

The V_{zz} component of the electric field gradient produced by the electrons of a given energy level J is:

$$V_{zz} = -e<r_q^{-3}><J\|\alpha\|J>[3J_z^2 - J(J+1)]. \quad (25)$$

The distortion of the charge cloud of the inner closed shells produces a change in the electric field gradient at the nucleus. This influence is taken into account by introducing the inner-shell shielding Sternheimer factor R. In the case of uranium, this shielding has been estimated to be $R_{5f} \sim 0.15$ (116, 117), and thus the electric field gradient acting on the nucleus is $V_{zz}^{eff} \simeq 0.85\ V_{zz}$.

3. Measurement of the Magnetic Dipole and Nuclear Quadrupole Moments of Free Ions

Experimental measurements of the hyperfine interactions allow the determination of the nuclear magnetic dipole and electric quadrupole moments. For complex atomic systems with more than one open shell, additional difficulaties are connected with the use of a proper coupling scheme. An example of this is uranium whose hyperfine structure for the 233 and 235 isotopes has been measured in free-atom optical spectra. Each of the levels involved in the optical transition shows hyperfine splitting, and the hyperfine structure of the optical lines is due to the difference in the splittings of these levels. After the hyperfine splitting of each level has been separated, the A and B parameters defined above can be calculated from differences in the positions for different values of F. This requires a knowledge of the J and I quantum numbers. The accuracy in estimation of the nuclear magnetic dipole and electric quadrupole moments from values of A and B depends on the accuracy with which some atomic parameters, especially the wavefunctions and the radial parameters, are known. For the lowest $^5L_6$ level of the ground configuration $5f^3\ 6d\ 7s^2$ of uranium atoms, the experimental A and B parameters and the moments μ and Q are connected (118) by

$$A = (2\beta_e\beta_n\mu/I)(a<r^{-3}>_{5f} + b<r^{-3}>_{6d})$$

$$B = e^2Q(c<r^{-3}>_{5f} + d<r^{-3}>_{6d}) \quad (26)$$

where a, b, c, and d depend on the intermediate coupling wavefunction. For the $^5L_6$ level, this is $0.875|(^4I)^5L> - 0.356|(^2H\ 2)^3K> + 0.234|(^4I)^3K> + 0.129|(^2H\ 1)^3K>$ (119) and a = 1.002, b = 0.388, c = 0.180, and d = 0.477, as compared to a' = 0.992, b' = 0.380, c' = 0.239, and d' = 0.512 for a pure Russell-Saunders ground level (118). The radial integral $<r^{-3}>_{5f}$ from equation (26) has been estimated from the value of $<r^{-3}>_{5f}$ for the neutral plutonium atom using the ratio for the spin-orbit parameters for the two atoms. Thus, a value of 5.9 a.u. was estimated for $<r^{-3}>_{5f}$, and a value for $<r^{-3}>_{6d}$ was taken as $0.6<r^{-3}>_{5f}$. With these quantities and the experimental values $A = -2.08\times10^{-3}$ cm^{-1} and $B = 138.5\times10^{-3}$ cm^{-1}, the values $\mu = -0.31\mu_n$ and Q = 6.4 barn for ^{235}U and $\mu = 0.487\mu_n$ and Q = 4.86 barn for ^{233}U were calculated (118).

Recent measurements by multistep laser photoionization gave $A = -1.98\times10^{-3}$ cm^{-1} and $B = 136.9\times10^{-3}$ cm^{-1} (120), or $A = -2.03\times10^{-3}$ cm^{-1} and $B = 138.73\times10^{-3}$ cm^{-1} (121), while laser-radiofrequency double resonance gave the values $A = 2.02\times10^{-3}$ cm^{-1} and $B = 136.9\times10^{-3}$ cm^{-1} (122). These parameters have also been measured for some excited levels (120, 121, 123).

The values of μ and Q depend on the accuracy with which the experimental A and B parameters have been measured and on the radial integral involved. While the parameters A and B, measured by different methods, show only very slight differences, the differences between various estimates of the radial integrals are fairly large. Thus, the relativistic calculations (25) show a clear 15% overestimate for the radial integral $<r^{-3}>_{5f}$ (118). Earlier estimates for ^{233}U have given $\mu = 0.73\mu_n$ and Q = 7.9

barn (124).

4. Hyperfine Interactions in Solids

The electronic properties of the ions in crystals are influenced by their neighbors, and this is manifested in the hyperfine interactions. The main effects in the case of the actinide ions in crystals are as follows:

(a) J mixing through the crystal field modifies the hyperfine splitting.

(b) When the crystal field interaction is of the same order or stronger than the spin-orbit coupling, the intermediate or even strong crystal field scheme must be used.

(c) The overlap, exchange, and covalency (charge transfer) effects modify the radial $<r^{-3}>$ integrals.

(d) When the neighboring nuclei possess magnetic or electric quadrupole moments, an additional interaction (known as super-hyperfine interaction) appears due to dipole interaction, overlap, or covalency.

(e) An additional quadrupole interaction due to the nonspherical electric charge distribution of the neighbors of the ion is produced. An additional polarization of the electronic shells of the ions takes place, and this can be expressed by an outer Sternheimer factor γ_∞ which is usually negative (antishielding) and has a very large value (for actinides about 100).

Due to the large line width compared to the hyperfine splitting, there are no data on hyperfine structure of the optical spectra for uranium ions in crystals. However, the above discussion is valid in the study of the hyperfine interaction of uranium ions in crystals by other methods, as for instance, EPR.

D. The Zeeman Effect

1. Zeeman Effect in a Free Atom without Nuclear Spin

In a free atom or ion whose nuclear spin is zero, each energy level is (2J + 1)-fold degenerate. This degeneracy can be lifted by an external magnetic field which splits the level into (2J + 1) components characterized by the magnetic quantum numbers M_J (Zeeman effect). When the energy levels are close to each other, and the external magnetic field is very strong, a mixing of the different levels through the Zeeman interaction also takes place.

The Zeeman effect is due to the interaction between the magnetic moment μ of the open electronic shell of the ion and the external magnetic field H_0, the energy of the interaction being:

$$W_Z = -\mu \bullet H_0.$$

In the case of a free atom or ion whose electrons in open-shells are characterized by the individual orbital l_i or spin s_i moments, the Hamiltonian of this interaction can be written as

$$H_Z = \beta H_0 \sum_{i=1} (l_i + g_S S_i) \qquad (27)$$

where β is the Bohr magneton, and g_S is the spin magnetic factor ($\mu_S = -g_S \beta s$) and amounts to 2.0023 (in the relativistic approximation) or 2 (in the non-relativistic approximation).

The Hamiltonian of equation 27 commutes with the operator J_Z but not with J^2, regardless of the coupling scheme, and its matrix elements are diagonal in M_J but not in J. For the Russell-Saunders coupling H_Z commutes also with L^2 and S^2, and its matrix elements are diagonal in L and S. The non-vanishing matrix elements of the Zeeman interaction are then

$$<\sigma SLM_J|L + g_S S|\sigma SLJ'M_J'> = (-1)^{J-M_J} \begin{pmatrix} J & 1 & J' \\ M_J & 0 & M_J \end{pmatrix} \times <\sigma SLJ|L + g_S S|\sigma SLJ'>. \qquad (28a)$$

The diagonal matrix elements are given by

$$<\sigma SLM_J|L + g_S S|\sigma SLJM_J> = g_J M_J \qquad (28b)$$

where g_J is the Lande factor

$$g_J = [1 + (g_S - 1)][J(J+1) - L(L+1) + S(S+1)]/2J(J+1).$$

The non-diagonal matrix elements are governed by the selection rule $|J - J'| = 1$.

According to equation 28b the Zeeman components of a level J are equidistant and form a symmetrical structure around the free-ion energy of the level. The Zeeman splitting is proportional to the Lande g-value. In real situations, when the intermediate coupling must be taken into account, the g-value can be sensibly different from the Lande factor.

2. Zeeman Effect and the Hyperfine Interaction in Free Atoms or Ions

When the nucleus of the atom or ion has

spin, in an external magnetic field, the hyperfine interaction will compete with the electronic Zeeman interaction (79) and with the nuclear Zeeman interaction $H_{zn} = \mu \bullet H_0 = g_I \beta_n H_0 \bullet I$.

For weak magnetic fields when the Zeeman interactions are small compared with the hyperfine interaction, the most appropriate coupling scheme for the hyperfine interaction is that of the coupling $J + I = F$. In this case the diagonal matrix elements in F are

$$<\sigma JIFM_F|H_z + H_{zn}|\sigma JIFM_F> =$$

$$\frac{M_F H_0}{2F(F+1)}\{[F(F+1)+J(J+1)-I(I+1)]g_j -$$

$$[F(F+1)+I(I+1)-J(J+1)\beta_n g_I\} =$$

$$\beta g_F M_F H_0. \qquad (29)$$

In very weak (of order 10 Gauss) magnetic fields, only these diagonal matrix elements are taken into account, and within this approximation each hyperfine-structure level F is split into (2F + 1) equally spaced components. In moderate magnetic fields the hyperfine structure is very complex and non-diagonal (in F) matrix elements must be considered.

For strong magnetic fields (10^3-10^4 Gauss) the coupling between the electronic angular momentum and the nuclear spin is broken, and the most appropriate scheme for characterization of the levels is ($JM_J Im_I$). The diagonal matrix elements are now:

$$<\sigma JM_J Im_I|H_z + H_{zn}|\sigma JM_J Im_I> =$$

$$H_0(g_J M_J - g_{Im_I}\beta_n/\beta) \qquad (30)$$

If the non-diagonal matrix elements can be neglected, each Zeeman level is split into (2I + 1) approximately equally spaced sublevels due to the hyperfine interaction $AM_J m_I$.

3. Zeeman Effect for Ions in Crystals

A crystal field can split the energy levels of the free ion and mix states characterized by different J values. As shown above for a weak crystal field, each level J is split in a crystal field according to the reduction of the irreducible representation D^J of the rotation group in the irreducible representations Γ_i of the symmetry point group of the crystal field. For the ions with even numbers of electrons, the resultant crystal field levels can be singlets, doublets, or triplets (the last ones only in cubic fields). For ions with odd numbers of electrons, the crystal field levels will be at least doubly degenerate, regardless of the symmetry of the crystal field. This residual degeneracy, known as Kramers degeneracy, results from the condition that the Hamiltonian of the system commutes with the time-reversal operator O. The two wavefunctions of the doublet are Kramers conjugates, i.e. if one of them can be written as a combination of states |J,M>:

$$|\zeta> = \sum_{J,M} C_{JM}|J,M>, \qquad (31a)$$

the other is

$$|\bar{\zeta}> = \sum_{J,M} C^*_{JM}(-1)^{J-M}|J,-M>. \qquad (31b)$$

For the intermediate crystal field, the eigenvalues of the crystal field plus spin-orbit coupling can be doublets Γ_6 or Γ_7 or quartets Γ_8 (the latter only in cubic fields). In this case the Kramers doublets cannot be described by states of equations 31a and 31b since the angular momentum J is no longer a good quantum number, and the wavefunction of each doublet contain mixtures from the other doublets which have the same transformation properties.

The Zeeman interaction can split the levels left degenerate by the crystal field, but the equations given for the free-ion case are no longer valid. As shown before, the states inside the doublets Γ_6 and Γ_7, the triplets Γ_4 and Γ_5, and the quartet Γ_8 can be classified according to the eigenstates of a fictitious angular momentum $\mathcal{J}$ with $\mathcal{J}$ equal to 1/2 (for the doublets), 1 (for the triplets), or 3/2 (for the quartets). The calculation of the Zeeman effect $-\mu \bullet H_0$ implies a knowledge of the matrix elements of the magnetic moment μ between crystal field electronic states. This calculation can be simplified if some symmetry properties are used. The matrix elements of a given operator V (which transforms according to the representation Γ of a certain group G) between the two wavefunctions which transform according to the representations Γ' and Γ'', respectively of the same group G is different from zero only if the decomposition of the product $\Gamma'^* \times \Gamma \times \Gamma''$ contains the unit representation of the group. If all of these representations have real characters (which is always the case with the representations encountered here), this condition is equivalent to the condition that the direct product $\Gamma' \times \Gamma''$ contains Γ. In this case the interaction V can remove partially the degeneracy of the different eigenvalues of the Hamiltonian H_0 which is invariant to the transformations of the group G. If the operator V is a vector V, and the representation Γ enters in the

decomposition of the direct product $\Gamma \times \Gamma''$ only once, the Wigner-Eckart theorem states that, inside a given J manifold, the operator V can be replaced by the equivalent operator αJ, where α is a proportionality factor depending on the vector V. When the Hamiltonian H_0 is invariant on the time-reversal operation Θ, the condition to lift the degeneracy under a perturbation of a lower symmetry is more restrictive (1). The kinetic and the electrostatic interactions as well as the spin-orbit coupling are invariant with regard to time reversal. For a system with an odd number of electrons, the square of the time-reversal operator Θ is -1, while for systems with even number of electrons, it is +1.

The set of functions $\phi_i\chi_j$ which spans the product of representations $\Gamma \times \Gamma'$ can be divided into a symmetrical subset $\frac{1}{2}\{\phi_i\chi_j + \phi_j\chi_i\}$ and an antisymmetrical subset $\frac{1}{2}\{\phi_i\chi_j - \phi_j\chi_i\}$ which do not mix, and the representations resulting from the decomposition of the product can thus be referred as symmetric or antisymmetric. If a symbol ϵ_V is introduced so that for time-odd operators V, it is equal to -1 and for time even operators, it is +1, the condition that the operator V which transforms according to Γ has non-vanishing matrix elements between the states characterized by Γ', is that, if $\Theta^2\epsilon_V > 0$, Γ must be contained in the symmetric direct product $[\Gamma \times \Gamma']_S$. If $\Theta^2\epsilon_V < 0$, it must be contained in the antisymmetric part of $\Gamma \times \Gamma'$.

The magnetic moment μ is an odd time operator which transforms according to the representation D^1 of the rotation group and to the representation Γ_4 of the cubic group. This implies that in the case of an ion with odd number of electrons, the Zeeman interaction can lift the degeneracy of a crystal field representation Γ' if Γ_4 appears at least once in the symmetric part of the decomposition of the direct product $\Gamma \times \Gamma'$. For the even-electron systems, this holds if Γ_4 belongs to the asymmetrical part of $\Gamma \times \Gamma'$.

As shown in Section II.B.3, the states of various representations of the cubic group can be classified as the states of a fictitious angular momentum. The Wigner-Eckart theorem shows that if the representation Γ_4 appears once (and in a proper way) in the decomposition $\Gamma \times \Gamma'$, the vector V can be replaced by $\alpha\tilde{J}$ where $\tilde{J}$ is the fictitious angular momentum of the representation Γ'. Thus, the magnetic momentum can be replaced by the fictitious momentum $\alpha\tilde{J}$ for the doublets Γ_6 and Γ_7 and the triplets Γ_4 and Γ_5. The decomposition of $\Gamma_3 \times \Gamma_3$ does not contain Γ_4, and thus the Zeeman interaction cannot lift the degeneracy of the doublet Γ_3. On the other hand, Γ_4 appears twice in the decomposition $\Gamma_8 \times \Gamma_8$; this case will be considered in more detail later.

3a. Zeeman Effect in a Kramers Doublet

Consider a Kramers doublet (the cubic Γ_6 or Γ_7 doublets for an ion with odd number of electrons or any doublet for such an ion in a crystal field of symmetry lower than cubic), well isolated from any other energy levels. The degeneracy of this doublet can be removed by the Zeeman effect. The time-odd operator μ has values opposite in sign in the two states of the doublet. As shown before, in this case the components of the vector μ can be considered proportional to the components of a fictitious angular momentum, or fictitious spin $\tilde{s}$ whose components are the Pauli matrices $\frac{1}{2}\sigma_1$, $\frac{1}{2}\sigma_2$, and $\frac{1}{2}\sigma_3$:

$$\mu_i = -\sum_j g_{ij}\tilde{S}_J. \tag{32}$$

The set of numbers q_{ij} represents the gyromagnetic factor (equivalent to the Landé factor introduced before), and the number of components g_{ij} depends on the symmetry of the crystal field. The set of numbers g_{ij} does not represent a tensor, and the common habit of calling the gyromagnetic factor a tensor comes from the confusion between the fictitious spin $\tilde{s}$ and a real electronic spin (1).

The numbers g_{ij} cannot be determined directly from experiment. In fact, for a given orientation of the external magnetic field with respect to the crystalline axes, the energy of the Zeeman levels is determined by an effective g-value

$$W = \pm\tfrac{1}{2}\beta g_{eff}H_0. \tag{33}$$

The effective g-value is connected to the gyromagnetic factors through the relation

$$g_{eff}^2 = |g\tilde{g}l|, \tag{34}$$

where $\tilde{g}$ is the transposed matrix g, and l represents the vector $(l_x l_y l_z)$ whose components are the direction cosines of the magnetic field in the laboratory system. The product $g^2 = g\tilde{g}$ represents a symmetrical tensor whose components can be determined by measuring the Zeeman energy transitions in three mutually perpendicular planes. It can be transformed in a diagonal form with a matrix L (125) so that

$$Lg^2L^+ = {}^dg^2. \tag{35}$$

The elements of the matrix L are the direction cosines which connect the principal (X, Y, Z)

axes of the tensors g^2 to the laboratory axes. After the principal components of g^2 are determined, the components g are determined by performing the square roots. As discussed before, in some situations the principal axes (X, Y, Z) can be connected with the geometrical axes of the system (for tetragonal, trigonal, and orthorhombic symmetry).

Once the elements of the ${}^{d}g^2$ have been determined, the effective g_{eff} value can be written simply as

$$g_{eff}^2 = g_{XX}^2 l_X^2 + g_Y^2 l_Y^2 + g_{ZZ}^2 l_Z^2, \qquad (36)$$

where l_X, l_Y, and l_Z are the direction cosines of the magnetic field in the reference frame (X, Y, Z) of the ${}^{d}g^2$ tensor. For cubic symmetry $g_{XX}^2 = g_{YY}^2 = g_{ZZ}^2 = g^2$, and in case of axial symmetry, $g_{XX}^2 = g_{YY}^2 = g_{\perp}^2$ and $g_{ZZ}^2 = g_{\parallel}^2$ (if Z is along the distortion axis).

Inside a given J the principal g-values are given by $g_{\parallel} = 2g_J\langle\zeta|J_Z|\zeta\rangle$ and $g_{\perp} = g_J\langle\zeta|J^+|\bar{\zeta}\rangle$.

3b. Zeeman Effect in a Triplet

In the case of a Γ_4 or Γ_5 triplet, the magnetic momentum μ can be replaced by a fictitious angular momentum $\mathcal{J}$, with $J = 1$. Since these triplet states appear only in cubic symmetry, the gyromagnetic factor has only one component: the triplet is split into three equidistant singlets, the splitting being proportional with the g-value and the intensity of the magnetic field, but independent of the orientation of the magnetic field with respect to the crystalline axes.

3c. Zeeman Effect in a Γ_8 Quadruplet

The representation Γ_4 appears twice in the decomposition of $\Gamma_8 \times \Gamma_8$. An adaptation of the Wigner-Eckart theorem shows (1, 126, 127) that the matrix elements of a time-odd vector within a manifold Γ_8 can be specified by two constants. The magnetic moment μ and the fictitious angular momentum $\mathcal{J} = 3/2$ can be connected by the relations (126):

$$\begin{aligned} \mu_z &= a\mathcal{J}_z + b\mathcal{J}_z^3 \\ \mu_x &= a\mathcal{J}_x + b\mathcal{J}_x^3 \\ \mu_y &= a\mathcal{J}_y + b\mathcal{J}_y^3 \end{aligned} \qquad (37)$$

such that

$$\pm\langle\pm 1/2|\mu_z|\pm 1/2\rangle = Q' = (4a+b)/8$$

$$\pm\langle\pm 3/2|\mu_z|\pm 3/2\rangle = P' = (12a+27b)/8 \qquad (38)$$

The electronic Zeeman interaction can thus be written as

$$\begin{aligned} H = g\beta\mathcal{J}H + u\beta[&\mathcal{J}_x^3 H_x + \\ &\mathcal{J}_y^3 H_y + \mathcal{J}_z^3 H_z - (\mathcal{J}\bullet H)\times \\ &3\mathcal{J}(\mathcal{J}+1)-1\}/5] \end{aligned} \qquad (39)$$

where the last term in the square bracket has been added to give to the Hamiltonian definite transformation properties.

The eigenvalues of this Hamiltonian, expressed in units E/H are obtained by solving the secular equation

$$\begin{aligned} &y^4 - (P^2 + Q^2)y^2 + P^2Q^2 + \\ &(P-3Q)(P+Q)^2(3P-Q)\times \\ &(n_1^2 n_2^2 + n_2^2 n_3^2 + n_3^2 n_1^2) = 0 \end{aligned} \qquad (40)$$

where n_i are the direction cosines of the external magnetic field relative to the cube edge, $P = g_i P'$ and $Q = g_i Q'$. The energy levels are not equidistant, and they depend on the magnitude of the external magnetic field and its orientation relative to the cubic axes. When the last term in the left side of equation 40 vanishes, i.e. when either $P = 3Q$ or $P = -Q$ or $3P = Q$, the Zeeman levels do not depend on the orientation. When Γ_8 enters more than once in the decomposition of J in the crystal field, its wavefunctions depend on the composition parameter x of the cubic crystal field potential and so do the positions of the Zeeman levels. An exact analytical solution of equation 40 cannot be given except for special orientations of the magnetic field:

(a) For H parallel to $|100|$, the four solutions of equation 40 are

$$Y_{1,2} = \pm P \text{ and } Y_{3,4} = \pm Q \qquad (41)$$

(b) For H parallel to $|111|$,

$$\begin{aligned} Y_{1,2} &= \pm\tfrac{1}{2}\sqrt{3(P^2 + Q^2) + 2PQ} \\ Y_{3,4} &= \pm\tfrac{1}{2}(P - Q) \end{aligned} \qquad (42)$$

(c) For H parallel to $|110|$,

$$Y_{1,2} =$$

$$\pm 1/\sqrt{2}\sqrt{P^2+Q^2+(P+Q)\sqrt{7(P^2+Q^2)-2PQ}}$$

$$Y_{3,4} =$$

$$\pm 1/\sqrt{2}\sqrt{P^2+Q^2-(P+Q)\sqrt{7(P^2+Q^2)-2PQ}} \qquad (43)$$

An axial distortion of the crystal field will split the Γ_8 quartet. If the distortion is tetragonal, the quartet is split into two doublets, while a trigonal distortion splits Γ_8 into a doublet and a pair of singlets. However, according to the Kramers theorem, those two singlets must have the same energy. If the distortions are weak enough, they can leave the wavefunctions of the levels unchanged, and in the tetragonal field one of the doublets can be characterized by the wavefunctions $|\pm 1/2>$ and the other by $|\pm 3/2>$. The Zeeman effect inside each of these doublets will be characterized by two g-values, $g_\parallel$ and $g_\perp$ as follows:

(a) In the case of a weak tetragonal distortion:

-inside the $|\pm 1/2>$ doublet,

$$g_\parallel = +2Q$$

$$\text{and } g_\perp = \tfrac{1}{2}|3P - Q| \qquad (44a)$$

-inside the $|\pm 3/2>$ doublet,

$$g_\parallel = -2P$$

$$\text{and } g_\perp = \tfrac{1}{2}|P - 3Q| \qquad (44b)$$

(b) In the case of a weak trigonal distortion:

-inside the $|1/2>$ doublet,

$$g_\parallel = |P - Q|$$

$$\text{and } g_\perp = P + Q \qquad (45a)$$

-inside the $|3/2>$ doublet, which in trigonal crystal fields is in fact composed of a pair of singlets $\Gamma_4{}^T$ and $\Gamma_5{}^T$, the tensor g^2 has one non-vanishing component

$$g_{ZZ}{}^2 = 3(P^2 + Q^2) + 2PQ \ . \qquad (45b)$$

3d. Zeeman Effect in the Case of a Cubic Γ_7 Doublet in Intermediate Crystal Field

The equations 13 for the two states of the cubic Γ_7 doublet lead to a g-value of

$$g_{\Gamma_7} = 2\cos^2\Theta - 8k_{a_2 t_2}\sin\Theta\cos\Theta/\sqrt{3} + 2(k_{t_2 t_2} - 1)\sin^2\Theta/3. \qquad (46)$$

As shown by this relation, g_{Γ_7} depends on the ratio of the spin-orbit parameter ζ to the crystal field splitting V and on the two orbital reduction parameters. The g-value for the excited $\Gamma_7{}'$ doublet is

$$g_{\Gamma_7}{}' = 2\sin^2\Theta - 8k_{a_2 t_2}\sin\Theta\cos\Theta/\sqrt{3} + 2(k_{t_2 t_2} - 1)\cos^2\Theta/3. \qquad (47)$$

These two g-values together with the energy interval

$$E_{\Gamma_7}{}' - E_{\Gamma_7} = 2\sqrt{3}k_{a_2 t_2}\zeta/\sin^2\Theta \qquad (48)$$

which can be measured by optical absorption, should make possible the estimation of the parameters $k_{a_2 t_2}$, $k_{t_2 t_2}$, and V (95). If the value of $g_{\Gamma_7}{}'$ cannot be measured, an approximate fitting procedure must be used.

4. Zeeman Effect and the Hyperfine Interaction in Crystals

For a given crystal field state characterized by a fictitious angular momentum $\mathcal{J}$, the hyperfine interaction can be written as

$$H_{hf} = \mathcal{J}AI = \sum_{i,j} \mathcal{J}_i A_{ij} I_j \qquad (49)$$

where the set of numbers A_{ij} represents the hyperfine interaction parameter and, like the gyromagnetic factor g_{ij}, it is not a tensor (1).

The treatment of the interaction for ions in crystals must take into account the relative strength of the hyperfine interaction as compared to the electronic and nuclear Zeeman interaction.

In the case of a Kramers doublet, the set A_{ij} can contain a large number of components and can be asymmetric. Usually the electronic Zeeman interaction is much stronger than the hyperfine interaction, and the electronic Zeeman interaction is much stronger than the hyperfine interaction, and the electronic and nuclear spins are quantized along different axes. When the nuclear quadrupole interaction can be neglected, the nuclear spin participates in the hyperfine and nuclear interaction. The nuclear Hamiltonian

$$H = \mathcal{J}AI - g_n\beta_n HI \qquad (50)$$

may be written as an interaction between the nuclear spin and an effective magnetic field

$$H = -g_n\beta_n H^{eff} I. \qquad (51)$$

This field is the sum of the external magnetic field and the hyperfine field H_{hf} created by the electrons at the site of the nucleus (128)

$$H^{eff} = H_{hf} + H = -(\mathcal{J}A + H)/g_n\beta_n. \quad (52)$$

Such a hyperfine field H_{hf} is the orbital field defined by equation 18. It depends on the electronic state. Thus in the case of a Kramers doublet, the hyperfine fields for the two electronic states are collinear and equal, but of opposite sign. These hyperfine fields add to the external magnetic field and the resulting effective fields are noncollinear and of different modulus. The nuclear spin is quantized in the effective field for each electronic state and the nuclear wavefunctions corresponding to a given electronic state M_J are connected to those corresponding to another state M_J by the relation:

$$|m(M_\mathcal{J})> = \sum_{m'} d_{mm'}^{(I)}(\omega)|m'(M'_\mathcal{J})> \quad (53)$$

where $d_{mm'}^{(I)}(\omega)$ are the matrix elements of the irreducible representation of the rotation group, and ω is the rotation which carries the direction $H_{M_\mathcal{J}}$ eff over into $H_{M'_\mathcal{J}}$ eff.

Three cases may be distinguished dependent on the relative magnitudes of H_{hf} and H in equation 52, viz.

(i) The hyperfine magnetic field is much stronger than the external magnetic field. This is the case for uranium ions, where an estimate of the orbital hyperfine magnetic field (106) gives values of the order 3.2×10^6 Oe for U^{5+}, 5.6×10^5 Oe for U^{4+}, and 4.9×10^6 Oe for U^{3+} as compared with the usual values 10^3-10^4 Oe for the external magnetic field. In this case the contribution of the external magnetic field to H^{eff} can safely be neglected, and the contribution of the nuclear Zeeman interaction is considered only as a perturbation.

(ii) The hyperfine and the external magnetic fields are of the same order of magnitude. This is of importance for the superhyperfine interaction and will be considered later.

(iii) The case when $|H| >> |H_{hf}|$ is of no importance for our discussion.

In the case (i) the procedure for the determination of the components A_{ij} is similar to that of the gyromagnetic factor. As before, a symmetrical A^2 tensor can be defined which can be diagonalized by a suitable choice of axes. An important problem is that of the simultaneous diagonalization of the gyromagnetic g_{ij} and hyperfine A_{ij} sets. This is possible if some restrictive assumptions on the spatial environment are made, and the wavefunctions of the Kramers doublet can be constructed from the wavefunctions of a single J level (1). The situation of simultaneous diagonalization of the gyromagnetic factor and hyperfine interaction is very common. The first-order contribution in the hyperfine energy can then be written as

$$H_{hf} = K M_\mathcal{J} m_I \quad (54)$$

where K is given by the relation

$$g^2K^2 = l_x^2 g_{xx}^2 A_{xx}^2 + l_y^2 g_{yy}^2 A_{yy}^2 + l_z^2 g_{zz}^2 A_{zz}^2 \quad (55)$$

for the case of rhombic symmetry and

$$g^2K^2 = g_\parallel^2 A_\parallel^2 \cos^2\Theta + g_\perp^2 A_\perp^2 \sin^2\Theta \quad (56)$$

for the axial symmetry. In the case of cubic symmetry, the hyperfine energy does not depend on the orientation of the magnetic field and K = A.

For the systems where we can neglect any influence of other manifolds of different J, a general relation

$$A_x/g_x = A_y/g_y = A_z/g_z = A_J/g_J \quad (57)$$

holds. Any deviation from this relation shows that the J mixing must be taken into account.

For the triplets Γ_4 and Γ_5, which arise only in cubic symmetry, the hyperfine Hamiltonian is characterized by a single parameter A and

$$H_{hf} = A\mathcal{J}I \quad (58)$$

with $\mathcal{J} = 1$.

In the case of a Γ_8 quartet, the same arguments as used in the deduction of the Zeeman interaction, lead to the following hyperfine Hamiltonian:

$$H_{hf} = A\,\mathcal{J}\,I + U\{\mathcal{J}_x^3 I_x + \mathcal{J}_y^3 I_y - \mathcal{J}_y^3 I_z - [\mathcal{J}\bullet I)(3\mathcal{J}(\mathcal{J}+1-1]/5\}. \quad (59)$$

When the nuclear spin $I \geq 1$, the nuclear quadrupole interaction must be taken into account. For a Kramers doublet, if the symmetry is rhombic, the quadrupole Hamiltonian is, as shown before

$$H_Q = P\{[I_z^2 - I(I+1)/3] + \eta(I_x^2 - I_y^2)/3\} \quad (60)$$

When the symmetry is axial, the "asymmetry parameter" η vanishes, and for cubic symmetry P is equal to zero.

In the case of the triplets Γ_4 and Γ_5 and the quadruplet Γ_8, the quadrupole interaction depends, not only on the parameter P, but also on two constants m and n, and can generally be written as (1):

$$H_Q = P[(m/6)\sum_{q=1}\{3I_q^2 - I(I+1)\} + (3n/4)\sum_{p\neq q}(I_pI_q + I_qI_p)(\mathcal{J}_p\mathcal{J}_q + \mathcal{J}_q\mathcal{J}_p)]. \quad (61)$$

When the superhyperfine interaction with the ligand nuclei is also present, it leads to an additional splitting of the energy levels. The superhyperfine Hamiltonian is a sum of individual contributions. If the symmetry of the crystal field is cubic, such an individual is of the axial form:

$$H_L = A_\parallel {}^L I_z {}^L\mathcal{J}_z + A_\perp {}^L(I_x {}^L\mathcal{J}_x + I_y {}^L\mathcal{J}_y) - g_n {}^L\beta_n H\bullet I^L, \quad (62)$$

where the symmetry axis is along the ion-ligand bond. Sometimes, when $I^L \geq 1$, a ligand nuclear quadrupole interaction $P_\parallel {}^L[(I_z {}^L)^2 - I^L(I^L + 1)/3]$ must be added to equation 62. When the symmetry of the crystal field is lower than cubic, more hyperfine parameters are necessary in equation 62. Thus, for a tetragonal distortion, the superhyperfine part is

$$H_L = \mathcal{J}\bullet A\bullet I$$

and depends (129) on five parameters:

$$A = \begin{vmatrix} A_1 & A_2 & A_4 \\ A_2 & A_1 & A_4 \\ A_5 & A_5 & A_3 \end{vmatrix}. \quad (63)$$

The superhyperfine interaction leads to a very complex splitting of the energy levels, depending on the number, nature, and the symmetry of the ligands around the central ion.

These considerations show that the Zeeman splitting in combination with (or without) the hyperfine interaction contains a large amount of information on the ion under study and on the host. However, the study of the Zeeman effect on the optical transitions of the ions in crystals is difficult since it amounts to much less than 1 cm^{-1}, and most information is lost because of the width of the optical transitions. A very useful method, which circumvents many of the difficulties encountered in the study of the optical Zeeman effect is EPR.

III. SURVEY ON PARAMAGNETIC RESONANCE

Usually, only the lowest Zeeman components, which are populated at the temperature at which the experiment is carried out, are involved in the resonance phenomena. The ensemble of these states are characterized as the states of a fictitious (or "effective") spin $\mathcal{S}$, $(2\mathcal{S} + 1)$ being the number of the levels involved in the resonance transitions. When the paramagnetic centers are ions in crystals, these levels are Zeeman components of the crystal field levels, and the effective spin $\mathcal{S}$ is usually different from the real spin S. In almost all cases only the states of a single crystal field level are involved in resonance, and the effective spin can be identical to the fictitious angular momentum $\mathcal{J}$ defined above. In this case, the electromagnetic field will induce transitions between states which are eigenfunctions of a so-called "spin Hamiltonian" which collects together all the interactions described in the Section II.D.4, written in the components of the effective spin: the electronic and nuclear Zeeman, the hyperfine, superhyperfine, and nuclear quadrupole interaction. In some situations the effective spin is larger than that determined from the number of levels involved in resonance. In this case, a zero-magnetic field splitting term (stronger than the electronic Zeeman interaction) must be added to the spin Hamiltonian in order to separate the levels which take part in the resonance phenomenon from the other levels which are not involved. A typical case is that of the resonance inside the doublet originating from a Γ_4 or Γ_5 triplet state due to an axial distortion. Though only two levels are involved in the resonance, the most suitable classification for them is as the states $|+1\rangle$ and $|-1\rangle$ of a fictitious spin $\mathcal{S} = 1$, and the state $|0\rangle$ is removed by adding a term $D[\mathcal{S}_z - \mathcal{S}(\mathcal{S}+1)]$ to the spin Hamiltonian.

An electromagnetic field interacts with the electronic magnetic moments through its magnetic component $H_1 \cos\omega t$,

$$H = -\mu\bullet H_1 \cos\omega t. \quad (64)$$

If we consider a paramagnetic ion without nuclear spin, whose ground state is a Kramers doublet and whose gyromagnetic factor is characterized by three values (g_x, g_y, and g_z), and if $H_1 << H_0$, the interaction of equation 64 will

induce between its two states, transitions with the probability P per unit time which is proportional to

$$P \sim H_1^2 |\langle M_S | g_x S_x + g_y S_y + g_z S_z | M_S' \rangle|^2 g(\nu). \quad (65)$$

The function $g(\nu)$ is the line shape function and expresses the effect of the various interactions which can lead to a finite width of the resonance lines. The source of broadening can be inhomogeneities in the applied magnetic field, interactions between spins, and so on. For a Kramers ion the line shape is usually symmetric and $g(\nu)$ can be expressed by Gaussian or Lorentzian functions centered on the frequency ν_0:

$$h\nu_0 = E_{M_S} - E_{M_S'}. \quad (66)$$

The matrix element in equation 65 shows that the transition is governed by the selection rule $|M_S - M_S'| = 1$, and the probability is maximum when the variable magnetic field is in the plane (x y).

For a Kramers doublet equation 66 establishes a connection between the electromagnetic field frequency and the external magnetic field H_0:

$$h\nu_0 = g_{eff} H_0. \quad (67)$$

For the usual magnetic fields of 10^3 - 10^4 Gauss, the frequency is of the order of 10^{10} Hz.

Spin-lattice relaxation can be accomplished through different processes based on the interaction of the paramagnetic ion with the lattice vibrations. This interaction leads to an exchange of energy between ion and lattice by absorption and/or emission of phonons (energy quanta of the lattice vibrations). The main processes of the spin-lattice relaxation are:

(a) The modulation of the interaction between spins due to the lattice vibrations. There are two such processes (130), a direct one by which the spin undergoes a resonance transition due to the absorption or emission of a resonant phonon ($\nu_p = \nu_0$), and biphononic (or Raman) process by which the spin interacts with a non-resonant phonon, undergoes a resonance transition and emits another phonon of frequency ($\nu_p \pm \nu_0$).

(b) the modulation of the crystal field due to the lattice vibrations (the Orbach process) (131, 132). This leads to a dynamic orbit-lattice interaction which, through the spin-orbit interaction causes relaxation of the spin. As in the previous case, there are direct and bi-phononic Orbach processes.

The spin-lattice relaxation time T_1 has a characteristic temperature dependence for each of the processes described above. The relaxation phenomena have a strong influence on the EPR experiments. They can broaden the lines and in many instances EPR can be observed only at very low temperatures, when the relaxation processes are less effective.

When a hyperfine interaction is present and it is much weaker than the electronic Zeeman interaction (the usual case), the nuclear spin will be, as shown below, quantized along the effective electronic magnetic field. As a result the nuclear eigenfunctions depend parametrically on the electronic quantum number M_S for each electronic state, and the wave function of the system can be written as a product $|M_S m(M_S)\rangle = |M_S\rangle|m(M_S)\rangle$.

In this case the transition probability in unity time is proportional to

$$P \sim H_1^2 |\langle M_S | g_x S_x + g_y S_y + g_z S_z | M_S' \rangle|^2 g(\nu) |d_{mm'}^{(I)}(\omega)|^2 \quad (68)$$

where $d_{mm'}^{(I)}(\omega)$ has been defined in Section II.C. When the angle between the two electronic effective fields is equal to π, $d_{mm'}^{(I)}(\pi) = 0$, and the selection rule for the hyperfine transitions is $m - m' = 0$. Each electronic transition will then be split into $(2I + 1)$ hyperfine components of equal intensity. If the angle ω is different from π, transitions with $m - m'$ different from zero can appear (forbidden hyperfine transitions).

The superhyperfine interaction leads to an additonal splitting of the resonance lines. In this case the effective electronic fields cannot be considered as collinear except for some orientations of the external magnetic field. For these special orientations only the allowed superhyperfine transitions with the selection rule $\Delta m^L = 0$ can occur, and each electronic transition is split into $(2I^L + 1)$ components. For all other orientations the spectra may contain forbidden superhyperfine transitions.

If the paramagnetic ion is surrounded by n equidistant ligands (ligands of the same isotopic species, at the same distance from the central ion), and the direction of the magnetic field makes the same angle with the central ion-ligand direction for all these ligands, the superhyperfine structure consists of $(2nI^L + 1)$ components whose intensity is symmetrically distributed

according to the binomial rule:

$$1 : n : n(n-1)/2 : .... :$$

$$n!/k!(n-k)! : ....:$$

$$n(n-1)/2 : n : 1.$$

In the case of an odd number of equivalent ligands, there will be an even number of superhyperfine components. When there are many groups of inequivalent nuclei, the superhyperfine structure from each group obeys the same rule, but the overall superhyperfine pattern is very complex. For arbitrary orientations of the magnetic field, this pattern is further complicated by the presence of the forbidden transitions. Usually the superhyperfine splitting is small and can be obscured by the linewidth. Also in many instances, it is impossible to make EPR superhyperfine measurements along the principal axes (which give directly the diagonal components of the interaction) because the structure due to the particular ligand is concealed by the unresolved structure due to the other ligands. In this case special techniques such as ENDOR (Electron Nuclear Double Resonance) must be used. This technique makes possible the measurement of the effect of a nuclear magnetic resonance-like transition ($\Delta m_I^L = 1$) on the electron paramagnetic resonance line by the simultaneous application of a strong microwave field and of a radiofrequency field of a frequency corresponding to the "nuclear" transition which is proportional to the superhyperfine splitting. This technique allows also the determination of some very fine effects as for instance the pseudonuclear g-value. This can arise when some low-lying excited states are admixed into the ground state, by the common action of the electronic Zeeman and hyperfine interaction or the pseudoquadrupole effect, which expresses the mixing of the excited states into the ground state through a second-order hyperfine interaction (133).

For a cubic triplet Γ_4 or Γ_5, the spin Hamiltonian (S = 1) contains an electronic Zeeman term with an isotropic g-value and a sum of terms $D_{ij}S_i \bullet S_j$, which express the small zero-field splitting produced by the lattice strains. At the same time, these strains can mix the three states of the triplet, and the magnetic microwave field can induce transitions with $\Delta M = 1$ between the states $|-1> \leftrightarrow |0>$ and $|0> \leftrightarrow |1>$ and transitions $\Delta M = 2$ between the states $|-1>$ and $|+1>$. These latter transitions are known as "half-field" transitions because they show up at an apparent g-value, g^{app}, of 2g. The transitions $\Delta M = 2$ can also be induced by the electric component of the microwave field. At very high intensities, transitions of the type $\Delta M = 2$ can be induced by the simultaneous absorption of two microwave quanta at $g^{app} = g$ (134). The normal $\Delta M = 1$ transitions are very broad because the M = 0 Zeeman level is very sensitive to the lattice strains, especially to those of axial symmetry. The distribution of these lattice strains leads to a strong broadening of the M = 0 level and of all the resonance transitions in which this level is involved. The levels M = +1 are broadened only due to the lower symmetry strains through a second-order effect, so the "half-field" transitions are much narrower than the M = 1 transitions. The double-quantum transitions are still narrower because they are influenced by the broadening of only one of the levels $|\pm 1>$. Thus the double quantum transitions show up as very sharp lines superimposed on the very broad lines with $\Delta M = 1$. In the case of an axial distortion, the triplets Γ_4 or Γ_5 are split into a doublet and a singlet. If the doublet is lowest, resonance transitions can be induced between its two levels. Though the resonance observed is inside of a doublet, which can be well isolated from any other levels, the best formalism to describe the resonance is an effective spin S = 1 formalism with two principal g-values ($g_\parallel$ and $g_\perp$) and with the axial zero-field splitting term $D[S_z^2 - S(S + 1)]$ added as explained before. The apparent g-values at which the resonance is observed are $g_\parallel^{app} = 2g_\parallel$ and $g_\perp^{app} \sim 0$. The term corresponding to the lattice strains is also included. For a triplet (Γ_4 or Γ_5) or a non-Kramers doublet, the presence of strains has a strong effect on the line shape, which is no longer symmetrical as in the case of Kramers ions but is broad on the low magnetic field side and sharp on the high field side. The hyperfine interaction shows similar features to the g-value, i.e, for a non-Kramers doublet $A_\parallel^{app} = 2A$, $A_\perp^{app} \sim 0$, and the quadrupole interaction has no effect upon the spectra.

The electron paramagnetic resonance for Γ_8 quartets is very unusual. The spin Hamiltonian when I = 0 is given by equation 3, and the energy eigenvalues can be obtained by solving the bi-quadratic secular equation 40. An accurate analytical solution for equation 40 cannot be obtained except for some special orientations of the external magnetic field with respect to the cubic axes. As expected from the form of equation 40, the Zeeman levels are anisotropic and are symmetric in pairs with respect to the zero energy. When the magnetic field is along the cube edge, three resonance transitions are

usually observed, the transition $|-\bar{1}/2> \leftrightarrow |\bar{1}/2>$ at an effective g-value of 2Q and with an intensity proportional to $(3P - Q)^2$, the line $|\bar{3}/2> \leftrightarrow |-\bar{3}/2>$ at 2P and with an intensity $(P - 3Q)^2$ and a line corresponding to the transitions $|\pm\bar{1}/2> \leftrightarrow |\pm\bar{3}/2>$ at P - Q, with an intensity $3(P + Q)^2$, the first two lines are sharp, but the third one is usually much broader, being very sensitive to any weak distortions of the cubic field. In many cases, because of its large line width and low intensity, this line is not seen in the spectra. The lines are usually very anisotropic. Thus the line at 2P with H along $|100|$ goes in $\sqrt{3(P^2 + Q^2) + 2PQ}$ with H along $|111|$ and in $\{2(P^2 + Q^2) - \frac{1}{2}(P + Q)\sqrt{7(P^2 + Q^2) - 2PQ}\}^{\frac{1}{2}}$ along $|110|$, while the line at 2Q with H along $|100|$ goes in P - Q with H along $|111|$ and $\{2(P^2 + Q^2) + \frac{1}{2}(P + Q)\sqrt{(7P^2 + Q^2) - 2PQ}\}^{\frac{1}{2}}$ with H parallel to $|110|$ (135). The intensity of the lines also dependent on orientation. For instance, around $|111|$ the lines $\bar{1}/2> \leftrightarrow |-\bar{1}/2>$ and $|\bar{3}/2> \leftrightarrow |-\bar{3}/2>$ drop almost completely while the transitions $\pm\bar{1}/2> \leftrightarrow |\pm\bar{3}/2>$ become strong. The parameters 2P and 2Q which characterize EPR of an ion whose ground state in a cubic field is a Γ_8 quartet can be connected with the composition parameter of the crystal field potential using the analytical expression for the wavefunctions given in Section II.B.7. Thus in the case of a Γ_8 state originating from a J = 9/2 level, the EPR parameters can be calculated using the wavefunction of equation 11a. Finally we get (79, 80)

$$2P = (3\cos^2\Theta - 5\sin^2\Theta)K_J g_J$$

$$2Q = (3\cos^2\Theta - 5\sin^2\Theta + 8\sqrt{21}\sin\Theta\cos\Theta)K_J g_J/3 \qquad (69)$$

where g_J is the Lande factor for the ground electronic state (in case of a pure $^4I_{9/2}$ state it is 8/11), K_J is a reduction factor for g_J and the fictitious angle Θ is defined by equation 11c. The knowledge of the resonance parameters 2P and 2Q allows one the determination of both 0 and K_J.

For a weak distortion, the usual resonance is observed inside the lowest Kramers doublet with g-values given by equation 44a or b or by equation 45a, depending on the symmetry and sign of the distortion. When a trigonal distortion leaves the doublet $|\pm 3/2>$ lowest, no resonance can be observed in this doublet.

We stress the fact that the strong g anisotropy given by equation 44a and b and 45a is connected only with the values of the cubic parameters P and Q and not with the intensity of the axial distortion. If the axial distortion is strong, it can admix other states in the Kramers doublet and the g-values will be different from those given in equations 44a and b and 45a and b.

Transitions between the Zeeman components of the crystal field levels of the paramagnetic ions in crystals can be induced not only by an electromagnetic field, but also by the oscillations of the crystal field caused by an external acoustic field of suitable frequency. This kind of resonance is known as acoustic paramagnetic resonance (APR) or ultrasonic paramagnetic resonance (UPR) and has been used in the study of U^{4+} in fluorite.

This brief account of the EPR method shows that is of great value in determining the properties of the lowest Zeeman levels of the ground state. Because the Zeeman interaction and the other interactions described by the spin Hamiltonia are perturbations on the eigenstates of the other interactions, the parameters determined in an EPR experiment can be useful to understand some general properties of the ion under study.

IV. EPR STUDIES OF URANIUM IONS

A. Studies of Hexavalent Uranium

Hexavalent uranium is diamagnetic and cannot be studied by EPR. However, some EPR studies on paramagnetic centers connected with hexavalent uranium or on paramagnetic U^{5+} centers obtained by transforming U^{6+} by trapping an electron on the lowest excited level (as discussed in Section II.A.3g) proved to be useful in obtaining information on the U^{6+} centers. This electron can be supplied by irradiating the crystals which contain U^{6+} with gamma or X-rays at room temperature. As examples we discuss the case of U^{6+} in alkali- and alkaline-earth fluorites. The bright green or yellow luminescence of the U^{6+} complexes in alkali (Li, Na, K) or alkaline-earth (Ca, Sr) fluorite crystals grown in the presence of oxygen has been known for a long time.

1. Alkali Fluorides

Many studies of optical absorption, luminescence, piezospectroscopic effects, Stark effect or chronospectroscopy on hexavalent uranium in alkali fluorides (136-145) have established that there is a great variety of luminescent centers, all connected with the presence of oxygen and the symmetry of the prevailing centers is C_{4v} or C_{2v}. In all these cases the direction $|100|$ plays a

particular role in the symmetry of the centers. For the main luminescent center in LiF and NaF, the symmetry has been established unambiguously as C_{4v}. The luminescence spectra from this center contain two series of lines, one of electric dipole nature (with zero-phonon lines at 5185 Å for LiF and 5528 Å for NaF) and one of magnetic dipole nature (5277 Å and 5636 Å). Because of its relatively small ionic radius, the hexavalent uranium (0.73 Å) can easily substitute for the alkali ions (Li^+, 0.68 Å; Na^+, 0.97 Å and K^+, 1.33 Å) while O^{2-} (1.34 Å) substitutes easily for F^- (1.33 Å), thus assuring the charge compensation. Some other point defects can also contribute to the charge compensation. Despite the large amount of work devoted to these systems, the optical studies could not give the answer to some very important problems such as:

(i) The nature of the uranium centers. Basically the models proposed can be divided into two groups (146): those based on a uranyl (UO_2^{2+}) group, and those based on a uranate structure (U^{6+} equally bonded to more oxygens). In the first case it has been assumed that the uranyl group substitute for F^- - M^+-F^- (along a |100| direction) (140, 143). A recent paper which disregards previously published data proposes a uranyl group directed along |111| substituting for the alkali ion and a fluorine vacancy on the same axis (147). This model gives a trigonal symmetry for the center, though the previous measurements have shown clearly that none of the U^{6+} luminescent centers in LiF has trigonal symmetry. In the second group of models, Runciman (137) proposed that the main luminescent center was an octahedral uranate group UO_6^{6-} which substituted for the group MF_6^{5-}. Feofilov (139) proposed a model with U^{6+} substituting for M^+ and five O^{2-} substituting for F^- in the nearest neighborhood of uranium. A model based on a planar square uranate group has also been proposed (144).

(ii) The nature of the vicinity of the active uranium center. All the models presented above, except that of Feofilov (139), cannot assure the complete charge compensation of uranium. This model also gives C_{4v} symmetry for the center. However, it cannot explain the large variety of the luminescent centers, and thus other models must also be considered. In the case of the uranyl-based models, the charge compensation has been assumed to be by some substitutional oxygen ions in the equatorial plane. The variety of the luminescent centers has been assumed to originate from the number of those substitutional O^{2-} ions. However, this model cannot explain the C_{4v} symmetry of the main luminescent center, except for the situation when a charge compensator is placed in the same direction as the uranyl axis.

For the octahedral uranate model proposed by Runciman, the extra negative charge has been assumed to be compensated either by a fluorine vacancy on the |111| direction (this would give a trigonal symmetry for the centers, which has not been confirmed by experiment) or by some substitutional high valence cations. This later model can explain a large variety of centers as well as the C_4 or C_{4v} symmetry. Runciman was able to check this assumption by introducing calcium or silicon into uranium-doped NaF and by observing their effect on the uranium luminescence or absorption spectra.

A recent model, based on luminescence and electrical conductivity measurements, assumes that the main U^{6+} center in NaF is a UO_6^{6-} complex associated with a F^- vacancy on the |100| axis (148-150).

EPR has proved to be very useful in giving information on the structure of these centers. Two main directions were investigated:

(a) In order to check the possibility of association of the octahedral uranate group with substitutional cations of valence higher than 1, paramagnetic ions of valence +2 (Cu^{2+}, Mn^{2+}), +3 (Fe^{3+}, Cr^{3+}) (151, 152), or +4 (Mn^{4+}) (153) have been introduced together with uranium in LiF and NaF.

The EPR spectra of these samples are very complex and show the presence of a large variety of paramagnetic centers involving either the paramagnetic dopant ion, or other ions accidentally present in the samples. Thus paramagnetic ions in valence states which generally cannot be obtained in the alkali fluorides could be stabilized this way. A typical example is the Cu^{2+} ion for which a large variety of centers have been obtained by co-doping LiF with uranium and copper oxides. Uranium is so effective in stabilizing Cu^{2+} in LiF that this ion shows up as an accidental impurity in almost all (even the purest) LiF:U crystals. The Cu^{2+} spectra show usually tetragonal or rhombic (|100| or |110|) symmetry, and in most cases a superhyperfine structure with less than six fluorine nuclei (151, 152). The very large anisotropy of the g-value and of the hyperfine structure as well as the

strong quadrupole interaction, show that these ions are submitted to the action of a strong axial distortion of the crystal field. This means that the Cu^{2+} ions are not placed randomly in the lattice, but in such a position that the first coordinating sphere contains not only F^- ions but also O^{2-}. Together with the strong crystal field distortion, this suggests that the Cu^{2+} ions are placed in the near neighborhood of the U^{6+} ion surrounded by an oxygen octahedron and contribute to the charge compensation. No trigonal Cu^{2+} centers have been observed, but in case of the EPR spectra of higher valence paramagnetic co-dopants, this symmetry predominates. Thus for Mn^{4+} in uranium doped LiF crystals (135), only a trigonal EPR spectrum corresponding to a very strong axial crystal field (the fine structure term D is stronger than the electronic Zeeman interaction) has been observed. It is difficult to give an accurate model for this Mn^{4+} center, but obviously its presence is connected with the presence of the hexavalent uranium.

Thus the EPR studies have shown that Runciman was correct in assuming that the hexavalent uranium can introduce in the alkali fluorite crystals more oxygen than necessary for its charge compensation and that the negative extra charge present can be compensated by introducing in the crystals cations with valence larger than +1. It was also shown that this aliovalent cation can occupy different substitutional positions around the uranium-oxygen complex, thus explaining, at least in part, the variety of the luminescent uranium centers in these crystals. The concentration of paramagnetic ions which could be introduced this way into the alkali fluorides was sensibly smaller than the total concentration of uranium centers.

(b) A more direct insight into the structure of luminescent U^{6+} centers in alkali fluorides is obtained if the U^{6+} ions can be converted into paramagnetic U^{5+} ions. From the characteristic features of the EPR spectra of these U^{5+} ions (symmetry, g-values, superhyperfine structure), the structure of the parent U^{6+} centers can sometimes be inferred. The irradiation at room temperature with X- or gamma rays has proven to be very effective in transforming U^{6+} into U^{5+} in LiF (154-156), NaF (155-157) and KF (158). A large variety of U^{5+} centers has been obtained whose study gives information about the parent U^{6+} centers too (146). It is concluded that even if a parent U^{6+} center can produce many U^{5+} centers by irradiation, the EPR studies show that there is a large variety of U^{6+} centers. The very small g-values of the EPR spectra show that the paramagnetic centers are uranate (V) species and not uranyl (UO_2^{+}) structures for which values of $g_\parallel \sim 4$ and $g_\perp \sim 0$ should be expected (as for the case of the neptunyl groups (159)). This rules out completely the uranyl-based models for the luminescent centers in alkali fluorides.

The symmetry of the U^{5+} centers is either cubic, tetragonal, orthorhombic, or of lower symmetry. For almost all the EPR spectra, the crystal |100| axis is one of the main symmetry axes. Rotations from this direction, observed for some low symmetry U^{5+} centers, can be connected with some defects associated with U^{5+} and are not connected with the original U^{6+} centers. No center of trigonal symmetry has been observed.

In LiF and NaF the prevailing U^{5+} center has tetragonal symmetry and shows superhyperfine stucture due to a F^- ligand placed on the symmetry axis. Measurements on selected samples (which contain almost only one type of luminescent center) have shown that this U^{5+} center can be connected with the main luminescent center of C_{4v} symmetry (154, 155, 160). This shows that the main luminescent U^{6+} center in LiF and NaF has the structural model proposed by Feofilov (130). The likelihood of this model has been stressed in some recent studies on absorption and laser excitation and MCD or U^{6+} in LiF (161, 162), using as argument the EPR studies on U^{5+} (155). This rules out the model (148-150) based on a UO_6^{6-} complex associated with a fluorine vacancy on the 100 axis.

The prevailing U^{5+} center in KF has quasi-tetragonal symmetry with a superhyperfine structure due to two ligand nuclei with I = 1/2. Centers of tetragonal or lower symmetry with such structure have been observed also in NaF and LiF (146, 156, 158). The superhyperfine splitting for these centers is much smaller than for the center discussed above and can be due either to two protons (in two OH^- groups or a H_2O^- group) or to two fluorine nuclei in a F_2^- group placed on the symmetry axis. Most probably, this association, which involves two I = 1/2 nuclei, is formed during irradiation by trapping one of them by the other which is originally connected with the U^{6+} center.

Many U^{5+} centers without superhyperfine structure and with a slight anisotropy have been observed in LiF:U co-doped with silver, copper, or gold, which originate in the parent uranate UO_6^{6-} groups.

A very anisotropic tetragonal U^{5+} center without superhyperfine structure can be

explained by a model implying a fluorine vacancy on the distortion axis. Most probably this vacancy is formed during irradiation.

2. Alkaline-earth Fluorides

The green luminescence of uranium in fluorite prepared in the presence of oxygen has been known for a long time (136, 163, 164), but a definite structural model for this center has not been inferred from these studies. The first model for this luminescent center assumed that U^{6+} enters substitutionally for Ca^{2+}, and four of the eight F^- ions are substituted by O^{2-} ions in order to preserve the charge neutrality (165). Thus the U^{6+} ion would be surrounded by two tetrahedra, one of F^- ions, the other of O^{2-} ions, resulting in a crystal field of inversionless symmetry. Recent Zeeman studies on the main luminescent line at 5212.5 Å have shown that the center has trigonal symmetry with inversion (166). Three structural models were proposed without a definite preference for one of them, viz.

(a) a substitutional uranyl ion with the axis along a cubic |111| direction;

(b) a substitutional U^{6+} ion surrounded by two fluorine vacancies on the same body diagonal of the cube, and with the other F^- ions substituted by O^{2-};

(c) an interstitial U^{6+} ion surrounded by six substitutional O^{2-} ions and two F^- ions on the same |111| direction.

All these models assure a complete charge compensation within the first coordination sphere of uranium. In order to select the right model, an EPR study of the transformation of the hexavalent uranium into pentavalent uranium under gamma irradiation has been performed. The samples contained before irradiation, besides the hexavalent uranium, three U^{5+} centers (167-169): a trigonal center (Tr), without superhyperfine structure, which consisted of a substitutional U^{5+} ion surrounded by six substitutional O^{2-} ions and two fluorine vacancies on the same |111| direction, a rhombic center (Rh_1) whose structure is similar to the Tr center except that there are only five substitutional O^{2-} ions and a F^- ligand in the first coordination sphere (these centers have also been identified in U^{4+}-doped fluorite (170-172)), and a low-symmetry U^{5+} center (Rh_3) without superhyperfine structure, which presumably has the same first coordination sphere as the Tr center plus a nearby additional charge compensating defect.

The gamma irradiation has a strong effect on the luminescent U^{6+} center, whose spectrum decreases with radiation dose while a similar increase is noticed in the intensity of the trigonal U^{5+} EPR spectrum. The dependence on dose is not smooth, probably because of some competitive processes such as the decrease of the intensity of the Rh_1 and Rh_3 U^{5+} EPR spectra or a transformation of part of the Tr centers due to irradiation. The parallel behavior of the luminescent U^{6+} centers and of the Tr U^{5+} centers under irradiation shows that their structure is similar, and thus the luminescent U^{6+} ion is substitutional and has six O^{2-} and two fluorine vacancies in the first coordination sphere. The absence of any EPR spectrum with resonance parameters close to those of UO_2^+ in the irradiated samples shows that no uranyl centers are present in the non-irradiated crystals.

The trigonal U^{6+} center has a strongly emitting level at 5212.5 Å. This luminescence line can be used in order to measure ultratrace levels of uranium in aqueous solutions (173, 174). Uranium is co-precipitated from solutions with calcium fluoride, the precipitates are calcined in air so as to assure the formation of the uranate centers described above and the luminescence is excited with a suitable laser. By a careful choice of the experimental conditions, amounts as low as 4×10^{-14} M (10^{-5} parts per billion or 0.01 picograms per milliliter) could be detected by this method (173).

These few examples show that the EPR measurements can be very useful in obtaining information on the structure of luminescent U^{6+} centers. Connected with luminescence (154, 160, 161, 167-171) or thermoluminescence (175) studies, the EPR measurements can also be useful in the study of the conversion U^{6+} U^{5+} during irradiation.

B. EPR of Pentavalent Uranium

As shown previously, because the actinide contraction is small at the beginning of the series, the 5f orbital is not so well localized as the 4f orbital in the lanthanide series. Thus, despite the large spin-orbit coupling in the actinides, the crystal field effects for the ions of $5f^1$ configuration can be for octahedral symmetry of the same order of magnitude or even stronger than the spin-orbit effects. For eightfold or tetrahedral symmetry, the crystal field effects are small, and a situation similar to the $4f^1$ ions is expected. The determination of the spectroscopic g-value by EPR is of great importance in obtaining information of the crystal field and bonding effects in crystals with U^{5+}. Some characteristics of the EPR of this ion are as follows:

(a) Because of the strong crystal field

effects with octahedrally-coordinated U^{5+} ions, the excited levels are high enough, so that the relaxation processes are slow, and the EPR spectra can be recorded at liquid nitrogen or even higher temperatures.

(b) For U^{5+} in extremely strong axial fields (e.g the groups UO_2^{+}) some of the excited levels could be lowered near the ground state, leading to a strong spin-lattice relaxation. This in turn causes a pronounced broadening of the lines and the spectra can be recorded only at liquid helium temperature.

(c) For eightfold cubic coordination the Γ_8 and Γ_6 levels originating from the ground $^2F_{5/2}$ level of the free ion are bunched together, a strong relaxation takes place, and the spectra can be recorded only at very low temperatures. A strong distortion may spread the crystal field levels, the relaxation is weakened, and the resonance could be, in principle, observed at somewhat higher temperatures. For a trigonal distortion the ground state could be the non-magnetic doublet Γ_3 and in such a case no resonance takes place.

(d) The sign of the g-value is negative.

(e) The effective g-values are usually very small, and high magnetic fields must be employed in order to observe the resonance.

1. U^{5+} in Octahedral Crystalline Fields

The EPR data for U^{5+} in diluted and concentrated systems are given in Appendix I and Appendix IV.

For the concentrated systems the lines are broad and slightly asymmetric, but in diluted systems they are sharp and symmetric, characteristic for Kramers ions.

1a. U^{5+} in Concentrated Systems

EPR measurements have been performed on concentrated halides and oxides of U^{5+}. While in the case of halides, the measurements have been successful (88, 91, 95, 176-180), no clear evidence for U^{5+} resonance have been obtained for oxides.

For many U^{5+} concentrated systems, optical data are available, and thus some of the characteristics of the crystal split levels (the crystal field splitting and the orbital reduction factors) can be estimated.

The g-values for the U^{5+} ion in concentrated halides are very low. Some general trends can be observed in case of the concentrated systems. The mean g-value (defined at $(2g_\perp + g_\parallel)/3$ in the case of axial symmetry) is around 0.6 to 0.77 when the ligands are F^- ions, 1.09 to 1.21 when the ligands are Cl^- and 1.2 to 1.39 for compounds with Br^-, i.e. the g-values are larger in the more covalent compounds. The same trend is observed for the energy difference between the Kramers doublets Γ_7 and Γ_7' which is of the order of 7300 to 7400 cm^{-1} in the compounds with F^-, 6700 to 7000 in compounds with chlorine and 6700-6850 in compounds with bromine (91). An analysis of the crystal field splitting based on these experimental data shows that for cubic complexes of pentavalent uranium, while the orbital reduction factor $k_{a_2 t_2}$ does not change much from compounds with F^- ($k_{a_2 t_2}$ = 0.935) to those with Br (0.906), the reduction factor $k_{t_2 t_2}$ is very sensitive to the neighborhood of uranium (0.9 for UF_6^-, 0.75 for UCl_6^-, and 0.50 for UBr_6^-). The crystal field splitting decreases strongly along this series, being respectively 3369 cm^{-1}, 1119 cm^{-1}, and 835 cm^{-1}. Unfortunately, the data given by different authors are not easily comparable, because different approximations have been used. Thus, many papers use a purely electrostatic crystal field, neglecting completely the orbital reduction. Other authors use the approximation $k_{a_2 t_2} = \sqrt{k_{t_2 t_2}}$, which has been assumed in the study of neptunium hexafluoride (85) and which shows up to be incorrect (91, 95). This explains why sometimes contradictory results on the same system are reported, as is the case of $CsUF_6$ (181, 182). A connection between the data obtained from EPR and those obtained from magnetic susceptibilty has been made (183).

A systematic search for U^{5+} EPR in some concentrated oxides of pentavalent uranium has been undertaken but none of the investigated compounds, namely $NaUO_3$, $LiUO_3$, KUO_3 and Ba_2ScUO_6 (perowskite structure), Li_3UO_4 and Na_3UO_4 (rock salt structure), and $BiUO_4$ (fluorite structure) has shown any detectable signal at temperatures as low as 7 K (184). More recent measurements on mixed oxides MUO_3 (M = Li, Na, K, Rb) have shown, even at room temperature, very broad signals with g-values between 2.4 and 4 (185). These resonances cannot be explained by simple crystal field models for U^{5+}.

1b. U^{5+} in Dilute Systems

If for concentrated compounds the problem of the structure of the paramagnetic center is not so difficult because crystallographic structural data can be used, with diluted systems the

problem is more complex. Two kinds of diluted systems have been studied, viz. systems for which the host cation has the same valence as the dopant and there is only one site of substitution, and systems where the valence of the host cation differs strongly from the dopant ion and the charge compensation mechanisms can give a large vaiety of paramagnetic centers.

1c. U^{5+} in Diluted Oxide Systems

The EPR studies on U^{5+} in $LiNbO_3$, $LiTaO_3$, and $BiNbO_3$ (184) refer to the first category. The U^{5+} ion gives a spectrum of g about 0.7, and the symmetry of the site appears to be almost perfectly octahedral. The energy diffrence between Γ_7 and Γ_7' is about 7050 cm^{-1}. From this transition and the lines corresponding to the $\Gamma_7 \leftrightarrow \Gamma_8$ and $\Gamma_7 \leftrightarrow \Gamma_6$ transitions, the reduction factors $k = 0.8$ and $k' = 0.34$ (in the assumption $k_{a_2 t_2} = \sqrt{k_{t_2 t_2}} = k$; $k_{t_1 t_1} = k'$ and $k_{t_1 t_2} = \sqrt{k_{t_1 t_1} k_{t_2 t_2}} = \sqrt{kk'}$) have been estimated. The search for EPR signals in some other U^{5+}-doped (1 to 5%) niobates or tantalates with octahedral coordination for the pentavalent cation has been unsuccessful (184).

1d. U^{5+} in Diluted Fluorides

There are two cases as follows:

(a)U^{5+} *in alkali fluorides.* As shown in Section IV.A, hexavalent uranium can be introduced substitutionally in alkali fluoride crystals grown in the presence of oxygen. The EPR and optical studies of the crystals show that they do not contain any paramagnetic uranium ion (U^{2+} to U^{5+}) and all the uranium is in the hexavalent form. These U^{6+} ions can be converted to U^{5+} by X- or gamma irradiation, and a great variety of paramagnetic centers can be formed this way, corresponding to the variety of initital U^{6+} centers. Moreover, a parent U^{6+} center can give rise to more types of U^{5+} centers. The structure and symmetry of these centers has been discussed in connection with the structure of the parent U^{6+} centers. As shown in Appendix I, taking into account the superhyperfine structure,these centers can be divided roughly into three groups: centers without superhyperfine structure, centers with a two-component and centers with a three-component superhyperfine structure (146). In Appendix I a cubic center C in LiF corresponds most probably to a U^{5+} ion surrounded by a regular octahedron of oxygens. The centers Tg4 and Rh5 for LiF:U^{5+} and the center Rh1 for NaF:U^{5+} most probably correspond to the same structure (UO_6), but the cubic crystal field is perturbed by a defect in the next cationic coordination sphere (such as a substitutional M^{2+} or M^{+} ion). The Tg3 center in LiF corresponds to a strong deformation of the crystal field due, probably, to an anionic vacancy in one of the corners of the octahedron. Two types of centers with two-line superhyperfine structure have been observed, which differ in the magnitude of splitting. The first type of such centers is characterized by superhyperfine splittings which can reach values up to $A_{\parallel}^{L} = 14.3 \times 10^{-4}$ cm^{-1} in LiF and $A_{\parallel}^{L} = 9.8 \times 10^{-4}$ cm^{-1} in NaF. These centers correspond to a substitutional U^{5+} ions surrounded by five substitutional O^{2-} ions and a F^- ion. In the case of the tetragonal centers Tg1 in LiF and NaF the negative extracharge of the complex is compensated far away. For the Rh1, Rh2, and Rh3 centers in LiF and for the center Rh2 in NaF, the extracharge compensation is done by a nearby point defect. Unfortunately, for such low-symmetry spectra, it is very difficult to make a clear connection between the symmetry axes of the g^2 tensor and the positions of the sources of the crystal field. For the second type of centers with two-line superhyperfine structure, the splitting is considerably smaller than in the first case, being of the order of 3 to 4×10^{-4} cm^{-1} (centers Tg3 and Rh3 in NaF). In this case the I = 1/2 ligand is obviously different from that in the previous group of centers. Tentative models for these centers imply complexes with U^{5+} surrounded by five O_2^- ions and a OH^- or $(FX)^-$ group (where X is a species without or with a small nuclear moment) for Tg3 and a similar structure perturbed by a nearby defect for Rh3. For the centers with three-component superhyperfine structure with an intensity ratio of 1:2:1, the splitting is sensibly smaller than the superhyperfine splitting in the case of the two-component structures due to a F^- ligand, but quite similar to the splitting observed for the second group of centers with two-line superhyperfine structure. This shows that the ligands which cause this structure are not isolated F^- ligands but either F_2^- groups, H_2O^-, or two OH^- ions (on the same cubic axis). A very slight rhombic distortion of the center Tg1 in KF and Tg2 in NaF as well as the presence of the Rh4 center in LiF seems to favor the first models, with a far away extracharge compensation in case of the Tg centers and a nearby one in case of the Rh4. Taking into account the similarity between the superhyperfine splitting in case of these three-component lines and in case of the second type of two-component centers, it is reasonable to assume that

the source of the splitting is the same for both cases. To check these models, ENDOR experiments in ^{2}D or ^{17}O-enriched samples would be necessary.

The low concentration as well as the great variety of centers prevents an accurate optical study of the U^{5+} centers. Using an ingenious combination of absorption, luminescence, and excitation measurements, Parrot et al. (186, 187) were able to measure all seven electronic transitions within the Tg1 center in LiF:U^{5+} and within another unidentified center. Unfortunately in their analysis of the splitting of the $5f^1$ configuration in a strong tetragonal field, they did not make use of the reduction parameters for each orbital, but left the spin-orbit coupling and the crystal field parameters B_k^q as parameters to be obtained by fitting the energy levels and the g-values. More sets of spin-orbit coupling and crystal field parameters have been obtained (186, 187) without a definite preference for one of them. The neglect of the reduction factors for the orbitals makes these parameters unreliable. A calculation of the g-value anisotropy defined as

$$\delta g = 3|g_{\parallel} - g_{\perp}|/|g_{\parallel} + 2g_{\perp}|$$

for various tetragonal U^{5+} centers with superhyperfine structure, gives values of 0.55 to 1.15 for LiF and 0.38 to 0.96 for NaF. The same situation holds for center Tg3 in LiF ($\delta g = 0.1$), which is assumed to correspond to an O_2^- octahedron, but not for the center Tg4 in LiF ($\delta g = 0.1$), which is assumed to correspond to an O_2^- octahedron slightly distorted by a cation impurity. This shows that for the centers whose source of distortion of the pure octahedron symmetry is placed in the first coordination sphere of uranium, the distortion is strong. Taking into account the comparison (Section II.B.3g) between the U^{6+} and U^{5+} hexa-coordinated complexes, this result confirms the recent interpretation of the optical spectra of the main tetragonal U^{6+} centers in LiF and NaF based upon the assumption of an axial distortion stronger than the coulombic inter-electronic interaction (188). This shows that the weak distortion model (189) is not valid in this case. This stresses the need for extreme care when comparing the properties of the uranate centers in alkali fluorides with those of other hexa-coordinated U^{6+} compounds as, for instance, UF_6.

(b) U^{5+} *in alkaline-earth* fluorides. Pentavalent uranium enters into calcium fluoride crystals during growth, accompanying U^{4+} (in green or yellow CaF-U crystals) or U^{6+} (in white cloudy samples). The green or yellow crystals may contain a (prevailing) trigonal U^{5+} center Tr and a rhombic Rh1 center. The trigonal symmetry, absence of any superhyperfine structure, and the low g-values show that the Tr center consists of a substitutional U^{5+} ion surrounded by six O^{2-} ions and two fluorine vacancies on the same |111| direction. Thus the vicinity of the uranium ion is a distorted octahedron rather than a distorted cube, and this explains the low g-values. The center Rh1 has a similar structure, but a F^- ion is left in the distorted octahedron. The heat treatment of the crystals or gamma irradiation at room temperature decreases the intensity of the Tr center, increases that of Rh1 and gives rise to a new center of rhombic symmetry. This new center shows superhyperfine structure of three components with the intensity ratio 1:2:1 for |001| (indicating two equivalent F^- ligands) which transforms to a two-line structure for |112| and |110|. It is difficult to give a precise model for this center, but it must include two F^- nearest neighbors. Since gamma irradiation and heat treatment up to 1000 °C have similar effects in producing the Rh1 and Rh2 centers, it has been assumed (172) that their main sources are some low symmetry U^{4+} centers compensated by substitutional oxygens and fluorine vacancies. Fluorine interstitials stimulated by gamma irradiation or heating migrate through the crystals and could be trapped on fluorine vacancies in the neighborhood of uranium. A rearrangement of charge could transform U^{4+} into U^{5+}.

In the as-grown white cloudy samples containing U^{6+}, the most intense EPR spectrum of U^{5+} belongs to a center of very low symmetry (Rh3 in Appendix I). The very sharp lines without superhyperfine structure and the close resemblance of the g-values of this center to those of the Tr center, show that the first coordination sphere of uranium is the same in both cases, but while with the Tr center, the negative extracharge of the complex $(U^{V}O_6)^{7-}$ as compared to $CaF_8)^{6-}$ is compensated far away, in case of the Rh3 center this is done in the neighborhood of the complex, possibly by a fluorine vacancy. No optical data on U^{5+} in fluorite have been measured.

The calculated mean g_0 value for the most symmetric U^{5+} centers in alkali and alkaline-earth fluorides are 0.33 to 0.4 for LiF, 0.49 to 0.58 for NaF, 0.55 for KF and 0.76 to 0.81 for CaF_2. This shows that for oxygen octahedrally-coordinated U^{5+} ions, the g-values can be equal or slightly larger than for F^- coordinated complexes, when the distance U-O is large (as in the case of alkaline-earth fluorides and niobates) but

becomes smaller as this distance decreases (the alkali fluorides). At the same time the distance $\Gamma_7' - \Gamma_7$ increases with decreasing length of the U-O bond (7050 cm^{-1} in niobates and 7878 cm^{-1} in Tg1 in LiF). This shows (190) a close relation between the g_0 and $E_{\Gamma_7'} - E_{\Gamma_7}$ and the spectrochemical series (191).

2. EPR of U^{5+} in Nonoctahedral Crystalline Fields

As shown previously, for the eightfold or tetrahedral symmetry the crystal field has a very small effect on the free state of a $5f^1$ ion, and its behavior would be similar to that of a $4f^1$ ion, i.e. the ground state is mainly determined by the $^2F_{5/2}$ level. of the free ion, with possible admixtures from the crystal-field states originated from the excited $^2F_{7/2}$ level In cubic symmetry the ground level can be Γ_6 or Γ_8. When Γ_6 is lowest, an isotropic resonance line with $g = 10/7$ is expected, while for Γ_8 some anisotropic transitions must be seen. An axial or lower symmetry distortion splits Γ_8, as discussed in the previous section.

Very few experimental data on systems with U^{5+} in nonoctahedral symmetry have been reported. Thus a line with $g \sim 1.25$ in uranium-doped ThO_2 powder could correspond to such a center, because the host cation Th^{4+} occupies the center of a regular cube of O^{2-} ions (192). However, no EPR measurement on U^{5+} in single crystals of ThO_2 has been reported in order to confirm this identification. An attempt to observe EPR in cubic UF_8M_3 (M = Na, Cs, Rb, NH_4) at liquid nitrogen temperature (193) was unsuccessful, but subsequent measurements (184) on polycrystalline UF_8Na_3 gave a broad resonance signal at $g = 1.2$. A very interesting aspect of this situation is the Rh_4 center of U^{5+} in fluorite (194). This center is observed in the uranium-doped fluorite samples heat-treated at 1200 °C in quartz ampoules sealed in air. This center appears regardless of the initial valence state of uranium and the means of charge compensation. The hyperfine structure for ^{235}U-doped samples shows that the center contains a uranium ion, while the symmetrical lineshape and the temperature of observation show that the valence state of uranium is +5 (195). While for the other U^{5+} centers in fluorite, the lines are sharp (of several Gauss), the line corresponding to this center are broad, of about a hundred Gauss with the magnetic field along the |100| direction. No superhyperfine structure was resolved for any orientation of the external magnetic field, but it is possible that the broad lines obscured an unresolved structure determined by a large number of ligands in the next coordination sphere. The g-values for this center (0.540, 2.775, and 0.471) and $\delta = 1.8°$ differ considerably from those observed for the other U^{5+} centers in fluorite and are very close to those reported for a rhombic Ce^{3+} ($4f^1$) ion in cerium oxide-doped fluorite, for which the main g-values are 3.286, 0.22, and 0.844 and $\delta = 13.8°$ (196).

The structure of this center as of other low-symmetry rare-earth centers in oxide-doped fluorite is not known. However, the g-values of the U^{5+} Rh4 center cannot be explained if the vicinity of uranium is assumed to be octahedral, and models with distorted eightfold or tetrahedral symmetry must be employed. The lack of a resolved superhyperfine structure shows that no fluorine ligands are present in the nearest neighborhood of uranium, but rather that this is formed by oxygen ions. Thus a structural model for this center must be based on a tetrahedral vicinity with, perhaps, one or two additional O^{2-} ions (in order to compensate the charge) placed in the first coordination sphere or in a near interstitial, to give a low symmetry to the center. The arrangement of this center could be connected (195) with the transition of fluorite crystals to the disordered superionic state at 1150 °C (197) when the F^- ions can migrate from their normal positions in interstitials leaving vacancies which can then be occupied by oxygens. They can also originate from some low-symmetry oxygen-coordinated U^{4+} centers.

3. EPR Hypefine Structure of U^{5+}

The EPR hyperfine structure corresponding to the isotope 235 uranium (I = 7/2) has been studied only in the case of U^{5+} in alkali fluorides and calcium fluorides, where the lines are sharp. Accurate measurements have been possible only for some axial centers (155, 156, 158, 171, 198, 199).

For the low-symmetry spectra the large number of lines belonging to the same center or to different centers present in the sample, the strong quadrupolar effects, and possible differences between the principal axes of the spectroscopic factor g and of the hyperfine interaction, make the analysis of the hyperfine structure extremely difficult. However, it was observed for all the U^{5+} spectra in alkali and alkaline-earth fluorides and has been used to prove that these centers belong to uranium.

Since the Tg1 center in NaF:U^{5+} is the only center for which all the spectra could be recorded at 9 GHz with a magnetic field up to 20 kGauss,

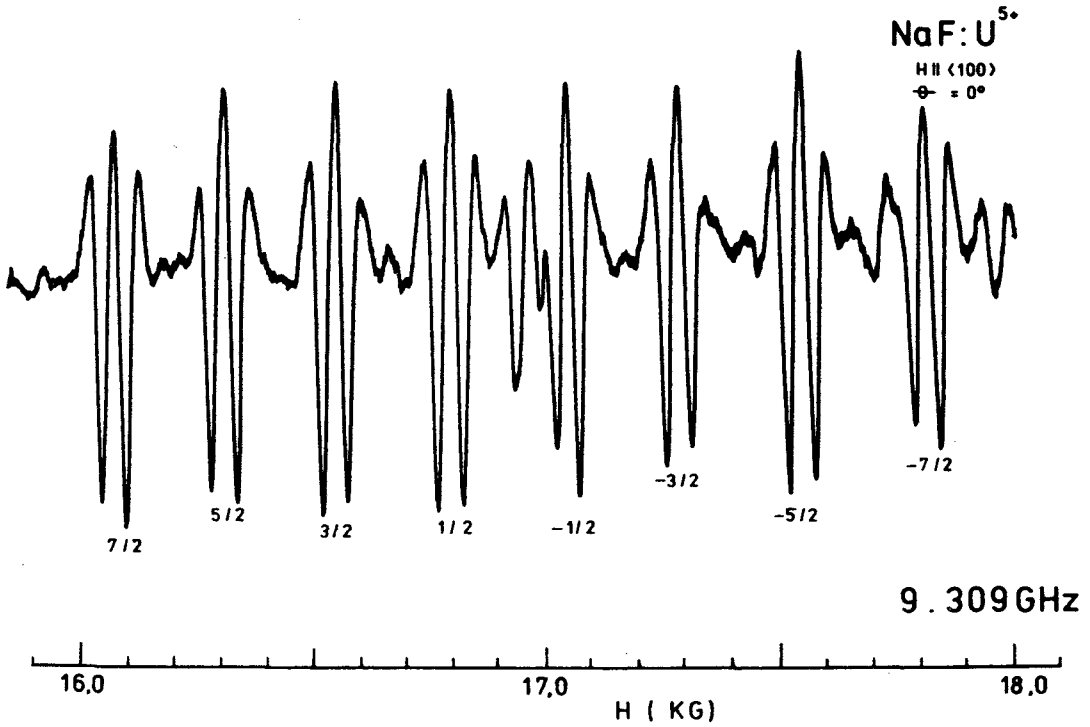

Figure 2. The parallel hyperfine structure for the Tg1 U^{5+} center in NaF.

we shall describe it as an illustrative example. For all the other axial centers, the EPR parameters for parallel orientation have been obtained from the angular dependence of the spectra. For the parallel orientation ($H \parallel |100|$), the hyperfine structure for the Tg1 $(^{235}U)^{5+}$ center in NaF consists of eight equally intense and almost equally split components. As Figure 2 shows, each hyperfine component is split into two because of the superhyperfine interaction with the F^- ligand placed on the distortion axis.

Approximately in the center of the hyperfine pattern, a line corresponding to ^{238}U is observed. The ratio of the total intensity of the hyperfine spectrum due to the 235 isotope to the intensity of the 238 isotope line is in this case about 13:1, faithfully reflecting the isotopical composition of the uranium oxide used as dopant. This fact has been used as a method for measuring the isotopic abundance of minute amounts of non-volatile uranium salts which can easily be dissolved in molten sodium fluorite in the presence of oxygen (200, 201). When the magnetic field is turned away from |100| in the (100) plane, the hyperfine pattern is drastically modified. If we denote the hyperfine components by m_I, when the angle between the external magnetic field and |100| becomes 20°, the splitting of the $\pm 1/2$ hyperfine lines is increased so that they overlap the $\pm 3/2$ components and for $\Theta = 45°$, they overlap the doublet $\pm 7/2$. This splitting of the other hyperfine doublets decreases as Θ increases and vanishes at $\Theta = 90°$ for the doublets $\pm 5/2$, $\pm 7/2$ (see Figure 3).

The lines 3 and 7 in Figure 3 correspond to the $\pm 1/2$ lines, the lines 4 and 6 to the $\pm 3/2$ doublet, and the line 5 to $\pm 5/2$ and $\pm 7/2$ components. The lines 1, 2, 8, and 9 are "forbidden" hyperfine transitions, which can be clearly observed at $\Theta > 60°$.

In order to describe this unusual hyperfine structure, a new perturbation scheme has been used (155). The spin Hamiltonian contains the axial Zeeman interaction, the axial hyperfine interaction, and the nuclear quadrupole interaction. The unusual behavior of the $\pm 1/2$ hyperfine doublet suggests that the nuclear electric quadrupole interaction is of the same order or stronger than the hyperfine interaction. In this case the eigenvalue problem of the spin Hamiltonian must be solved numerically. In order to obtain the starting values for the parameters (which are then improved by a numerical diagonalization), a preliminary analytical treatment was used assuming that the magnitude of the interactions in the spin Hamiltonian are in the

order: Zeeman electronic, quadrupole interaction, and hyperfine interaction. In such a case the quadrupole interaction splits the nuclear spin degeneracy into four levels, degenerate after $\pm m_I$, and subsequently the hyperfine interaction is block diagonalized within each of these doublets. The resonance condition given by such a treatment is:

(a) for the doublet $\pm 1/2$,

$$h\nu = g\beta H \pm \tfrac{1}{2}K$$

with

$$g = (g_\parallel^2 \cos^2\Theta + g_\perp^2 \sin^2\Theta)^{\frac{1}{2}}$$

and

$$Kg = (A_\parallel^2 g_\parallel^2 \cos^2\Theta + 16A_\perp^2 g_\perp^2 \sin^2\Theta)^{\frac{1}{2}},$$

(b) for the doublets $\pm 3/2$, $\pm 5/2$, $\pm 7/2$,

$$h\nu = g\beta H + A_\parallel g_\parallel m_I \cos\Theta/g.$$

The doublet $\pm 3/2$ is split by second-order effects.

In the same way the angular dependence for the forbidden hyperfine lines has been obtained and was used to estimate the electric quadrupole parameter.

This analytical treatment predicts a maximum splitting for the hyperfine doublet $\pm 1/2$ at an angle Θ given by (168):

$$\cos^2\Theta = 1 + \frac{A_\parallel^2 g_\parallel^2 (2g_\perp^2 - g_\parallel^2) - 16A_\perp^2 g_\parallel^2 g_\perp^2}{A_\parallel^2 g_\parallel^2 (g_\parallel^2 - g_\perp^2) - 16A_\perp^2 g_\perp^2 (g_\parallel^2 - g_\perp^2)}$$

The spin Hamiltonian parameters obtained in this analytical treatment have been improved by numerical exact diagonalization of a 16×16 matrix. Similar hyperfine behavior has been observed for other U^{5+} centers (in alkali and alkaline-earth fluorides), and the determination of the parameters has been done in the same way. From an inspection of the hyperfine data given in Appendix I, the importance of the nuclear quadrupole effects is seen. For many centers (Tg1 in NaF, Tg1 in KF, Tr in CaF_2) the electric quadrupole parameter is larger than the magnetic hyperfine parameters, and in the case of Tg1 in LiF, they are of the same order of magnitude. A similar situation has been observed for the isoelectronic Np^{6+} ion (202). Thus, the hyperfine behaviour of the $5f^1$ ions in octahedral coordination parallel the electronic behaviour characterized by crystal field effects stronger than the spin-orbit coupling.

C. EPR of Tetravalent Uranium

As shown before, the ground level of the non-Kramers ion U^{4+} (f^2 ground configuration) in a crystal can be a singlet, doublet, or triplet depending on the symmetry of the crystal field, on the composition of the crystal field potential, and on the effect of the intermediate coupling and J mixing through the crystal field. Thus in the case of octahedral symmetry, the ground state is always a Γ_1 singlet. In the case of eightfold and tetrahedral cubic symmetry, the ground level can be a Γ_1 or a Γ_5 triplet, depending on the ratio of the fourth- to sixth-order terms in the crystal field potential. In lower symmetries the ground level can be either a singlet or a non-Kramers doublet. This explains why many systems of interest, for which the crystal field is octahedral or of lower symmetry, cannot be studied by EPR. The most suitable hosts for EPR studies on U^{4+} are those with eightfold cubic cationic positions. An EPR study of uranium-doped ThO_2 (192) shows at room temperature a line with $g \sim 2.7$, which has been attributed to U^{4+}. However, a calculation of the spin-lattice relaxation time for U^{4+} in cubic crystalline fields (203) shows that this becomes too short already at the liquid nitrogen temperature to allow an observable EPR signal from U^{4+}. Thus the nature of this center is uncertain. Unfortunately, no EPR study on single crystals of ThO_2 doped with uranium (preferably enriched in the 235 isotope) has been reported to check this identification (192).

More studies have been devoted to U^{4+} in alkaline-earth fluorides. In the case of calcium fluoride, the composition of the eightfold cubic crystal field potential favors Γ_5 as a ground level, and its states can be characterized as the eigenfunctions of a fictitious spin $S = 1$. Using the wavefunction of the Γ_5 triplet, single quantum transitions at $g = 2$ (governed by the selection rule $\Delta M_S = 1$) and at $g = 4$ (selection rule $\Delta M_S = 2$) and double-quantum transitions at $g = 2$ (selection rule $\Delta_S = 2$) are expected, as in the case of the cubic Pr^{3+} ($4f^2$) center in fluorite (134). A single isotropic line of $g \sim 2$ has been observed for CaF_2:U, which has been attributed to U^{4+} in cubic sites (204). However, this line does not show any superhyperfine splitting, as expected for substitutional cationic sites. A further confirmation of this spectrum especially using ^{235}U-doped samples is necessary. The difficulties connected with the charge compensation for a cubic center of U^{4+} in CaF_2 must also be taken into account.

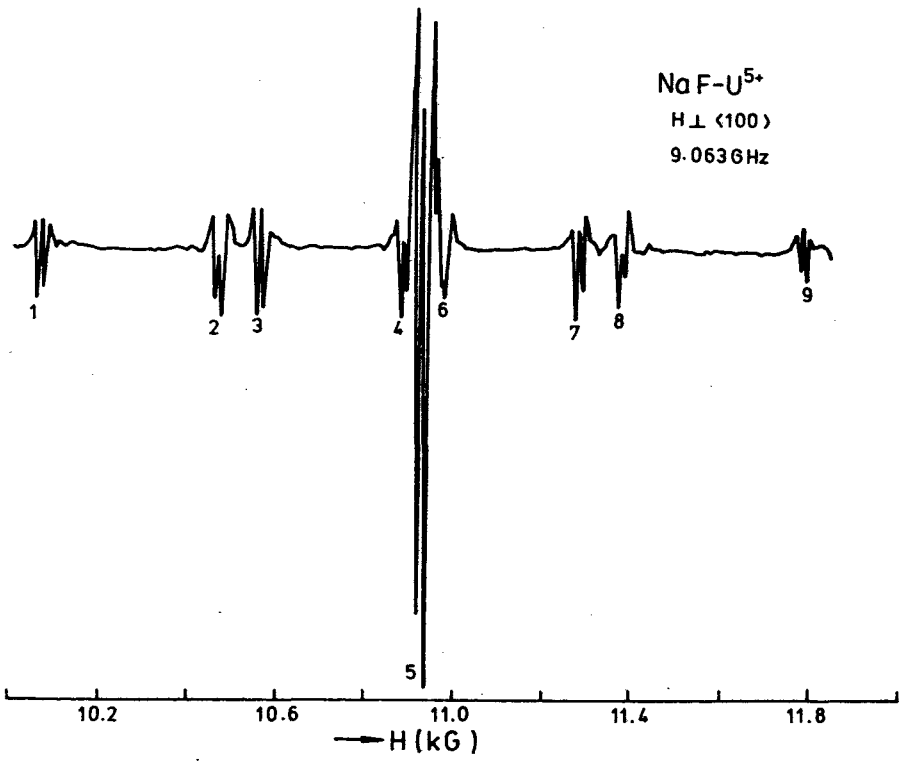

Figure 3. The perpendicular hyperfine structure for the Tg1 U^{5+} center in NaF.

An axial distortion (as caused, for instance, by charge compensating point defects) splits the Γ_5 triplet into a doublet and a singlet. The relative positions of the two components are given by the sign of the axial distortion. Thus a tetragonal distortion, due for instance to the presence of a charge-compensating interstitial anion (F^- or O^{2-}) in the empty cube next to uranium, leaves the singlet lowest, as occurs in the fluorine-compensated tetragonal Pr^{3+} ($4f^2$) centers in fluoride (205), and no EPR transition is expected. A trigonal distortion leaves the doublet lowest, and paramagnetic resonance transitions can be induced between its two states in the presence of an external magnetic field. As shown before, the most suitable spin Hamiltonian for such a non-Kramers doublet corresponds (206, 207) to a fictitious spin $S = 1$, and a strong additional zero-field splitting term must be added in order to remove the singlet. Three trigonal centers have been attributed to U^{4+} in CaF_2. Various EPR and acoustic paramagnetic resonance studies on the center Tr1 (204, 208-217) have shown that the center is inversionless, and the resonance transitions are induced mainly by the electric component of the microwave field. The superhyperfine structure shows that the U^{4+} ion occupies a substitutional lattice site and is surrounded by eight fluorine ligands. The interaction with two of them placed on the same body diagonal, is stronger than that corresponding to the other six. The distortion of the cube can be due to a static Jahn-Teller effect or, most probably, to the presence of a charge compensator which gives inversionless symmetry to the crystal field. The fact that the green or yellow crystals which contain this center can be grown if the dopant is UF_4 or if care is taken in order to eliminate the oxygen leads usually to the conclusion that the oxygen does not take part in this center. However, the presence of oxygen-coordinated U^{5+} centers (170-172) in some high quality green or yellow crystals containing the Tr1 U^{4+} center shows that the oxygen can be present in these crystals. Most probably, the charge compensation for this U^{4+} center is effected by a substitutional O^{2-} ion in the first empty cube along the $|111|$ direction. A compensation with

two interstitial F^- ions is improbable, because this would give a centrosymmetric complex.

The apparent g-value for this center is very close to that expected if a very slight distortion, which leaves the wavefunctions of the levels almost unaltered, is taken into account. An optical study of this system (43, 44) gave for the crystal field parameters values which lead to $g_\parallel \sim 4.8$. The disagreement between the EPR and optical data is due mainly to the fact that the crystal field parameters were determined to fit the splitting of a large number of levels and may not correspond to the best-fit values for the ground state.

In the case of the Tr2 U^{4+} center in fluorite, the superhyperfine structure due to the F^- ligands suggests a center with inversion symmetry (218). The fact that the superhyperfine structure is best resolved when the magnetic field is along the $|111|$ shows that all the U^{4+}-F^- bonds are equivalent with respect to this direction, and this is possible only if no F^- is placed on the distortion axis. The odd number of components and the intensity ratios show that there are six F^- in the first coordination sphere. In such cases the charge compensation can be due to two substitutional O^{2-} ions on the distortion axis. This model gives a distortion of the right sign to assure the doublet as a ground level and a mixing of states which can explain the value of $g_\parallel$. The presence of the oxygens can explain why this center appears in the crystals doped with uranium oxide, or in samples obtained by heat treatment of U^{3+}-doped fluorite at 1200 °C in quartz ampoules sealed in vacuum (for which the quartz, evidently attacked during the treatment, can supply the necessary oxygen).

The nature of the Tr3 center in CaF_2 (and Tr centers in SrF_2 and BaF_2) is not established (219-222). From the crystal growth procedure it was concluded that a remnant contamination of the samples with oxygen is possible and, as a logical possible model, that given for the center Tr2 above has been proposed. However, the superhyperfine interaction with 24 ligands of I = 1/2 shows that this model cannot be correct for the Tr3 center. It is also impossible to explain the g-value by a trigonal distortion of the cube, since the dominant $A_2^0 \langle r^2 \rangle$ term of the distortion would give apparent g-values larger than 4 if its sign is taken as to leave the doublet lowest (223). The fluorite crystals which contain the Tr3 center show an optical absorption spectrum (43, 44) sensibly different from that observed for the crystals containing the Tr1 center. Hargreaves attributed this optical spectrum to a U^{2+} ion with $5f^3$ 7s ground configuration, which at the same time has been considered as responsible for the EPR Tr3 center observed in the same crystal (224). The crystal growth conditions which were considered able to eliminate completely the oxygen, as well as the valence conversion of the uranium ions in fluorite under uv and X-irradiation were set forth in order to support this identification.

A chemical method of analysis of different uranium-doped fluorite samples, connected with optical absorption measurements (225), led to the conclusion that the samples studied by Hargreaves (43, 44) contain U^{4+} and not U^{2+}. The paper (225) connects the color of the CaF:U crystals with the valence state of uranium and the means of charge compensation. We note, however, that in discussing this problem, the very complex situation of the CaF_2:U system must be taken into account, in which many valence states and types of centers can be simultaneously present in a given sample. These centers make themselves conspiculous in different manner with respect to different measurements; thus the conclusions of (225) must be used with caution. As an example, in many good quality (low scattering, good cleavage) green CaF_2:U crystals, we found besides the Tr1 U^{4+} center, various U^{5+} centers; the same situation may be observed in the yellow crystals.

The crystal growth conditions reported in different papers must be considered prudently. Both uranium and calcium have a strong tendency to oxidize, and sometimes strong reducing conditions may not be sufficient in order to eliminate all the oxygen from the system. There are cases when in a crystal containing a prevailing uranium center without oxygen, inclusions of calcium oxide or uranium dioxide are also present. The nature of a given center can be clarified only if a physical model which allows an estimate of a given parameter in agreement with the observed value is proposed.

Recently a new tentative model for the Tr3 center in CaF_2:U has been proposed (226): a U^{4+} ion substitutes a Ca^{2+} ion, and the nearest cube of fluorines is replaced by five oxygens. Two of the oxygens are placed on the same body diagonal while the other three form a triangle which can replace one of the original F^- triangles (normal to the body diagonal in question) or may be displaced towards the equatorial site of the complex. This model can easily explain the g-values on the basis of a strong trigonal field acting on the $^3H_4$ ground level of the free ion. According to this model the observed superhyperfine structure is due to the 24 fluorine ions in the next-nearest positions.

The hyperfine structure of $(^{235}U)^{4+}$ in fluorite has been studied in (218). The spectra show a hyperfine structure of eight allowed $\Delta m = 0$ components from which the apparent A parameter has been determined. The absence of the forbidden transitions in the spectra prevented the determination of the nuclear quadrupole parameter, although it is expected to be large. A pecularity of this hyperfine structure must be noted. For the actinide ions the relation $A_J/g_J = A_x/g_x = A_y/g_y = A_z/g_z$, which is usually valid for the lanthanide ions, is expected to hold regardless of the host crystal. However, a marked difference in the ratio $A_\parallel/g_\parallel$ for the Tr1 and Tr2 U^{4+} centers in fluorite is observed. In the first case this ratio is 26.6, while in the second case it is 41.9 (in units of 10^{-4}). This prevents an estimate of the magnetic moment of the 235 isotope of uranium from the EPR hyperfine structure of the U^{4+} centers. The difference between the two cases can be accounted for only if we allow for crystal field effects which can produce a considerable mixing of the free-ion levels.

The EPR studies on U^{4+} in crystals can be explained under the assumption of weak to intermediate crystal effects on a given free-ion energy level, if the intermediate coupling and J mixing are taken into account. Thus a qualitative difference between U^{5+} and U^{4+} appears in that they are separated by the limit between the intermediate and weak crystal field effects.

D. EPR of Trivalent Uranium

The trivalent uranium ion has a $5f^3$ ground configuration with a J = 9/2 ground level composed of 83% ^4I and 15% ^2H intermediate coupling components. In a cubic field this level is split into a doublet Γ_6 and two Γ_8 quartets. In octahedral coordination the doublet is lowest, while in eightfold or tetrahedral cubic symmetry, the lowest is either Γ_6 or Γ_8, depending on the composition parameter x of the cubic crystalline potential. A tetragonal distortion splits the quartet into two doublets, while a trigonal distortion splits it into a doublet and a degenerate pair of singlets. In a strong trigonal field, the lowest of the components can be either a singlet or a Kramers doublet.

The paramagnetic resonance studies on U^{3+} are concentrated on two types of hosts, the alkaline-earth fluorides and the lanthanum chloride. Most of those studies refer to calcium fluoride. The trivalent uranium ion can easily replace a Ca^{2+} ion, and the charge difference can be compensated in various ways (227) by (i) an interstitial F^- ion, (ii) a substitutional M^+ cation, (iii) a substitutional O^{2-} ion, and (iv) substitution of three Ca^{2+} ions by two U^{3+} ions. The presence of the charge compensators in the vicinity of the uranium ion leads to a distortion of the cubic crystal field. If the charge compensator is far from the uranium ion, the distortion of the cubic field can be safely neglected in most cases.

If we express the position of the charge compensator in units of the lattice parameter taking U^{3+} as the origin, an interstitial F_i^- ion can occupy a (l, m, n) site characterized by (l + m + n) equal to an odd number, at a distance of $(l^2 + m^2 + n^2)^{\frac{1}{2}}a_0$ from uranium, where a_0 is the lattice parameter (in case of CaF_2, $a_0 = 2.726$ Å). The main sites of F_i^- in the vicinity of uranium are of the type (1, 0, 0), (1, 1, 1), (2, 1, 0), and (2, 2, 1). A substitutional M_S^+ ion can occupy sites with (l + m + n) equal to an even number, and the main position in the vicinity of uranium are (1, 1, 0), (2, 0, 0) and (2, 1, 1). The main nearest substituional position of O^{2-} is $(\frac{1}{2}, \frac{1}{2}, \frac{1}{2})$.

In the eightfold cubic substitutional sites of CaF_2, a Γ_8 ground level is expected for U^{3+}. The first attempt (228) to observe EPR from cubic sites of U^{3+} in CaF_2 produced spectra which did not follow the predicted (126) angular dependence. These results have been criticized (221, 222) where a new center has been reported as cubic U^{3+}. This center can be approximately described by the Γ_8 theory only if the sixth-order parameter in the cubic potential is taken equal to zero. This is in contradiction with the observations on other actinide or rare earth ions in fluorite or in other cubic crystal field. Recent studies (79, 135, 229, 230) have unearthed a new center in fluorite (the center C in Appendix III), which is well described by the Γ_8 resonance theory and have shown that this is the substitutional cubic U^{3+} center. When the magnetic field is parallel to the cube edge, two strong resonance lines with a resolved superhyperfine structure of an odd number of components are observed. An analysis of this structure shows that it is due to an interaction with eight equivalent fluorine ligands. The superhyperfine components of the low magnetic field transitions have individual linewidths (between the points of maximum slope) of about 7 Gauss and are split apart at 10.2 Gauss. When the magnetic field is turned away from the |100| direction in the (110) or (100) plane, the line positions and intensities change drastically (Figure 4).

Around the |111| direction the intensity of the two transitions drops, and a very broad line appears between them. The two strong and sharp lines have been attributed to the

transitions $|1/2> \leftrightarrow |-1/2>$ (the line at high magnetic field with an effective g-value of 2Q) and $|3/2> \leftrightarrow |3/2>$ (the line at low magnetic field with an effective g-value of 2P). As shown in the previous sections since the Γ_8 representations enter twice in the decomposition of $D^{9/2}$, the wavefunctions of each Γ_8 quartet depend on the composition parameter x. This makes the resonance parameters P and Q dependent on x and can be used to determine it. An estimation of x from data on this center using equation 69 gives -0.4959 (from the value of Q) and -0.4582 (from the value of P), if we take for g_J the Landé factor of the ground state corrected for the intermediate coupling and $K_J = 1$. A unique x parameter of -0.4873, which fits both P and Q parameters, can be obtained if a reduced value for $K_J g_J$ of 0.6794 (the reduction factor K_J being 0.918) is used. Three major sources for the reduction of g_J can be considered (135, 229, 230), but an accurate calculation of this effect is for the moment impossible because the positions of the excited states in the crystal field are not known:

(a) The J mixing through the cubic crystal field. As shown in Section 2.II.A.3d, there are many free-ion energy levels not very far from the ground state; thus at least six or seven Γ_8 quartets closer than 10,000 cm^{-1} to the ground state can appear in a cubic field, and these can be admixed to the ground Γ_8 level. An estimation of the effect of the first excited level J = 11/2 shows that it lowers the g_J value of the ground state.

(b) The covalency effects. The presence of covalency is clearly shown by the superhyperfine structure. A previous estimation (231), shows that the covalency effects could be important in the case of cubic U^{3+} centers in fluorite.

(c) A dynamic Jahn-Teller effect (232).

The composition parameter x determined for this center is in very good agreement with the values obtained for the $4f^3$ ions Pr^{2+} (233, 234) and Nd^{3+} (230, 235) in cubic sites in fluorite or for the isoelectronic Np^{4+} in ThO_2 (236). Using this x value and the parameters β_J and γ_J for U^{3+} corrected for the intermediate coupling, a value of 0.177 for the ratio $A_6<r^6>/A_4<r^4>$ has been obtained, in very good agreement with the values obtained for the various rare-earth ions in fluorite and for the actinide ions in various eightfold or sixfold cubic lattices. We mention that a comparison between the data obtained for cubic U^{3+} ($5f^3$) and those on cubic $4f^3$ ions (Pr^{2+} and Nd^{3+}) in fluorite shows that U^{3+} is in many respects (the value of x, the superhyperfine structure) more similar to Pr^{2+} than to Nd^{3+} (230). With these arguments in favor of this center, it is very difficult to explain the nature of the spectrum reported by Title (221, 222).

The g-values of the tetragonal Tg2 center in CaF_2 doped with uranium and sodium (237) can be related to the P and Q parameters of the cubic center (135, 229, 230) by equation 44b, i.e. the tetragonal distortion in this case is characterized by a positive $A_2^0<r^2>$ parameter and splits the quartet into two doublets, leaving the doublet $|\pm 3/2>$ lowest with its wavefunction almost unchanged. The superhyperfine structure of an odd number of components observed for this center is best resolved with the external magnetic field along the distortion axis. A rough analysis shows that it consists of an interaction with eight almost equivalent F^- ligands and a weaker interaction with four other F^- ions which form a square normal to the distortion axis. This structure shows that no interstitial F^- ion is involved in the charge compensation. The most plausible model for this center is that of a substitutional Na_S^+ at a lattice site (2, 0, 0) relative to uranium. Such type of centers have previously been reported in fluorite doped with neodymium and sodium, or with cerium and sodium (238). In this paper (238) the assignement Na_S^+ (2, 0, 0) has been rejected on the argument that this ion is too remote from the rare-earth ion to induce such a large g-anisotropy. It can be shown (237) that the g-values for Nd^{3+} in such a center can be related to the values reported for cubic Nd^{3+} in fluorite (230, 235) in exactly the same way as in the case of uranium. In fact, as equation 44a shows, the g-anisotropy in such a case depends on the cubic parameters and not on the magnitude of the distortion and can be very large. Tetragonal centers have recently been observed in CaF_2 doped with uranium and either Li^+, K^+, or Ag^+ (239). This proves again that the center C (135, 229, 230) is the substitutional cubic U^{3+} center in fluorite.

When the charge compensation is done by an interstitial F_i (1, 0, 0) (219, 227, 240), the g-values (center Tg1 in Appendix III) cannot be related in a simple way to the cubic parameters, because a considerable mixing of states is induced by the strong tetragonal component. The same is also true for the rhombic Rh2 center compensated by a substitutional M^+ ion (M = Li, Na, K, Ag) at a (1, 1, 0) lattice site (239, 241). Thus, while the tetragonal M_S^+ (2, 0, 0) centers have similar EPR spectra, the rhombic M_S^+ (1, 1, 0) depends markedly on the compensating alkali ion (239).

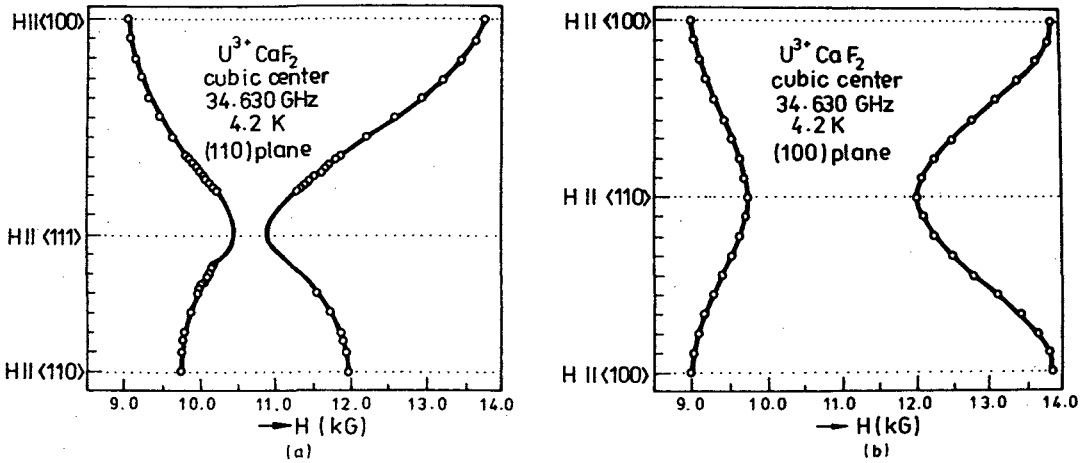

Figure 4. The angular variation of the two main transitions in the cubic U^{3+} center in CaF_2.

The tetragonal center Tg1 in the fluorite lattice is the most studied uranium center. We also mention studies on linear electric field effects (242), electron spin-lattice relaxation (240, 243-247), ^{19}F NMR (248-250), the study of the superhyperfine structure by ENDOR (251, 252), discrete saturation (DS) (253, 254) and radiofrequency discrete saturation (RDS) (257) and optical detection of EPR (258). The EPR spectra of this center show a well resolved hyperfine structure with a large number of components due to an odd number of fluorine ligands. This shows that an interstitial fluorine ion is placed in the vicinity of uranium. Counting the superhyperfine components in an EPR spectrum with many ligands (which can be grouped in nonequivalent sets) is difficult, because the outer lines may be lost. Also a determination of the superhyperfine interaction parameters may prove impossible, because as many as five superhyperfine parameters are necessary to characterize the interaction with the nearest neighboring nuclei, when the symmetry of the crystal field is tetragonal. A fortunate situation is the case of cubic symmetry or for the ligand on the distortion axis, when only two superhyperfine parameters are necessary. The parameters of the superhyperfine interaction with the ligands from different coordination spheres can be determined with great accuracy by using ENDOR, DS, or RDS. These parameters can then be used in order to determine the dipolar and covalent contributions to the superhyperfine interaction and the displacements of the various ligands and of the paramagnetic ion from their equilibrium positions in the unperturbed fluorite lattice. The measurements on the Tg1 U^{3+} center in CaF_2 have given a configuration of the charge-compensation model with an interstitial fluorine ion at a (1, 0, 0) lattice site and have produced a displacement d = 0.09 (252) (i.e. of the order of 0.12 Å) of the U^{3+} ion towards the interstitial fluorine.

A low symmetry center Rh1 in fluorite doped with $NaUF_4$ has been assumed to originate from a substitutional U^{3+} center compensated by a fluorine ion at a (2, 2, 1) lattice site (259). Since the experimental angular dependence observed (259) does not show all the lines predicted by theory for such a center, this spectrum has been reinterpretated (260) as due to a F_i^- compensation at a (2, 1, 0) lattice site, and thermodynamical arguments were presented to show that such a center is more probable than that assumed (240). However, a recent record of the entire resonance spectrum (261) shows that the symmetry assignment (259) is correct. A structural model for this center is difficult, because for such low symmetry centers, the principal axes do not necessarily point toward the sources of the distortion. It seems, however, that the co-doping with alkali fluorides increases its probability because it appears frequently in the fluorite crystals doped with uranium and with NaF, KF, or LiF. It is possible that these fluorides supply

the F^- ions and help in its stabilization in such a position as to contradict the calculated thermodynamical distribution (260).

A remarkable fact is the absence of any trigonal U^{3+} EPR center in fluorite, in spite of the fact that a F^- ion can occupy easily the interstitial position (1, 1, 1). As shown (135) if the distortion potential $A_2 \langle r^2 \rangle$ created by such a F^- ion is positive, as in the case of some trigonal rare-earth centers in fluorite compensated this way, and if the condition of weak distortion is achieved, it will leave as the ground state the doublet $|\pm\bar{3}/2\rangle$, which is non-magnetic. Thus no EPR signal can be observed for the trigonal U^{3+} centers in fluorite even if they do exist. The same is true for the Nd^{3+} ion.

The tetragonal center Tg1 compensated by F_i^- (1, 0, 0) has also been observed in SrF_2 (227, 262). This center shows superhyperfine structure and an ENDOR study (252) shows that the displacement d of U^{3+} toward F_i^- is only 0.05. A low symmetry center Rh1 similar to Rh1 in CaF_2 has also been observed (262), but the direction x is no longer directed toward the direction (2, 2, 1), but makes an angle of only 15° ± 0.5 with the direction |110|.

Neither the SrF_2:U^{3+} crystals compensated with F_i^- or M_S^+ have shown cubic U^{3+} centers. Instead, the crystals compensated with M_S^+ (where M = Na or K) show (263, 264) two new tetragonal centers with the g-values Tg2, $g_\parallel$ = 2.824 and $g_\perp$ = 1.97 and for center Tg3, $g_\parallel$ = 1.72 and $g_\perp$ = 2.49. These g-values can be deduced in a very good approximation from a unique set of EPR cubic crystal field parameters of a Γ_8 quartet if it is assumed that the two tetragonal distortions are weak and leave as the lowest doublet for center Tg3, the cubic pair of wavefunctions $|\pm\bar{1}/2\rangle$ and for center T2, the pair $|\pm\bar{3}/2\rangle$. The resonance parameters of this virtual cubic center are 2P = -2.824 and 2Q = 1.72, from which a value of -0.4928 for the composition parameter x and a value of 0.9473 for K_J can be reduced. These values are in a normal connection with the existing EPR data on the rare-earth ions in cubic sites in alkaline-earth fluorides. They show that in going from CaF_2 to SrF_2, the value of the composition parameter x and that of K_J increase. Due to the similarity of the center Tg2 with the center M_S^+ (2, 0, 0) in CaF_2, it has been assumed that they have the same structure. As concerns the center Tg3, whose EPR lines are broader, it was attributed to a far-compensated substitutional U^{3+} ion slightly displaced towards one of the cube faces (263, 264).

In barium fluoride only the TfF_i^- (1, 0, 0) center has been studied (242, 265, 266). An analysis of the hyperfine structure by RDS (266) shows that the U^{3+} ion is displaced by 0.20 Å toward the interstitial compensator.

In a strong trigonal field the situation can be completely different from that in the weak distortion case, and a Kramers doublet can be left as a ground state. This is the case of U^{3+} in lanthanum chloride (268-270) for which a trigonal spectrum with sharp lines without superhyperfine structure has been observed. The spin-lattice relaxation for this center (271, 272), and the interaction of U^{3+} pairs in $LaCl_3$ (273) have also been studied.

These EPR studies show that the ground state of the U^{3+} ion can be interpreted as arising from the splitting of the lowest level J = 9/2 of the ground configuration $5f^3$ in a weak crystal field. The wavefunctions for the Kramers doublet in axial crystal fields, calculated from the resonance data can be expressed in terms of the $|M_J\rangle$ components of the J = 9/2 level as follows:

(a) for Tg1 (F_i^- (1, 0, 0)) in CaF_2, SrF_2, and BaF_2, $\alpha|\pm 9/2\rangle + \beta|\pm 7/2\rangle + \gamma|\pm 1/2\rangle$ with α^2 equal, respectively, to 0.48, 0.47, and 0.43; $\beta^2 \sim 0$ in all three cases and γ^2 equal to 0.52, 0.45, and 0.57 (223).

(b) for Tg2 (M_S^+ (2, 0, 0)) in CaF_2 (237) and SrF_2 (263, 264), $a|\pm 3/2\rangle + b|\mp 5/2\rangle$ with a^2 equal respectively to 0.1209 and 0.1126, and b^2 equal to 0.8791 and 0.8874.

(c) for U^{3+} in $LaCl_3$ (271), $0.9578|\pm 7/2\rangle + 0.2873|\pm 5/2\rangle$.

There is only one report on EPR of U^{3+} in non-halide crystals, that referring to the tetragonal orthophosphates $ScPO_4$ and $LuPO_4$ (267). In these crystals U^{3+} enters substitutionally. As can be seen from the g-value anisotropy, the differences in the crystal field parameters for the two crystals are fairly large.

The hyperfine structure of the isotope 233 of uranium has been studied in the case of the Tr center in $LaCl_3$ (268, 270) and that of ^{235}U for the Tr center in $LaCl_3$ (269, 270), the centers C (135, 230), Tg1, Tg2, and Rh2 in CaF_2 and for Tg1 in SrF_2 (271). From the hyperfine structure of the spectra in $LaCl_3$, the magnetic dipole and electric quadrupole moments have been estimated (268-270) as follows: for ^{233}U, $\mu = 0.51\mu_n$ and Q = 3.4 barn and for ^{235}U, $\mu = 0.33\mu_n$ and Q = 4.0 barn.

The values of the nuclear moments estimated from the measured hyperfine parameters are very sensitive to the details of calculation, especially to the values used for the parameters

$<r^{-3}>$. The value of 50 $Å^{-3}$ used for $<r^{-3}>$ has been estimated from the spin-orbit coupling, and no correction was made for the core polarization and J mixing. By using more precise ENDOR data on the same system from an unpublished work of Lerner and Hutchison in a calculation which takes into account the intermediate coupling, the relativistic radial parameters $<r^{-3}>$ given by equation 15 and equation 17 for the free-ion hyperfine parameter A, Lewis et al. (25) obtained a value of 0.45 μ_n for the nuclear magnetic moment of ^{235}U. However, they could not find the source of the discrepency between this value and that reported in (245, 246). The ratios A_i/g_i along the main symmetry axes i for a large variety of $(^{235}U)^{2+}$ centers in CaF_2, SrF_2, and $LaCl_3$ show a good grouping around an average value of 41×10^{-4} cm^{-1} (274). This value was used in equation 57 in order to determine the free-ion hyperfine parameter A_J and re-estimate the nuclear moment for ^{235}U using equation 17 with the relativistic radial parameters (25) or an effective relativistic expression for the hyperfine parameter

$$A_J=(2\beta_e\beta_n\mu_I/4\pi I)<r^{-3}>_{eff}<J\|N\|J>. \quad (70)$$

This is similar to the non-relativistic expression (275) with $<r^{-3}>$ replaced by $<r^{-3}>_{eff}$. The operator N, whose reduced matrix elements enter in equation 70, is given in the square bracket of equation 19. The effective radial integral $<r^{-3}>_{eff}$ used to re-estimate the magnetic moment μ_I for ^{235}U has been estimated using three methods: (a) with equation 19 and the D-S parameters (25), $<r^{-3}>_{eff}$ was equal to 5.633 a.u; (b) the degeneracy-weighted value using the $<r^{-3}>_{jj}$, MDF paramters (26) is equal to 5.630 a.u.; (c) the value estimated from the spin-orbit parameter using relativistic corrections is equal to 5.53 a.u These three values agree very well and converge towards a value of 5.6 a.u. With this value and with A_J/g_J equal to 41×10^{-4} cm^{-1} and using the intermediate coupling wavefunctions for the ground state of U^{3+}, a value of $-(0.46\pm0.03)\mu_n$ has been estimated for $\mu_I{}^{235}$ (274). This estimate does not take into account explicitly the core polarization effects. It must be noted that this neglect is partly compensated by the neglect of reduction of the hyperfine parameter in crystals as compared to the free-ion value. This new value of μ_I for ^{235}U is about 30-40% larger than the values previously reported; this difference is, obviously, a relativistic effect.

E. Divalent Uranium

No firm EPR data on divalent uranium have been reported. As shown before, the assignment of the trigonal EPR spectrum Tr3 in CaF_2:U described in Section IV.C to U^{2+} (43, 44) has been contested (225) on arguments based on a chemical analysis and optical absorption measurements. Even disregarding these arguments, it is difficult to explain how such a symmetry for the center and the g-values can originate from a U^{2+} ion. The ground configuration of U^{2+} is not firmly established, but as shown before, the possible configurations give either $^5I_4$ or $^5L_6$ as the lowest level. In an eightfold cubic crystal field, the ground level of $^5I_4$ is a singlet Γ_1. This has been confirmed, for instance, in the case of Pu^{4+} (276, 277) in eightfold cubic coordination, and for Np^{3+} in trichlorides, tribromides, and triiodides (278) or for centers of tetragonal or trigonal symmetry in CaF_2 (279). On the other hand Pm^{3+} ($4f^4$, $^5I_4$) in lanthanum ethyl sulfate gives an EPR spectrum with $g_\| = 0.432$ and $g_\perp \sim 0$ (279). Both these situations are not compatible with the Tr3 center in CaF_2. The same difficulties appear if a ground level $^5L_6$ is considered, because the ground state in crystals is either a singlet or the nonmagnetic doublet Γ_3. If this doublet is split by a second-order Zeeman effect, very large g-values are expected. Thus, a definitive answer regarding the nature of the Tr3 center in CaF_2:U cannot be given, but it is difficult to explain its g-values on the basis of a U^{2+} ion. We think, however, that there is enough evidence to assume that the U^{2+} ion in the eightfold coordination of the fluorite lattice does not have a magnetic ground state, and the center Tr3 corresponds better to the tentative model U^{4+} (226).

F. EPR in Concentrated Uranium Compounds

EPR on the concentrated compounds have given inconsistent results. Many concentrated systems of a given valence for uranium show strong EPR signals at temperatures much higher than the corresponding ions in diluted systems. Many times the g-values are far from those expected from a crystal field model.

The only cases where unambiguous EPR results have been obtained are the concentrated U(V) halide compounds discussed in Section IV.B.

Many concentrated compounds of trivalent or tetravalent uranium show strong and very broad EPR signals at room temperature. In some instnaces the spectrum was observed only for powdered samples and not in highly stoichiometric bulk samples.

Thus UF_3 powder shows (280, 281) at room temperature strong signals characterized by $g_\parallel = 2.8\text{-}2.9$ and $g_\perp = 2.1\text{-}2.2$. Even if combinations of free-ion $|M_J>$ wavefunctions can be found which can explain these g-values, it is difficult to understand an EPR signal at room temperature.

Uranium tetrafluoride powder has shown at room temperature an EPR signal with g = 2.15 (281). However, the stoichiometric bulk samples did not show any signal either at room or at liquid nitrogen temperature (282).

Uranium dioxide powder shows at room temperature a signal of g equal to 2.33 (283, 284), but this is not observed in the stoichiometric bulk samples (282). Other uranium oxides show at room temperature EPR signals with g-values equal to 4.04 in U_2O_5 (284), 5.42 in U_3O_8 (284), 2.31 in U_4O_9 (285). The large g-values for U_2O_5 and U_3O_8 have been attributed to U^{4+} in trigonal sites. Signals arose with g-values 2.41 in Li_2UO_4 (285), 2.18 in $BaUO_4$ (285), 2.10 in $MgUO_{3.8}$ (286), 2.10 in $MgU_3O_{8.9}$ (286), 2.04 in $CaUO_3$ (286), 2.61 in CaU_6O_{12} (286), 2.14 in $SrUO_{3.67}$ (286), 2.31 in $SrU_4O_{12.8}$ (286), 2.08 in $BaUO_{3.5}$ (286) and 2.08 in $Ba_2U_3O_{12}$ (285). Because many MUO_4 (M = Mg, Ca, Sr, Ba) compounds are deficient in oxygen (287) and $SrU_4O_{12.8}$ contains pentavalent uranium (288), the EPR signals reported for many of these systems could be due to U^{5+}, but it is difficult to explain the g-values on a simple crystal field model.

Recent EPR studies between 4.2 and 300 K on uranium trichalcongenides US_3 and UTe_3 show two lines with almost isotropic g-values of about 4 and 2 (289). The first of these lines was attributed to Fe^{3+} impurities in a strong crystal field, and the second line was assigned either to U^{5+} or to a localized electron arising from a broken bond. This last line shows a g-shift with temperature which was explained as due to the interaction of the paramagnetic center with a host U^{4+} ion.

V. CONCLUSION

Electron paramagnetic resonance is a very useful tool in obtaining information on uranium ions (1-3, 290-293). As shown in this review, some of the peculiarities of the actinide 5f configurations have a great impact on the EPR parameters. The uranium ions form a family which encompasses the first three $5f^n$ configurations, i.e. those where the identity of the actinides is best represented. The resonance data show clearly that a boundary line separates the U^{5+} ($5f^1$) ion in octahedral symmetry from the other ions of uranium as concerns the crystal field effects. Strong effects of the intermediate coupling and J mixing and intermediate coupling must be considered. All these uranium ions show covalency effects, manifested in orbital reduction factors and in the superhyperfine structure of the spectra. Details of the crystal field interaction could be determined, as for instance the ratio $A_4 <r^4>/A_6 <r^6>$ for trivalent uranium in cubic symmetry and the reduction of the free-ion g_J-value in crystals. The valence state of the uranium ions could be in most cases unambiguously determined, except for peculiar situations such as the concentrated systems. Very useful information about the symmetry and structure of the uranium centers in diluted systems have been obtained. The hyperfine structure studies have been effective in determination of the nuclear spin, nuclear magnetic dipole moment and nuclear electric quadrupole moments. The need for using the relativistic radial parameters in these estimations is now evident.

Still more information can be obtained if these studies are extended to encompass systematically a whole family of crystals. Thus, the studies on a given crystal, for instance calcium fluoride, should be extended to the whole family of eightfold cubic fluorides in order to find a closer correlation between the resonance parameters and the structural details of the system. More advanced techniques such as ENDOR or RDS should be employed in order to study finer effects such as the pseudonuclear g-value or pseudoquadrupole effects. A closer correlation of the data obtained by EPR and other methods is also necessary.

Very useful information could be obtained from a study of isoelectronic actinide ions $Pa^{(n-1)+}$ - U^{n+} -$Np^{(n+1)+}$ - $Pu^{(n+2)+}$ or of the isovalent Pa^{n+} - U^{n+} -Np^{n+} - Pu^{n+} ions in the same lattice.

Note Added in Proof. A recent observation of the ^{235}U NMR signal in UF_6 (294) leads to a nuclear magnetic moment of ^{235}U of $-0.35999\mu_n$. The discrepency between this value and that determined from EPR of U^{3+} using a relativistic radial parameter could be accounted for only if large core polarization effects (of the order of 25%) in the hyperfine structure of $^{235}U^{3+}$ are supposed.

REFERENCES

[1] A. Abragam and B. Bleaney, *Electron*

Paramagnetic Resonance of Transition Ions, Clarendon Press, Oxford , 1971.

[2] L. A. Boatner and M. M. Abragam, *Rep. Progr. Phys.* **41,** 87 (1978).

[3] I Ursu, *Rezonanta Magnetica in Compusi cu Uraniu* (*Magnetic Resonance of* Uranium Compounds), Ed., Acad. R. S. Romania, Bucharest, 1979 (in Romanian); *Magnitny Rezonans v Soedynenyah Urana*, Energoatomizdat, Moscow, 1983 (updated edition, in Russian).

[4] *C. R. C. Handbook of Chemistry and Physics*, 53rd Edition, CRC Press, 1972-1973.

[5] W. H. Zachariasen, in *The Actinide Elements*, G. T. Seaborg and J. J. Katz, Eds., McGraw Hill Co., New York, 1954, p. 769.

[6] N. Bohr, *Nature* **112,** 30 (1923).

[7] O. Hahn, *Angew. Chem.* **42,** 924 (1929).

[8] E. U. Condon and G. H. Shortley, *The Theory of Atomic Spectra*, Cambridge Univ. Press, Cambridge, 1935.

[9] B. R. Judd, *Operator Techniques in Atomic Spectroscopy*, McGraw-Hill Co., New York, 1963.

[10] B. G. Wybourne, *Spectroscopic Properties of Rare Earths*, Interscience Publ., New York, 1965.

[11] D. R. Hartree, *Proc. Cambr. Phil. Soc.* **24,** 89 (1928).

[12] V. Fock, *Z. Physik* **61,** 126 (1930).

[13] J. C. Slater, *Phys. Rev.* **81,** 385 (1951).

[14] W. Kohn and J. Sham, *Phys. Rev., A* **140,** 1133 (1965).

[15] I. Lindgren, *Phys. Lett.* **19,** 382 (1965).

[16] J. C. Slater, T. M. Wilson, and J. H. Wood, *Phys. Rev* **179,** 28 (1969).

[17] H. A. Bethe and E. E. Salpeter, *Quantum Mechanics of One- and Two-Electron Atoms*, Springer Verlag, Berlin, 1957.

[18] S. Cohen, *Phys. Rev.* **118,** 489 (1960).

[19] B. Swirles, *Proc. Roy. Soc., Ser. A* **152,** 625 (1935).

[20] J. P. Grant, *Proc. Roy. Soc., Ser. A* **262,** 555 (1961).

[21] D. A. Liberman, J. T. Waber, and D. T. Cromer, *Phys. Rev., A* **137,** 37 (1965).

[22] I. P. Grant, *Adv. in Phys.* **19,** 747 (1970).

[23] J. P. Desclaux and N. Bessis, *Phys. Rev., A* **2,** 1633 (1970).

[24] C. J. Lenander, *Phys. Rev.* **130,** 1033 (1963).

[25] W. B. Lewis, J. B. Mann, D. A. Liberman, and D. T. Cromer, *J. Chem. Phys.* **53,** 809 (1970).

[26] A. J. Freeman, J. P. Desclaux, G. H. Lander, and J. Faber, *Phys. Rev. B* **13,** 1168 (1976).

[27] D. W. Steinhaus, L. J. Radziemski, R. D. Cowan, J. Blaise, G. Guelaschvili, Z. Ben Osman, and J. Vergen, *Present Status of the Analysis of the First and Second Spectra of Uranium (U I and U II) as Derived from Measurements of Optical Spectra*, Los Alamos Sci. Lab. Report, Los Alamos, 1971, LA-4501.

[28] J. Blaise and L. J. Radziemski, *J. Opt. Soc. Am.* **66,** 644 (1976).

[29] L. R. Carlson, J. A. Paisner, E. F. Worden, S. A. Johnson, C. A. May, and R. W. Solarz, *J. Opt. Soc. Am.* **66,** 846 (1976).

[30] R. W. Solarz, Z. A. Paisner, L. R. Carlson, S. A. Johnson, E. F. Worden, and C. A. May, *Opt. Commun.* **18,** 29 (1976).

[31] R. W. Solarz, C. A. May, L. A. Paisner, and L. A. Radziemski, *Phys. Rev., A* **14,** 1129 (1976).

[32] E. Miron, L. A. Levin, and G. Erez, *Opt. Commun.* **18,** 66 (1976).

[33] E. Miron, L. A. Leven, G. Erez, and S. Lavi, *Opt. Commun.* **18,** 536 (1976).

[34] C. C. Kiess, C. J. Humphreys, and D. D. Laun, *J. Opt. Soc. Am.* **66,** 644 (1976); *J. Res. Nat. Bur. Std.* **37,** 57 (1946).

[35] P. Schuurmans, *Physica* **11,** 419 (1946).

[36] W. C. Marten, L. Hagen, J. Reader, and J. Sugar, *J. Phys. Chem. Ref. Data* 771 (1974).

[37] J. C. Van den Bosch and G. J. Van den Berg, *Physica* **15,** 329 (1949).

[38] M. Diringer, *Ann. Phys.* (*Leipzig*) **10,** 89 (1966).

[39] N. Spector, *Phys. Rev., A* **8,** 3270 (1973).

[40] S. Imoto, H. Adachi, and S. Asai, in *Proc. 2nd Int. Conf. on Electronic Structure of the Actinides, Wroclaw, 1976*, J. Mulak, W. Suski, and R. Troc, Eds., Ossolineum, Wroclaw, 1976, p. 61.

[41] B. R. Judd, *J. Opt. Soc. Am.* **58,** 1311 (1968).

[42] K. L. Van der Sluis and L. J. Nugent, *J. Opt. Soc. Am.* **64,** 687 (1974).

[43] W. A. Hargreaves, *Phys. Rev.* **156,** 331 (1967).

[44] W. A. Hargreaves, *Phys. Rev., B* **2,** 2273 (1970).

[45] W. T. Carnall and B. G. Wybourne, *J. Chem. Phys.* **40,** 3428 (1964).

[46] W. F. Krupke and J. B. Gruber, *J. Chem. Phys.* **46,** 542 (1967).

[47] A. Natarajan, S. D. Wang, and J. O. Artman, *J. Chem. Phys.* **62,** 2707 (1975).

[48] J. G. Conway, *J. Chem. Phys.* **41,** 904 (1964).

[49] H. Crosswhite and H. M. Crosswhite, *J. Opt. Soc. Am.* **60,** 1556 A (1970).

[50] H. J. Stapleton, C. D. Jeffries, and D. A. Shirley, *Phys. Rev.* **124,** 1455 (1961).

[51] R. Zalubas, *J. Opt. Soc. Am.* **58,** 1195

(1968).
[52] P. F. A. Klinkenberg, *Physica* **16,** 618 (1950).
[53] G. Racah, *Physica* **16,** 651 (1950).
[54] P. F. A. Klinkenberg and R. J. Lang, *Physica* **15,** 774 (1949).
[55] P. P. Sorokin and M. J. Stevenson, *Phys. Rev. Lett.* **5,** 557 (1960).
[56] G. D. Boyd, R. J. Collins, S. P. S. Porto, A. Yariv, and W. A. Hargreaves, *Phys. Rev. Lett.* **8,** 269 (1962).
[57] S. P. S. Porto and A. Yariv, in *Quantum Electronics*, P. Grivet and N. Bloembergen, Eds., Columbia Univ. Press, New York, 1964, p. 717.
[58] J. G. Conway, *J. Chem. Phys.* **31,** 1002 (1959).
[59] R. McLaughlin, *J. Chem. Phys.* **36,** 2699 (1962).
[60] R. A. Satten, D. Young, and D. M. Gruen, *J. Chem. Phys.* **33,** 1140 (1960).
[61] J. F. Wyart, V. Kaufman, and J. Sugar, *Phys. Scripta* **22,** 389 (1980).
[62] C. H. H. Van Deurzen, K. Rajnak, and J. G. Conway, *Rept. LBL-15924*, Lawrence Berkeley Lab. (1983).
[63] V. Kaufman and L. J. Radziemski, *J. Opt. Soc. Am.* **66,** 599 (1976).
[64] W. B. Lewis, L. B. Asprey, L. H. Jones, R. S. McDowell, S. W. Rabideau, A. H. Zeltman, and R. T. Paine, *J. Chem. Phys.* **65,** 2707 (1976).
[65] M. Boring and H. G. Hecht, *J. Chem. Phys.* **69,** 112 (1978).
[66] M. Boring and J. H. Wood *J. Chem. Phys.* **71,** 32 (1979).
[67] P. J. Hay, W. R. Wadt, L. R. Kahn, R. C. Raffenetti, and D. H. Phillips, *J. Chem. Phys.* **71,** 1767 (1979).
[68] S. de Silvestri, O. Svelto, and F. Zaraga, *Appl. Phys.* **21,** 1 (1980).
[69] D. A. Case and C. Y. Yang, *J. Chem. Phys.* **72,** 3443 (1980).
[70] D. J. Newman, *Adv. Phys.* **20,** 197 (1971).
[71] C. Morrison, D. R. Mason, and D. Kikuchi, *Phys. Lett. A* **24,** 607 (1976).
[72] H. A. Bethe, *Ann. Phys.* **3,** 133 (1929).
[73] M. T. Hutchings, *Solid State Phys.* **16,** 227 (1964).
[74] K. W. H. Steven, *Proc. Phys. Soc.* **65,** 209 (1952).
[75] C. W. Nielson and G. F. Koster, *Spectroscopic Coefficients for the p^n, d^n, and f^n Configurations*, MIT Press, Cambridge, Mass., 1963.
[76] P. Erös and H. A. Razafimandimby, *Helv. Phys. Acta* **51,** 12 (1978).
[77] M. I. Bradbury and D. J. Newman, *Chem. Phys. Lett.* **1,** 44 (1967).
[78] K. R. Lea, M. J. M. Leask, and W. P. Wolf, *J. Phys. Chem. Solids* **23,** 1381 (1962).
[79] V. Lupei, C. Stoicescu, and I. Ursu, *Bull. Magn. Reson.* **5,** 205 (1983).
[80] V. Lupei and C. Stoicescu, *J. Phys., C* in press.
[81] S. K. Chan and D. J. Lam, in *The Actinides: Electronic Structure and Related Properties*, A. J. Freeman and J. B. Darby, Eds., Academic Press, New York, 1974, Vol. I, p. 1.
[82] S. K. Chan and D. J. Lam, in *Plutonium 1970*, W. N. Miner, Ed., Met. Soc. AIME, New York, 1970, p. 219.
[83] B. G. Wybourne, *J. Chem. Phys.* **43,** 4506 (1965).
[84] A. J. Freeman and D. J. Koeling, in *The Actinides: Electronic Structure and Related Properties*, A. J. Freeman and J. B. Darby, Eds., Academic Press, New York, 1974, Vol. I, p. 51.
[85] J. C. Eisenstein and M. H. L. Pryce, *Proc. Roy. Soc., Ser. A* **255,** 181 (1960).
[86] C. A. Hutchison and B. Weinstock, *J. Chem. Phys.* **32,** 56 (1960).
[87] M. J. Reisfeld and G. A. Crosby, *Inorg. Chem.* **4,** 65 (1965).
[88] P. Rigny and P. Plurien, *J. Phys. Chem. Solids* **28,** 2589 (1967).
[89] J. Selbin and J. D. Ortego, *Chem. Rev.* **69,** 657 (1969).
[90] C. J. Ballhausen, *Theor. Chim. Acta* **24,** 234 (1972).
[91] J. Selbin, C. J. Ballhausen, and D. G. Durrett, *Inorg. Chem.* **11,** 510 (1972).
[92] J. L. Ryan, *MPT Int. Rev. Sci., Inorg. Chem. Ser. 1*, K. W. Bagnall, Ed., Butterworths, London, 1972, Vol. 7.
[93] W. B. Lewis, H. G. Hecht, and M. P. Eastman, *Inorg. Chem.* **12,** 1634 (1973).
[94] M. Drifford and E. Soulie, *Coll. Int. du C.N.R.S., Nr. 225* CNRS, Ed., Lyon, 1976, Paris, 1977, p. 95.
[95] N. Edelstein, *Rev. Chem. Miner.* **14,** 149 (1977).
[96] R. E. Tress, *Phys. Rev.* **83,** 756 (1951).
[97] B. R. Judd, *Adv. Chem. Phys.* **14,** 91 (1969).
[98] B. R. Judd, H. M. Crosswhite, and H. Crosswhite, *Phys. Rev.* **169,** 130 (1968).
[99] M. Born and J. R. Oppenheimer, *Ann. Phys.* **84,** 457 (1927).
[100] M. Born and K. Huang, *Dynamical Theory of Crystal Lattices*, Oxford Univ. Press, Oxford, 1954.
[101] H. A. Jahn and E. Teller, *Proc. Roy. Soc., Ser. A* **161,** 220 (1937).
[102] F. S. Ham, in *Electron Paramagnetic Resonance*, S. Geschwind, Ed., Plenum Press, New

York, 1972, p. 1.

[103] R. Englman, *The Jahn-Teller Effect in Molecules and Crystals*, Wiley, New York, 1972.

[104] T. L. Estle, *N.A.T.O. Summer School on Optical Interactions in Solids*, Erice, 1975.

[105] B. R. Judd, in *Proc. 2nd Conf. on Electronic Structure of the Actinides, Wroclaw, 1976*, J. Mulak, W. Suski, and R. Troc, Eds., Ossolineum, Wroclaw, 1977, p. 93.

[106] B. P. Dunlap and G. M. Kalvius, in *The Actinides: Electronic Structure and Related Properties*, A. J. Freeman and J. B. Darby, Eds., Academic Press, New York, 1974, Vol. I, p. 237.

[107] C. Schwartz, *Phys. Rev.* **97,** 380 (1955).

[108] G. H. Sandars and J. Beck, *Proc. Roy. Soc., Ser. A* **289,** 97 (1965).

[109] L. Armstrong, Jr., *Theory of Hyperfine Stucture of Free Atoms*, Wiley, New York (1971).

[110] S. Feneuille and L. Armstrong, Jr., *Phys. Rev., A* **8,** 1173 (1973).

[111] B. Bleaney, in *Hyperfine Interactions*, A. J. Freeman and R. B. Frankel, Eds., Academic Press, New York, 1967, p. 12.

[112] E. Fermi, *Z. Physik* **60,** 320 (1930).

[113] B. G. Wybourne, *J. Chem. Phys.* **37,** 1807 (1962).

[114] N. Edelstein and R. Mehlhorn, *Phys. Rev., B* **2,** 1225 (1970).

[115] H. B. G. Casimir, *On the Interaction between Atomic Nuclei and Electrons*, W. E. Freeman, San Francisco, 1963.

[116] R. M. Sternheimer, *Phys. Rev.* **84,** 244 (1951).

[117] R. M. Sternheimer, *Phys. Rev.* **146,** 140 (1966).

[118] S. Gerstenkorn, P. Luc, Cl. Bauche-Arnoult, and D. Merle, *J. Phys. (Paris)* **34,** 805 (1973).

[119] F. Guyon, Thesis, Orsay (1972).

[120] H. D. V. Bohm, W. Michaelis, and C. Wetkamp, *Opt. Commun.* **26,** 177 (1978).

[121] L. A. Hackel, C. F. Bender, M. A. Johnsson, and M. C. Rushford, *J. Opt. Soc. Am.* **69,** 230 (1979).

[122] W. J. Childs, O. Poulsen, and L. S. Goodman, *Opt. Lett* **4,** 35 (1979).

[123] W. J. Childs, O. Poulsen, and L. S. Goodman, *Opt. Lett.* **4,** 63 (1979).

[124] T. Ben Mena, J. M. Gagné, and J. M. Helber, *J. Phys. (Paris)* **30,** C 1-79 (1969).

[125] J. E. Wertz and J. R. Bolton, *Electron Spin Resonance*, McGraw Hill Co., New York, 1972.

[126] B. Bleaney, *Proc. Phys. Soc. (London)* **73,** 939 (1959).

[127] Y. Ayant, E. Belorizky, and J. Rosset, *J. Phys. Rad.* **23,** 201 (1962).

[128] J. A. Weil and J. H. Anderson, *J. Chem. Phys.* **35,** 1410 (1961).

[129] J. M. Baker, E. R. Davies, and J. P. Hurrell, *Proc. Roy. Soc., Ser. A* **308,** 403 (1968).

[130] I. Waller, *Z. Physik* **79,** 270 (1932).

[131] J. H. Van Vleck, *Phys. Rev.* **57,** 426 (1940).

[132] R. Orbach, *Proc. Roy. Soc., Ser. A* **264,** 458 (1961).

[133] J. M. Baker and B. Bleaney, *Proc. Roy. Soc., Ser. A* **245,** 156 (1958).

[134] V. Lupei, *J. Phys., C* **12,** L 45 (1979).

[135] V. Lupei and C. Stoicescu, *Rev. Roum. Phys.* **23,** 353 (1978).

[136] E. L. Nicholas and M. K. Slattery, *J. Opt. Soc. Am.* **12,** 449 (1926).

[137] W. A. Runciman, *Nature* **175,** 1082 (1955).

[138] W. A. Runciman, *Proc. Roy. Soc., Ser. A* **237,** 39 (1956).

[139] P. P. Feofilov, *Opt. Spectros.* **7,** 493 (1959); **8,** 433 (1960).

[140] A. A. Kaplyanskii and N. A. Moskvin, *Opt. Spectros.* **14,** 357 (1963).

[141] A. A. Kaplyanskii, N. A. Moskvin, and P. P. Feofilov, *Opt. Spectros.* **16,** 339 (1964).

[142] O. Risgin and A. G. Becker, *Appl. Opt.* **5,** 639 (1966).

[143] O. D. Gavrilov, A. A. Kaplyanskii, V. N. Medvedev, and N. A. Moskvin, *Opt. Spectros.* **27,** 521 (1969).

[144] D. D. Pant, D. N. Sanval, and J. C. Joschi, *Indian J. Pure Appl. Phys.* **7,** 103 (1969).

[145] S. Georgescu, H. Totia, F. Domsa, and V. Lupei, *J. Phys. E. Sci. Instrum.* **12,** 473 (1979).

[146] V. Lupei and A. Lupei, *Phys. Status Solidi, B* **94,** 301 (1979).

[147] K. K. Bagai and A. V. R. Warrier, *J. Phys., C* **10,** L 437 (1977).

[148] C. K. Bleijenberg and C. W. M. Timmermans, *Phys. Status Solidi, A* **47,** 589 (1978).

[149] C. K. Bleijenberg and P. P. Bredels, *J. Chem. Phys.* **72,** 5390 (1980).

[150] C. K. Bleijenberg, *Structure and Bonding* **42,** 97 (1980).

[151] V. Lupei and P. H. Yuster, *Proc. XVIIth Congress Ampere, Turku, Finland, 1972*, V. Hovi, Ed., North Holland Publ. Co., Amsterdam, 1973, p. 535.

[152] V. Lupei and C. Lupu, unpublished results.

[153] V. Lupei and I. Voicu, *J. Phys. Chem. Solids* **37,** 1093 (1976).

[154] V. Lupei and I. Ursu, *Proc. XVIIIth Ampere Congress, Nottingham, 1974* P. S. Allen, E. R. Andrew, and C. A. Bates, Eds., University of Nottingham Press, 1974, Vol. I, p. 177.

[155] V. Lupei, A. Lupei, S. Georgescu, and I.

Ursu, *J. Phys.*, *C* **9,** 2619 (1976).

[156] V. Lupei, A. Lupei, S. Georgescu, and I. Ursu, *Proc. XIXth Ampere Congress, Heidelberg, 1976* H. Brunner, K. H. Hausser, and D. Schweitzer, Eds., Groupment Ampere, Heidelberg, 1976, p. 554.

[157] V. Lupei, S. Georgescu, and I. Ursu, *Rev. Roum. Phys.* **21,** 25 (1976).

[158] V. Lupei, A. Lupei, and S. Georgescu, *Rev. Roum. Phys.* **21,** 906 (1976).

[159] J. C. Eisenstein and M. H. L. Pryce *Proc. Roy. Soc., Ser. A* **229,** 20 (1955).

[160] A. Lupei, V. Lupei, and I. Ursu, *J. Phys., C* **15,** 5489 (1982).

[161] W. A. Runciman and E. Y. Wong, *J. Chem. Phys.* **71,** 1838 (1979).

[162] W. A. Runciman, B. T. Thangavadivei, and N. B. Manson, *J. Luminesc.* **24/25,** 209 (1981).

[163] F. A. Kroger, *Physica* **14,** 488 (1948).

[164] W. A. Runciman, *Britt. J. Appl. Phys. Suppl.* **4,** 578 (1955).

[165] J. V. Nicholas, *Phys. Rev.* **155,** 151 (1967).

[166] N. B. Manson, G. H. Shah, and W. A Runciman, *Solid State Commun.* **16,** 645 (1975).

[167] A. Lupei and V. Lupei, *J. Phys., C* **12,** 1123 (1979).

[168] V. Lupei, A. Lupei, and I. Ursu, *Proc. XXth Ampere Congress, Tallin, 1978*, E. Kundla, E. Lippmaa, and T. Saluvere, Eds., Springer-Verlag, Berlin, 1979, p. 294.

[169] I. Ursu, V. Lupei, and A. Lupei, *Rev. Roum. Phys.* **23,** 673 (1978).

[170] V. Lupei, and A. Lupei, *Rev. Roum. Phys.* **22,** 869 (1977).

[171] V. Lupei, A. Lupei, and I. Ursu, *J. Phys., C* **10,** 4587 (1977).

[172] A. Lupei and V. Lupei, *J. Phys., C* **11,** 2861 (1978).

[173] D. L. Perry, S. M. Klainer, H. R. Bowman, F. P. Milanovich, T. Hirschfeld, and S. Miller, *Anal. Chem.* **53,** 1048 (1981).

[174] M. V. Johnston and J. C. Wright, *Anal. Chem.* **53,** 1050 (1981).

[175] I. Ursu, V. Lupei, and F. Domsa, *Ann. Sess. Central Inst of Phys. Bucharest*, paper 15, 1976, p. 169.

[176] M. Drifford, P. Rigny, and P. Plurien, *Phys.Lett.* **27A,** 620 (1968).

[177] P. Rigny, A. J. Dianoux, and P. Plurien, *J. Phys. Chem. Solids* **32,** 1175 (1971).

[178] J. Selbin, J. D. Ortego, and G. Gritzner, *Inorg. Chem.* **7,** 976 (1968).

[179] C. Miyake, K. Fuji, and S. Imoto, *Inorg. Nucl. Chem. Lett.* **13,** 53 (1977).

[180] J. Selbin and H. J. Sherill, *Inorg. Chem.* **13,** 1235 (1974).

[181] A. F. Leung, *Can. J. Phys.* **54,** 178 (1978).

[182] E. Soulie, *J. Phys. Chem. Solids* **39,** 695 (1978).

[183] J. Mulak and Z. Zolnierek, *Bull. Pol. Acad. Aci., Ser. Sci. Chem.* **20,** 1081 (1972).

[184] W. B. Lewis, H. G. Hecht, and M. P. Eastman, *Inorg. Chem.* **12,** 1634 (1973).

[185] C. Miyake, K. Fuji, and S. Imoto, *Chem. Phys. Lett.* **61,** 124 (1979).

[186] R. Parrot, C. Nau, C. J. Delbecq, and P. H. Yuster, *Phys. Rev., B* **15,** 137 (1977).

[187] R. Parrot and C. Naud, *Proc. 2nd Int. Conf. on Electronic Structure of the Actinides, Wroclaw, 1976*, Wroclaw, Sept. 1976, J. Mulak, W. Suski, and R. Troc, Eds., Ossolineum, Wroclaw, 1977, p. 133.

[188] V. Lupei and A. Lupei, *J. Phys., C* in press.

[189] K. C. Bleijenberg, *J. Chem. Phys.* **73,** 617 (1980).

[190] V. Lupei, unpublished.

[191] J. S. Griffith, *Theory of Transition Metal Ions*, Cambridge Univ. Press, 1961.

[192] P. M. Llewellyn, Thesis, Oxford University, 1965.

[193] P. Rigney, A. J. Dianoux, and P. Plurien, *J. Phys. Chem. Solids* **32,** 1901 (1971).

[194] V. Lupei and A. Lupei, *Rev. Roum. Phys.* **23,** 363 (1978).

[195] A. Lupei and V. Lupei, *Phys. Stat. Solids, B* **95,** K69 (1979).

[196] S. D. McLaughlan and P. A. Forrester, *Phys. Rev.* **151,** 311 (1966).

[197] C. R. A. Catlow, J. D. Comins, F. A. German, T. R. Harley, and W. Hayes, *J. Phys., C* **11,** 3197 (1978).

[198] V. Lupei, A. Lupei, and S. Georgescu, *Phys. Stat. Solids, B* **83,** 71 (1977).

[199] A. Lupei and V. Lupei, *Rev. Roum. Phys.* **22,** 1005 (1977).

[200] I. Ursu and V. Lupei, *Ann. Sci. Sess. of the Central Inst. of Phys., Bucharest*, paper 29, 1976, p. 231.

[201] I. Urus, V. Lupei, and I. Voicu, *Rev. Roum. Phys.* **24,** 229 (1979).

[202] B. Bleaney, P. M. Llewelyn, M. H. L. Pryce, and G. R. Hall, *Phil. Mag.* **45,** 992 (1954).

[203] Y. Obata and K. Sasaki *J. Phys. Soc. Jap.* **42,** 36 (1977).

[204] S. D. McLaughlan, *Phys. Rev.* **150,** 118 (1966).

[205] W. A. Hargreaves, *Phys. Rev.* B **6,** 3417 (1972).

[206] K. A. Müller, *Phys. Rev.* **171,** 350 (1968).

[207] C. M. Bowden, H. C. Meyer, and P. L. Donoho, *Int. J. Quant. Chem.* **3 S,** 617 (1970).
[208] G. C. Wetsel and P. L. Donoho, *Phys. Rev.* **139,** A 334 (1965).
[209] H. C. Meyer, P. F. McDonald, J. D. Stettler, and P. L. Donoho, *Phys. Lett.* **24 A,** 569 (1967).
[210] P. F. McDonald, H. C. Meyer, and P. L. Donoho, *Sol. State Commun.* **6,** 367 (1969).
[211] G. C. Wetzel, *J. Appl. Phys.* **39,** 692 (1968).
[212] P. F. McDonald, *Phys. Rev.* **177,** 447 (1969).
[213] C. M. Bowden, H. C. Mayer, and P. F. Donald, *Phys. Rev. Lett.* **22,** 224 (1969).
[214] C. M. Bowden, H. C. Meyer, P. F. McDonald, and J. D. Stettler, *J. Phys. Chem. Solids* **30,** 1535 (1969).
[215] C. M. Bowden, H. C. Meyer, and P. L. Donoho, *Phys. Rev., B* **3,** 656 (1971).
[216] P. F. Wunsch, Ph.D. Thesis, Rice Univ. (1972).
[217] P. K. Wunsch and P. L. Donoho, in *Proc. XVIIth Ampere Congress Turku, 1972,* V. Hovi, Ed., North Holland Publ. Co., 1973, p. 312.
[218] V. Lupei and C. Stoicescu, *J. Phys., C* **12,** 4585 (1979).
[219] A. Yariv, *Phys. Rev.* **128,** 1588 (1962).
[220] A. Yariv, in *Proc. Int. Conf. on Paramagnetic Resonance,* W. Low, Ed., Academic Press, New York, 1963, Vol. I, p. 189.
[221] R. S. Title, P. P. Sorokin, M. J. Stevenson, G. D. Pettit, J. E. Scardefield, and J. R. Landard, *Phys. Rev.* **128,** 62 (1962).
[222] R. S. Title, in *Proc. Int. Conf. on Paramagnetic Resonance,* W. Low, Ed., Academic Press, New York, 1963, Vol. I, p. 178.
[223] W. Hayes, in *Crystals with the Fluorite Structure,* W. Hayes, Ed., Clarendon Press, Oxford, 1974, p. 392.
[224] P. F. McDonald, E. L. Wilkinson, and R. A. Jensen, *Phys. Chem. Solids* **28,** 1629 (1967).
[225] M. McDonald, U. Abend, J. G. Conway, N. Edelstein, and E. H. Huffman, *J. Chem. Phys.* **53,** 2030 (1970).
[226] V. Lupei, *Rev. Roum. Phys.* **29,** 000 (1984).
[227] B. Bleaney, P. M. Llewellyn, and D. A. Jones, *Proc. Phys. Soc., B* **69,** 858 (1956).
[228] G. Vincow and W. Low, *Phys. Rev.* **122,** 1390 (1961).
[229] V. Lupei and C. Stoicescu, in *Proc. XIXth Ampere Congress, Heidelberg, 1976,* M. Brunner, K. H. Hausser, and D. Schweitzer, Eds., Groupment Ampere, Heidelberg, 1976, p. 243.
[230] V. Lupei and C. Stoicescu, unpublished results.
[231] D. Sengupta and J. O. Artman, *J. Chem. Phys.* **54,** 1010 (1971).
[232] C. Stoicescu and V. Lupei, unpublished results.
[233] F. R. Meritt, H. Guggenheim, and C. G. B. Garrett, *Phys. Rev.* **145,** 188 (1966).
[234] E. R. Bernstein and L. W. Dennis, *Phys. Rev., B* **20,** 870 (1979).
[235] I. E. Kask and L. S. Kornienko, *J.E.T.Ph.* **53,** 504 (1967).
[236] P. R. Richardson and J. B. Gruber, *J. Chem. Phys.* **56,** 256 (1972).
[237] V. Lupei, C. Stoicescu, and I. Ursu, *J. Phys., C* **9,** L 317 (1967).
[238] S. D. MacLaughlan, *Phys. Rev.* **160,** 287 (1967).
[239] V. Lupei and C. Stoicescu, *Bull. Magn. Reson.* **2,** 179 (1981).
[240] T. D. Black and P. L. Donoho, *Phys. Rev.* **170,** 462 (1968).
[241] V. Lupei, C. Stoicescu, and I. Voicu, *Rev. Roum. Phys.* **22,** 549 (1977).
[242] A. Kiel and W. B. Mims, *Phys. Rev., B* **7,** 2917 (1973).
[243] B. G. Berulava, T. I. Sanadza, and O. G. Khakhanashvili, *Sov. Phys. Sol. State* **7,** 509 (1965).
[244] P. L. Donoho and T. D. Black, in *Proc. XIVth Ampere Congress Ljubljana, 1966,* R. Blinc, Ed., North Holland Publ. Co., Amsterdam, 1967, p. 244.
[245] T. I. Sanadze and B. G. Berulava, *Izv. Acad. Nauk. SSSR, Ser. Fiz.* **31,** 1973 (1967).
[246] V. P. Shekun, *Fiz. Tverd. Tela, Leningrad* **13,** 1741 (1971).
[247] T. D. Black, *Phys. Lett.* **37,** A 303 (1971).
[248] L. W. Leppelmeier and J. Jeener, *Phys. Rev.* **175,** 498 (1968).
[249] G. R. Khutsishvili, *Comments Sol. St. Phys.* **5,** 23 (1972).
[250] G. R. Khutsishvili and B. D. Mikaberidze, in *Proc. XVIIIth Ampere Congress, Nottingham, 1974,* P. S. Allen, E. R. Andrew, and C. A. Bates, Eds., University of Nottingham Press, 1974, Vol. II, p. 471.
[251] E. Secemski, D. Kiro, W. Low, and D. J. Schipper, *Phys. Lett.* **31,** A 45 (1970).
[252] E. Secemski and W. Low, in *Proc. XVIIth Ampere Congress, Turku, 1972,* W. Hovi, Ed., North Holland Publ. Co., Amsterdam, 1973, p. 315.
[253] P. I. Bekauri, B. G. Berulava, T. I. Sanadze, O. K. Khanashvili, and G. R. Khutsishvili, *J.E.T.Ph.* **59,** 368 (1970).
[254] T. I. Sanadze and G. R. Khutshishvili, *J.E.T.Ph.* **59,** 753 (1970).
[255] T. A. Abramovskaya, B. G. Berulava, and

T. I. Sanadze, *Pisma J.E.T.Ph.* **16,** 555 (1972).

[256] T. A. Abramovskaya, B. G. Berulava, and T. I. Sanadze, *J.E.T.Ph.* **66,** 306 (1974).

[257] G. R. Khutsishivili and T. I. Sanadze, in *Proc. XVIIIth Ampere Congress, Nottingham, 1974,* P. S. Allen, E. R. Andrew, and C. A. Bates, Eds., University of Nottingham Press, 1974, Vol. I, p. 17.

[258] A. A. Antipin and V. S. Zapaskii, *Fiz. Tverd. Tela, Leningrad* **21,** 3562 (1979).

[259] E. Mahlab, V. Volterra, W. Low, and A. Yariv, *Phys. Rev.* **131,** 920 (1963).

[260] R. H. Heist and F. K. Fong, *Phys. Rev., B* **1,** 2970 (1970).

[261] V. Lupei, *Rev. Roum. Phys.* **25,** (1980).

[262] E. D. Dahlberg and T. D. Black, *Phys. Rev., B* **10,** 3756 (1974).

[263] V. Lupei, *Bull. Magn. Reson.* **2,** 180 (1981).

[264] V. Lupei, *J. Phys., C* **16,** 6623 (1983).

[265] B. G. Berulava and G. I. Sanadze, in *Paramagnitny Rezonans,* Univ. of Kazan, 1960, p. 11 (in Russian).

[266] P. I. Mirianashvili, *Fiz. Tverd. Tela, Leningrad* **20,** 2074 (1978).

[267] M M. Abraham, L. A. Boatner, J. O. Ramey, and M. Rappaz, *J. Chem. Phys.* **78,** 3 (1983).

[268] B. Bleaney, C. A. Hutchison, Jr., P. M. Lewellyn, and D. F. D. Pope, *Proc. Phys. Soc., B* **69,** 1167 (1956).

[269] C. A. Hutchison, Jr., P. M. Llewellyn, E. Wong, and P. Dorain, *Phys. Rev.* **102,** 292 (1956).

[270] P. Dorain, C. A. Hutchison, Jr., and W. Wong, *Phys. Rev.* **105,** 1307 (1957).

[271] R. Furrer, F. Seiff, and J. Pelzl, *Phys. Stat. Solids, B* **63,** 549 (1974).

[272] R. L. Marchand, G. E. Fish, and H. J. Stapleton, *Phys. Rev., B* **11,** 23 (1975).

[273] T. C. L. G. Sollner and R. N. Rogers, *A. I. P. Conf. Proc.* **18,** 550 (1974).

[274] V. Lupei, *J. Phys., C* **16,** 6627 (1983).

[275] R. J. Elliott and K. W. H. Stevens, *Proc. Roy. Soc., Ser. A* **219,** 387 (1953).

[276] C. A. Candela, C. A. Hutchison, Jr., and W. B. Lewis, *J. Chem. Phys.* **30,** 246 (1959).

[277] G. Raphael and R. Lallement, *Sol. State Commun.* **6,** 383 (1968).

[278] E. R. Jones, M. E. Hendricks, J. A. Stone, and D. G. Karraker, *J. Chem. Phys.* **60,** 2088 (1974).

[279] A. Natarajan, S. D. Wang, and J. O. Artman, *J. Chem. Phys.* **62,** 2707 (1975).

[280] H. J. Stapleton, C. D. Jeffries, and D. A. Shirley, *Phys. Rev.* **124,** 1455 (1961).

[281] S. N. Ghosh, W. Gordy, and D. G. Hill, *Phys. Rev.* **96,** 36 (1954).

[282] J. Mulak, Z. Zolnierek, V. Lupei, A. Lupei, and C. Stoicescu, unpublished results.

[283] A. T. Tench, J. F. J. Kibblewhite, and V. J. Wheeler, in *Reactivity of Solids, Proc. 7th Int. Sym. Bristol,* Chapman and Hall, London, 1972, p. 38.

[284] J. J. Verbist, J. Riga, C. Tenret-Noel, J. J. Pireaux, G. D'Ursel, R. Caudano, and E. G. Derouane, in *Plutonium and other Actinides,* H. Black and R. Linder, Eds., North Holland Publ. Co., Amsterdam, 1976, p. 409.

[285] E. Thibaut, J. J. Pireaux, J. Riga, C. Tenret-Noel, R. Caudano, E. G. Derouane, and J. Verbist, in *Proc. 2nd Int. Conf. on Electronic Structure of the Actinides, Wroclaw, 1976,* Wroclaw 1976, J. Mulak, W. Suski, and R. Troc, Eds., Ossolineum, Wroclaw, 1977, p. 61.

[286] A. C. Allen, A. J. Griffiths, and Ch. W. Suckling, *Chem. Phys. Lett.* **53,** 309 (1978).

[287] D. Jakes and I. Krivy, *J. Inorg. Nucl. Chem.* **39,** 51 (1974).

[288] E. H. P. Cordfunke and B. O. Loopstra, *J. Inorg. Nucl. Chem.* **39,** 51 (1976).

[289] M. Baran, H. Szymczak, B. Janus, and W. Suski, *Sol. State Commun.* **48,** 569 (1983).

[290] I. Ursu, *Rev. Roum. Phys.* **26,** 783 (1981).

[291] I. Ursu and V. Lupei, *Proc. Div. Conf. EPS, Nuclear and Atomic Physics with Heavy Ions,* Publ. by Central Inst. of Physics, Bucharest, 1982, p. 39.

[292] I. Ursu and V. Lupei, *Int. Magn. Reson. Rev., in press.*

[293] I. Ursu and V. Lupei, *Bull. Magn. Reson.* **5,** 136 (1983).

[294] H. Le Bail, C. Chachaty, P. Rigny, R. Bougon, *J. Physique Lett.* **44,** L 1017 (1983).

Appendix I. (1)

Electron Paramagnetic Resonance data on U^{5+}

C denotes cubic, Tg tetragonal, Tr trigonal and Rh rhombic and centers at lower symmetry

Host	Center	T	| g |	Hyperfine structure (^{235}U, I = 7/2) (10^{-4} cm^{-1})	Superhyperfine structure (10^{-4} cm^{-1})	Ref.	Comments
LiF	C	77	0.333 ± 0.001		No	[146]	
LiF	Tg1	77	$g_{\parallel}$ = 0.253 ± 0.001 $g_{\perp}$ = 0.4716 ± 0.0005	$A_{\parallel}$ = 45 ± 1 $A_{\perp}$ = 45.5 ± 0.5 P = 50.5 ± 0.5	n_L = 1, I_L = 1/2 $A^L_{\parallel}$ = 14.3 ± 0.2 $A^L_{\perp}$ = 7.5 ± 0.2	[154], [156] [156]	
LiF	Tg2	77	$g_{\parallel} < 0.1$ $g_{\perp}$ = 0.587 ± 0.001		n = 2, I = 1/2 $A^L_{\perp} \sim$ 5.5	[146]	
LiF	Tg3	77	$g_{\parallel}$ = 0.13 ± 0.05 $g_{\perp}$ = 0.59 ± 0.001		No	[146]	
LiF	Tg4	77	$g_{\parallel}$ = 0.326 ± 0.01 $g_{\perp}$ = 0.362 ± 0.01		No	[146]	
LiF	Rh1	77	g_X = 0.517 ± 0.001 g_Y = 0.387 ± 0.001 g_Z = 0.20 ± 0.05		n_L = 1, I_L = 1/2	[146]	X ∥ |100|, Y and Z in plane (110) at δ = 10.8° from (110) and (001)

Appendix I. (2)

Host	Center	T	| g |	Hyperfine structure (^{235}U, I = 7/2) (10^{-4} cm^{-1})	Superhyperfine structure (10^{-4} cm^{-1})	Ref.	Comments
LiF	Rh2	77	$g_X = 0.562 \pm 0.001$ $g_Y = 0.563 \pm 0.001$ $g_Z = 0.337 \pm 0.005$		$n_L = 1$, $I_L = 1/2$	[146]	Y ∥ |001|, X and Z in plane (001) at $\delta = 5.7^\circ$ from |110| and |110|
LiF	Rh3	77	$g_X = 1.110 \pm 0.001$ $g_Y = 0.537 \pm 0.001$ $g_Z = 0.20 \pm 0.05$		$n_L = 1$, $I_L = 1/2$	[146]	Transformation matrix from |110|,|001|,|110| to XYZ: $\mathcal{L} = \begin{vmatrix} 0.973 & 0.075 & 0.217 \\ 0.177 & 0.846 & 0.503 \\ -0.146 & -0.528 & -0.837 \end{vmatrix}$
LiF	Rh4	77	$g_X = 0.937 \pm 0.001$ $g_Y = 0.15 \pm 0.05$ $g_Z = 0.543 \pm 0.001$		$n_L = 2$, $I_L = 1/2$ $A_Z^L \sim 4.8$	[146]	Z ∥ |001|, X and Y in plane (110) at $\delta = 7.8^\circ$ from |110| and |010|
LiF	Rh5	77	$g_X = 0.360 \pm 0.001$ $g_Y = 0.328 \pm 0.001$ $g_Z = 0.343 \pm 0.001$		No	[146]	X ∥ |110|, Y ∥ |110|, Z ∥ |001|
NaF	Tg1	77	$g_\parallel = 0.3935 \pm 0.0005$ $g_\perp = 0.5912 \pm 0.0005$	$A_\parallel = 46.0 \pm 0.2$ $A_\perp = 56.5 \pm 0.2$ $P = 75.0 \pm 0.5$	$n_L = 1$, $I_L = 1/2$ $A_\parallel^L = 9.8$ $A_\perp^L = 4.5$	[155], [156] [157]	

Appendix I. (3)

Host	Center	T	|g|	Hyperfine structure (^{235}U, I = 7/2) (10^{-4} cm^{-1})	Superhyperfine structure (10^{-4} cm^{-1})	Ref.	Comments
NaF	Tg2	77	$g_{\parallel} = 0.109 \pm 0.001$ $g_{\perp} = 0.6813 \pm 0.0005$	$A_{\parallel} = 34 \pm 1$ $A_{\perp} = 58 \pm 0.5$ $P = 93 \pm 0.5$	$n_L = 2$, $I_L = 1/2$ $A_{\perp}^{L} = 3.2$	[155], [156]	
NaF	Tg3	77	$g_{\parallel} = 0.16 \pm 0.01$ $g_{\perp} = 0.677 \pm 0.001$		$n_L = 1$, $I_L = 1/2$ $A_{\perp} = 3.1$	[160]	
NaF	Rh1	77	$g_X = 0.5894 \pm 0.0001$ $g_Y = 0.5940 \pm 0.0001$ $g_Z = 0.5442 \pm 0.0001$		No	[157]	X ∥ |110|, Y ∥ |110|, Z ∥ |001|
NaF	Rh2	77	$g_X = 0.794 \pm 0.001$ $g_Y = 0.581 \pm 0.001$ $g_Z = 0.332 \pm 0.01$		$n_L = 1$, $I_L = 1/2$ $A_X^L = 4.6$ $A_Y^L = 4.7$ $A_Z^L = 9.5$	[160]	Y ∥ |001|, X and Z in plane (001) at $\delta = 15.5^{\circ}$ from 100 and 010
NaF	Rh3	77	$g_X = 0.766 \pm 0.001$ $g_Y = 0.659 \pm 0.001$ $g_Z = 0.15 \pm 0.01$		$n_L = 1$, $I_L = 1/2$ $A_X = 3.2$ $A_Y = 3.8$	[160]	Y ∥ |001|, X and Z in plane (001) at $\delta = 1.8^{\circ}$ from 100 and 010

Appendix I. (4)

Host	Center	T	|g|	Hyperfine structure (^{235}U, I = 7/2) (10^{-4} cm^{-1})	Superhyperfine structure (10^{-4} cm^{-1})	Ref.	Comments
KF	Tg1	77	$g_{\parallel} = 0.169 \pm 0.001$ $g_{\perp} = 0.7258 \pm 0.0005$	$A_{\parallel} = 36 \pm 1$ $A_{\perp} = 59 \pm 0.5$ $P = 110.5 \pm 0.5$	$n_L = 2$, $I_L = 1/2$ $A_{\perp}^{L} = 2.7$	[158], [198]	
CaF_2	Tr	77	$g_{\parallel} = 0.190 \pm 0.005$ $g_{\perp} = 1.047 \pm 0.001$	$A_{\parallel} = 24.0 \pm 1$ $A_{\perp} = 66.0 \pm 0.5$ $P = 107.0 \pm 0.5$	No	[168], [170] [171], [199]	
CaF_2	Rh1	77	$g_X = 1.388 \pm 0.001$ $g_Y = 0.820 \pm 0.001$ $g_Z = 0.22 \pm 0.05$		$n_L = 1$, $I_L = 1/2$ $A^{L} = 9.2$ at 40° from 001	[168], [172]	X along |110|, Z and Y in plane (110) at $\delta = 0.7^{\circ}$ from |111| and |112|
CaF_2	Rh2	77	$g_X = 0.880 \pm 0.001$ $g_Y = 1.614 \pm 0.001$ $g_Z = 0.17 \pm 0.05$		$n_L = 2$, $I_L = 1/2$	[168], [172]	X along |110|, Z and Y in plane (110) at $\delta \sim 4^{\circ}$ from |111| and |112|
CaF_2	Rh3	77	$g_X = 1.019 \pm 0.001$ $g_Y = 1.054 \pm 0.001$ $g_Z = 0.20 \pm 0.05$		No	[167], [169]	Transformation matrix from |111|, |110|, |112| to XYZ: 0.9984 -0.0553 0.005 0.0552 0.9983 0.005 -0.005 -0.012 0.9999
CaF_2	Rh4	77	$g_X = 0.540 \pm 0.001$ $g_Y = 2.775 \pm 0.001$ $g_Z = 0.471 \pm 0.001$		No	[191], [195]	Z ∥ |110|, X and Y in plane (110) at $\delta = 1.8^{\circ}$ from |001| and |110|

Appendix II. (1)

Electron Paramagnetic Resonance data on $U^{4+}(5f^2)$

Host	Center	T	g^{app}	Hyperfine structure A^{app} (10^{-4} cm^{-1})	Ref.	Comments
ThO_2 Powder		290	~ 2.7		[192]	a)
CaF_2	C	1.4	~ 2		[204]	a)
CaF_2	Tr1	1.4; 4.2	$g_{\parallel} = 4.02 \pm 0.01$ $g_{\perp} \leq 0.1$		[204]	Superhyperfine structure with eight fluorine ligands
		4.2	$g_{\parallel} = 4.03 \pm 0.01$ $g_{\perp} \leq 0.1$	$A_{\parallel} = 107 \pm 0.5$	[218]	
CaF_2	Tr2	1.4	$g_{\parallel} = 5.66 \pm 0.02$ $g_{\perp} \leq 0.1$		[204]	
		4.2	$g_{\parallel} = 5.60 \pm 0.02$ $g_{\perp} \leq 0.1$	$A_{\parallel} = 234.5 \pm 1$	[218]	Superhyperfine structure with six fluorine ligands
CaF_2	Tr3	4.2	$g_{\parallel} = 3.238 \pm 0.005$ $g_{\perp} = 0.00 \pm 0.15$		[219], [220]	Superhyperfine structure with 24 fluorine ligands
			$g_{\parallel} = 3.27 \pm 0.05$ $g_{\perp} = 0.0 \pm 0.2$		[221], [222]	
SrF_2	Tr	4.2	$g_{\parallel} = 2.85 \pm 0.005$ $g_{\perp} = 0.0 \pm 0.15$		[219 - 222]	a)
BaF_2	Tr	4.2	$g_{\parallel} \sim 3$ $g_{\perp} \sim 0$		[219], [220]	a)

a) Nature of the center not firmly established.

Appendix III. (1)

Electron Paramagnetic Resonance data on U^{3+} ($5f^3$)

Host	Center	T	g	Hyperfine structure (10^{-4} cm^{-1})	Ref.	Comments
CaF_2	C	4.2	$2P = -2.740 \pm 0.005$ $2Q = 1.793 \pm 0.005$	106.1 ± 1 82.8 ± 1	[135], [229] [230]	Superhyperfine structure
CaF_2	Tg1	20	$g_{\parallel} = 3.501 \pm 0.008$ $g_{\perp} = 1.866 \pm 0.002$		[227]	Superhyperfine structure
		4	$g_{\parallel} = 3.528 \pm 0.005$ $g_{\perp} = 1.875 \pm 0.005$		[219]	
		4	$g_{\parallel} = 3.531 \pm 0.004$ $g_{\perp} = 1.878 \pm 0.001$		[240]	
		4.2	$g_{\parallel} = 3.533 \pm 0.002$ $g_{\perp} = 1.876 \pm 0.002$	$A_{\parallel} = 164.1 \pm 0.5$ $A_{\perp} = 64.8 \pm 0.5$	[274]	
CaF_2	Tg2(Na)	4.2	$g_{\parallel} = 2.740 \pm 0.003$ $g_{\perp} = 2.029 \pm 0.005$	$A_{\parallel} = 106 \pm 0.5$ $A_{\perp} = 92.5 \pm 1$	[237], [239], [274]	Co-doped with Na; Superhyperfine structure
CaF_2	Tg2(Li)	4.2	$g_{\parallel} = 2.746 \pm 0.005$ $g_{\perp} = 2.022 \pm 0.005$		[239]	Co-doped with Li
CaF_2	Tg2(K)	4.2	$g_{\parallel} = 2.747 \pm 0.005$ $g_{\perp} = 2.013 \pm 0.005$		[239]	Co-doped with K
CaF_2	Tg2(Ag)	4.2	$g_{\parallel} = 2.742 \pm 0.005$ $g_{\perp} = 2.017 \pm 0.005$		[239]	Co-doped with Ag

Appendix III. (2)

Host	Center	T	g	Hyperfine structure (10^{-4} cm^{-1})	Ref.	Comments
CaF_2	Rh1	20	$g_x = 1.38 \pm 0.001$ $g_y = 2.85 \pm 0.02$ $g_z = 2.94 \pm 0.01$		[259]	Z ∥ |110|, X ∥ |221|
		4.2	$g_x = 1.378 \pm 0.010$ $g_y = 2.838 \pm 0.008$ $g_z = 2.927 \pm 0.008$		[261]	
CaF_2	Rh2(Na)	4.2	$g_x = 2.308 \pm 0.002$ $g_y = 2.126 \pm 0.005$ $g_z = 1.090 \pm 0.005$	$A_x = 103 \pm 1$ $A_y = 82.6 \pm 1$ $A_z = 43.6 \pm 1$	[241], [274]	x ∥ |001|, y ∥ |110|, z ∥ |110| Co-doped with Na
CaF_2	Rh2(Li)	4.2	$g_x = 2.438 \pm 0.005$ $g_y = 2.210 \pm 0.005$ $g_z = 2.119 \pm 0.005$		[239]	Co-doped with Li
CaF_2	Rh2(K)	4.2	$g_x = 2.298 \pm 0.005$ $g_y = 2.112 \pm 0.005$ $g_z = 1.147 \pm 0.005$		[239]	Co-doped with K
CaF_2	Rh2(Ag)	4.2	$g_x = 2.137 \pm 0.005$ $g_y = 2.359 \pm 0.005$ $g_z = 1.850 \pm 0.005$		[239]	Co-doped with Ag
SrF_2	Tg1	20	$g_{\parallel} = 3.433 \pm 0.008$ $g_{\perp} = 1.971 \pm 0.002$		[227]	
		4.2	$g_{\parallel} = 3.489 \pm 0.0005$ $g_{\perp} = 1.9831 \pm 0.0005$		[262]	
		4.2	$g_{\parallel} = 3.4882 \pm 0.0008$ $g_{\perp} = 1.9830 \pm 0.0008$	$A_{\parallel} = 158.3$	[274]	

Appendix III. (3)

Host	Center	T	g	Hyperfine structure (10^{-4} cm^{-1})	Ref.	Comments
SrF_2	Tg2	4.2	$g_{\parallel} = 2.824 \pm 0.005$ $g_{\perp} = 1.97 \pm 0.01$	$A_{\parallel} = 111.09$	[263], [264] [274]	Co-doped with Na or K
SrF_2	Tg3	4.2	$g_{\parallel} = 1.72 \pm 0.01$ $g_{\perp} = 2.49 \pm 0.01$		[263], [264]	Co-doped with Na or K
SrF_2	Rh1	4.2	$g_x = 1.3276 \pm 0.0005$ $g_y = 2.88 \pm 0.01$ $g_z = 3.183 \pm 0.002$		[262]	z ∥ |110|, x in plane (110) a (15+0.5)° from (110)
BaF_2	Tg1	10-20	$g_{\parallel} = 3.337 \pm 0.002$ $g_{\perp} = 2.115 \pm 0.001$		[265]	
		4.2	$g_{\parallel} = 3.233 \pm 0.008$ $g_{\perp} = 2.108 \pm 0.002$		[242]	
$LaCl_3$	Tr	4.2; 20	$g_{\parallel} = 4.153 \pm 0.005$ $g_{\perp} = 1.520 \pm 0.002$	$A_{\parallel}^{235} = 176 \pm 1$ $A_{\perp}^{235} = 58.5 \pm 0.5$ $P^{235} = 5.5 \pm 0.5$	[268], [269]	
			$g_{\parallel} = 4.149$ $g_{\perp} = 1.520$	$A_{\parallel}^{233} = 378.6 \pm 1.2$ $A_{\perp}^{233} = 123.6 \pm 1.0$ $P^{233} = 9.9$		
$ScPO_4$	Tg	4.2	$g_{\parallel} = 1.370$ $g_{\perp} = 1.736$		[267]	
$LuPO_4$	Tg	4.2	$g_{\parallel} = 3.13$ $g_{\perp} = 0.9$		[267]	

Appendix IV. (1)

Electron Paramagnetic Resonance Data on Concentrated Uranium Compounds

Host	T	g	Ref.	Comments
ThO_2 powder	77	1.25	[192]	
UF_6Li	77	$g_{\parallel} = 0.801$ $g_{\perp} = 0.753$	[88], [176] [177]	U^{5+} Trigonal Center
UF_6Na	77	$g_{\parallel} = 0.817$ $g_{\perp} = 0.708$	[88], [176] [177]	U^{5+} Trigonal Center
UF_6Cs	77	$g_{\parallel} = 0.928$ $g_{\perp} = 0.681$	[88], [176] [177]	U^{5+} Trigonal Center
UCl_6Rb powder	R.T.	~ 1.1	[178]	
UCl_5	77	1.1882	[179]	Linewidth 734 G
$UCl_5 \cdot SOCl_2$	R.T.	1.097	[178]	
$UCl_5 \cdot PCl_5$	R.T.	1.11	[178]	
$(n - C_3H_7)_4 NUCl_6$	R.T.	~ 1.1	[178]	
$UCl_5 \cdot TCAC$	R.T.	1.095	[178]	
$NOUF_6$	77	0.748	[177]	
UOF_5^{2-} complexes	R.T.	0.58	[180]	Linewidth 8000G
UCl_6^- complexes	R.T.	1.12	[180]	Linewidth 1200G

Host	T	g	Ref.	Comments
$UOCl_5^{2-}$ complexes	R.T.	1.09	[180]	Linewidth 1400G
UBr_6^- complexes	R.T.	1.21	[180]	Linewidth 850
$UOB_{M_5}^{2-}$ complexes	R.T.	1.24	[180]	Linewidth 1600G
Na_3UF_8	7	1.2	[184]	
$LiNbO_3$	R.T. 77	0.727	[184]	
$LiTaO_3$	R.T. 77	$g_{\parallel} = 0.773$ $g_{\perp} = 0.658$	[184]	
$BiNbO_3$	7	~ 0.7	[184]	
$LiUO_3$	R.T. 77	2.49 2.57	[185]	Linewidth 1658G at R.T. and 1660G at 77K
$NaUO_3$	R.T. 77	3.49 4	[185]	Linewidth 1296G at R.T. and 1726G at 77K
KUO_3	R.T. 77	2.42 2.61	[185]	Linewidth 1571 at R.T. and 1604G at 77K
$RbUO_3$	R.T. 77	2.43 2.48	[185]	Linewidth 1641 at R.T. and 1654G at 77K
US_3	R.T. 4.2	2; 4	[289]	
UTe_3	R.T. 4.2	2; 4	[289]	

Appendix IV (3)

Host	T	g	Ref.	Comments
UF_3	R.T.	g = 2.8 - 2.9 g = 2.1 - 2.2	[280] [281]	Powder sample
UF_4	R.T.	2.15	[281]	Powder sample
UO_2	R.T.	2.33	[283, 284]	Powder sample